GABA Accumulation and the Hypersensitive Response in Isolated Mesophyll Cells Treated with the G Protein Activator, Mastoparan

Lisa J. Allen, Honours B. Sc. (Biochemistry)
Department of Biological Sciences

Submitted in partial fulfillment of the requirements
for the degree of Master of Science

August, 1997
Brock University
St. Catharines, Ontario

Abstract

GABA (γ-amino butyric acid) is a non-protein amino acid synthesized through the α-decarboxylation of L-glutamate. This reaction is catalyzed by L-glutamate decarboxylase (EC 4.1.1.15), a cytosolic Ca^{2+}/calmodulin-stimulated enzyme. The purpose of this study is to determine whether or not GABA accumulation is associated with the hypersensitive response of isolated *Asparagus sprengeri* mesophyll cells.

The addition of 25 μM mastoparan, a G protein activator, to suspensions of isolated asparagus mesophyll cells significantly increased GABA synthesis and cell death. Cell death was assessed using Evan's blue dye and fluorescein diacetate tests for cell viability. In addition, mastoparan stimulated pH-dependent alkalinization of the external medium, and a rapid and large O_2 consumption followed by a loss of photosynthetic activity. The rate of O_2 consumption and the net decrease in O_2 in the dark was enhanced by light. The inactive mastoparan analogue Mas17 was ineffective in stimulating GABA accumulation, medium alkalinization, O_2 uptake and cell death. Accumulation of H_2O_2 in response to mastoparan was not detected, however, mastoparan caused the cell-dependent degradation of added H_2O_2. The pH dependence of mastoparan-stimulated alkalinization suggests cellular electrolyte leakage, while the consumption of O_2 corresponds to the oxidative burst in which O_2 at the cell surface is reduced to form various active oxygen species. The results are indicative of the "hypersensitive response" of plants to pathogen attack, namely, the death of cells in the locality of pathogen invasion.

The data are compatible with a model in which mastoparan triggers G protein activity, subsequent intracellular signal transduction pathway/s, and the hypersensitive response. It is postulated that the physiological elicitation of the hypersensitive response involves G protein signal transduction. The synthesis of GABA during the hypersensitive response has not been documented previously; however the role/s of GABA synthesis in the hypersensitive response, if any, remain unclear.

Acknowledgements

I wish to express my deep gratitude to Dr. Alan Bown for his time, encouragement and support throughout this project. His passion for research and commitment to the clear communication of scientific knowledge have both challenged and inspired me.

Thanks to Lesley, Glen, Ray, Stephanie and Al who have worked with me in the Bown laboratory over the past two years. I have enjoyed your companionship. Special thanks to my colleagues Randy -- for your friendship, empathy, pep talks and invaluable technical assistance -- and Richard -- for your friendship, stimulating conversations, and computer expertise.

Thank you to my family whose pride in my accomplishments has always motivated me to reach higher.

I can't thank Dan enough. He has gone through this program with me and has cheerfully eaten leftovers for the last two years. His encouragement is appreciated beyond words.

I dedicate this volume to the memory of my dad, John N. Kamphuis, who is sorely missed. He would have loved to read this.

Table of Contents

Lists of Figures, Tables and Models

Figures

Tables

Models

1. Introduction

GABA is a ubiquitous non-protein amino acid. GABA is synthesized in plant cells predominantly by the α-decarboxylation of L-glutamate, a proton-consuming reaction catalyzed by the cytosolic enzyme, L-glutamate decarboxylase (EC 4.1.1.15) (GAD). *In vitro* data demonstrate that GAD activity and GABA accumulation are stimulated by elevated cytosolic Ca^{2+} ions. GAD has a calmodulin-binding domain and is activated by elevated Ca^{2+}/calmodulin concentrations (Baum *et al.*, 1993; Snedden *et al.*, 1995).

GABA accumulates rapidly in response to a variety of stresses as diverse as hypoxia, cold and hot temperatures, UV irradiation, mechanical manipulation and viral attack (Wallace *et al.*, 1984; Bown and Shelp, 1989). The observed rapidity of GABA accumulation indicates that it is not due to the *de novo* synthesis of GAD. Instead, GABA accumulation is attributed to the activation of GAD. Large and rapid increases in cytosolic Ca^{2+} concentrations in response to wind, touch, fungal elicitor application and cold temperature shock have also been shown (Knight *et al.*, 1991; Cholewa *et al.*, 1997). Thus, GABA accumulation may be the result of an intracellular signal transduction pathway leading to increased cytosolic Ca^{2+} and subsequent GAD activation.

Roberts and colleagues (1992) observed GABA accumulation in conjunction with the death of maize root tip cells subjected to hypoxia. This caused them to hypothesize that GABA accumulation may be "a metabolic marker for dead or dying...plant cells." The combination of GABA accumulation and cell death suggested the involvement of GABA accumulation with the hypersensitive response (HR).

The hypersensitive response is an induced plant defense. It is defined as the

death of cells in the area of pathogen invasion to limit the spread of infection. A rise in Ca^{2+} has been demonstrated to be essential for the hypersensitive response (Schwacke and Hager, 1992). The involvement of Ca^{2+} ions in the elicitation of the hypersensitive response also indicates the involvement of an intracellular signal transduction pathway, linking the extracellular perception of an elicitor to the cellular response.

In both GABA accumulation and the hypersensitive response, the mechanisms of signal transduction are a matter for investigation. In a preliminary study, treatment of asparagus mesophyll cells with the G protein activator, mastoparan, led to GABA accumulation and cell death (Allen, 1995). This suggested that GABA production may be a component of the HR. Alternatively, mastoparan may merely be cytotoxic. To elucidate the relationship between GABA accumulation and the hypersensitive response, it must be demonstrated that mastoparan is causing cell death via the hypersensitive response. Thus, the focus of this investigation is the influence of the G protein activator, mastoparan, on GABA accumulation and the hypersensitive response in isolated *Asparagus sprengeri* mesophyll cells. The research questions posed were:

1. Does mastoparan induce death in asparagus mesophyll cells?
2. Is GABA accumulation "a metabolic marker for dead or dying...plant cells" as Roberts and colleagues (1992) have postulated?
3. Does MP induce the hypersensitive response via G protein activation in asparagus mesophyll cells?
4. Are GABA accumulation and the hypersensitive response causally related?
5. Does light play a role in the mastoparan-stimulated hypersensitive response of photosynthetic asparagus mesophyll cells?

2. Literature Review

2.1. GABA

2.1.1. GABA metabolism

GABA, or γ-amino butyric acid, is present in virtually all plant tissues. It often constitutes a significant portion of the total free amino acid pool. Though GABA possesses both amino and acid functional groups, it is not an α-type amino acid, nor is it incorporated into protein (Bown and Shelp, 1989).

Glutamate decarboxylase (GAD; EC 4.1.1.15), a pyridoxal-phosphate-dependent enzyme, is primarily responsible for GABA synthesis by catalysing the α-decarboxylation of L-glutamate. This reaction consumes a proton and is normally irreversible because one of the products, CO_2 gas, is irretrievable because of diffusion [Figure 2.1. Reaction i)]. GABA in the presence of pyruvate can undergo transamination to produce succinic semialdehyde and alanine in a reversible reaction catalyzed by GABA-pyruvate transaminase (GABA-T; EC 2.6.1.19) [Figure 2.1. Reaction ii)]. Together succinic semialdehyde and $NAD(P)^+$ undergo a redox reaction catalysed by succinic semialdehyde dehydrogenase (SSADH; EC 1.2.1.16), resulting in succinate and NAD(P)H [Figure 2.1. Reaction iii)]. The above three reactions compose "the GABA shunt." This pathway allows L-glutamate carbon to enter the tricarboxylic acid (TCA) cycle as succinate.

Figure 2.1: GABA Shunt Reactions

i) H^+ + L-glutamate ---> GABA + CO_2

ii) GABA + pyruvate <----> Succinic semialdehyde + alanine

iii) Succinic semialdehyde + $NAD(P)^+$ + H_2O ---> Succinate + NAD(P)H

The subcellular locations of the enzymes of the GABA shunt have only recently been established using delicate soybean cotelydonary protoplasts (Breitkreuz and Shelp, 1995). Organellar fractions were gently purified with continuous Percoll-gradient centrifugation to preserve intact mitochondria and microbodies. GAD activity was found to be located exclusively in the cytosolic fraction while both GABA-T and SSADH activities were found exclusively in the mitochondrial fraction. It was speculated that, analogous to mammalian systems, GABA-T and SSADH may associate to form a stable complex to promote efficient substrate channeling (Breitkreuz and Shelp, 1995). What has not been characterized is the system for GABA transport into the mitochondria following its synthesis.

GABA production may also occur by the hydrolysis of 4-guanidinobutyrate as well as by the 2-step conversion of putrescine to GABA (Bown and Shelp, 1989).

2.1.2. GABA accumulation in response to stress

Extensive literature exists to document rapid accumulation of GABA in response to various unrelated environmental stresses including hypoxia, mechanical manipulation and mechanical injury, cold and hot temperature shocks, anaerobiosis, γ-radiation, viral attack, water stress and phytohormone application (reviewed by Bown and Shelp, 1989; Satya Narayan and Nair, 1990; Bown and Shelp, 1997). An elegant example is provided by Wallace *et al.* (1984). GABA levels increased approximately 23-fold within 5 min of transfer of soybean leaflets from 35°C to 22°C and 6°C. This increase was paralleled by a reduction in glutamate concentration. The conversion of glutamate to GABA was also confirmed with [^{14}C]-labeling experiments. The ratio of the activities of GAD to GABA-T or SSADH was high, suggesting that increased GABA synthesis was responsible for its accumulation versus decreased GABA metabolism.

More recently, Ramputh and Bown (1996) demonstrated that mechanical touch and mechanical damage of soybean leaflets, intended to simulate the movement and feeding behaviour of phytophagous insects on the leaflets, caused anywhere from 9- to 25-fold increases in GABA within 1-4 min. In each of these cases, the rapidity of GABA synthesis precludes the possibility of *de novo* synthesis of GAD. Consequently rapid GABA accumulation must involve the activation of GAD.

The addition of L-Glu to the medium of a suspension of *Asparagus sprengeri* mesophyll cells induced transient alkalinization of the medium, uptake of L-Glu by the cells (McCutcheon and Bown, 1987), and GABA synthesis (Chung *et al.*, 1992). These phenomena provide evidence for the existence of a H^+/L-Glu symport across the plasma membrane of *A. sprengeri* mesophyll cells.

Newly synthesized GABA did not remain in the cytosol but left the cell (Chung *et al.*, 1992). The measurement of high GABA levels in *A. sprengeri* xylem fluid initially suggested the possibility of efflux from cells and further studies with radiolabeling confirmed the efflux phenomenon. Incubation of isolated *A. sprengeri* mesophyll cells with L-[U-^{14}C]Glu led to its uptake via the H^+/L-Glu symport and its α-decarboxylation in the cytosol. Alanine levels rose in the cytosol while radiolabeled GABA levels increased in the medium. The specific activity of extracellular GABA was 18 nanocuries per nanomole while intracellular GABA had a specific activity of approximately 0.2 nanocuries per nanomole. Thus, it appears that the newly synthesized GABA pool is distinct from previously synthesized GABA and that it is the former that is subject to efflux. These data support the selective efflux of newly synthesized GABA although the mechanism of efflux remains unclear. The intracellular concentration of GABA is 24 or 600 times that of the medium in the presence or absence of L-Glu, respectively, suggesting a passive mechanism of efflux.

These and numerous other data invite a pair of questions regarding GABA accumulation. The first question involves mechanism: how do these diverse environmental stimuli culminate in the activation of GAD and the accumulation of GABA--is there more than one possibility? Secondly, the significance of GABA is questioned: what role(s) does GABA accumulation play?

2.1.3. GAD regulation

Early attempts to answer the question of mechanism included the idea that the compartmentation of glutamate or a GAD-effector molecule was disrupted or specifically altered to stimulate the α-decarboxylation of glutamate by GAD (Bown and Shelp, 1989). Since that time, localization of GAD and glutamate to the cytosol as well as new insights into the regulation of GAD do not support this hypothesis.

2.1.3.1 GAD regulation by pH

One of the first pieces of evidence for direct regulation of GAD was the determination of the enzyme's pH optimum. Plant GAD activity exhibits a pH optimum of 5.8 (Snedden *et al.*, 1992). Around neutrality, GAD activity is only a fraction of its maximum. Thus, acidification of the cytosol which is usually maintained between 7.0-7.5 (Kurkdjian and Guern, 1989) should theoretically cause increased GABA production.

In vivo experiments with isolated asparagus mesophyll cells involving acidosis were performed to test this hypothesis (Crawford *et al.*, 1994). The treatments used to cause cytosolic acidification included hypoxia and incubation with butyrate, a permeant weak acid. While 60 min of these treatments stimulated GABA production from 100-1800%, 15 seconds of incubation with butyrate at pH 5.0 was sufficient to cause increases in GABA between 200-300%.

Subsequently, Carroll and associates (1994) made a similar observation using *in vivo* ^{15}N NMR spectroscopy to observe nitrogen assimilation in carrot cell cultures. A decrease in cytosolic pH of approximately 0.18 pH units following the addition of [^{15}N]-labeled ammonium chloride resulted in increased GABA levels. The pH decline was rectified following GABA production, supporting the hypothesis that a role for GABA accumulation is to alleviate cytosolic acidosis. The basis for this hypothesis is the H^+-consuming nature of the α-decarboxylation reaction of GAD.

A critical statement from the article by Crawford *et al.* (1994) proposes that "a reduced cytosolic pH appears to be a sufficient but not a necessary requirement for stimulated GABA synthesis." Although H^+ ions are involved in regulation of GAD activity, not all stresses leading to GABA accumulation can be attributed to a lowering of pH. Several examples include cold and hot temperature shocks, fungal elicitation, and mechanical stresses. The involvement of Ca^{2+}, the ubiquitous second messenger, was suggested to be involved in GAD regulation in these cases.

2.1.3.2 GAD regulation by Ca^{2+}

Preliminary evidence for Ca^{2+} regulation of plant GAD was limited and incoherent. Ca^{2+} ions were known to regulate many processes by binding to Ca^{2+}-dependent kinases and to the Ca^{2+}-binding protein calmodulin (CaM). Tobacco plants had been engineered to express the Ca^{2+}-sensitive luminescent coelenterate protein aequorin. Cold and mechanical stresses, which cause increased GABA levels (Wallace *et al.*, 1984), were also observed to cause rapid and transient increases in

intercellular Ca^{2+} levels indicated by luminescence in these transgenic tobacco leaves (Knight *et al.*, 1991). Cytosolic Ca^{2+} levels were found to increase when cytosolic H^+ ions levels increased (Gehring *et al.*, 1990). Furthermore, in a random search for plant CaM-binding proteins by screening plant cDNA libraries with a ^{35}S-labeled recombinant calmodulin probe, it was discovered that petunia GAD has a CaM-binding domain (Baum *et al.*, 1993).

2.1.3.2.1 *In vitro* data

The CaM-binding property of petunia GAD opened the door for the *in vitro* investigation of the Ca^{2+} regulation of GAD. A 62-kD CaM-binding protein from fava bean was isolated, purified and determined by microsequence analysis to be GAD (Ling *et al.*, 1994). Furthermore, the *in vitro* activity of this enzyme was stimulated by 50% with 100 μM Ca^{2+}, by 100% with 100 μM Ca^{2+} plus 100 nM CaM, and not significantly stimulated by CaM without added Ca^{2+}. These data indicate that there exist some tightly associated GAD/CaM complexes which are stable even in the absence of Ca^{2+}. It is these that are activated when 100 μM Ca^{2+} is added.

Soybean GAD activity was also stimulated by Ca^{2+}/CaM (Snedden *et al.*, 1995). It was further noted that the 2- to 8-fold stimulation of GAD by Ca^{2+}/CaM at pH 7 was absent at pH 5.8, the optimum pH for enzyme activity. Thus, GAD appears to be responsive to Ca^{2+}/CaM at physiological pH values.

Low levels of GAD activity in the absence of exogenous Ca^{2+}/CaM have been observed in fava bean (Ling *et al.*, 1994), soybean (Snedden *et al.*, 1995), petunia

(Arazi *et al.*, 1995) and tobacco (Baum *et al.*, 1996). This activity is understood to be residual activity resulting from GAD/CaM complexes formed during extraction. The lack of significant GAD activity in the absence of Ca2+/CaM predicts a model reminiscent of many animal CaM-binding proteins where the CaM-binding domain is an autoinhibitory domain, preventing enzyme activity by physically blocking substrate access to the active site (Snedden *et al.*, 1995). Upon binding of Ca^{2+}/CaM, the CaM-binding domain moves aside, exposing the active site and allowing substrate turnover. Proteolysis of the CaM-binding domain of soybean GAD during purification yielded a Ca^{2+}/CaM-insensitive yet active enzyme (Snedden *et al.*, 1995). In this case, proteolytic cleavage of the CaM-binding domain has the same effect as Ca^{2+}/CaM binding to this domain. This observation is consistent with the model presented.

2.1.3.2.2 *In vivo* data

In vivo data on the role of Ca^{2+} in the regulation of GAD is much more scarce due to the difficulty in measuring cytosolic Ca^{2+} concentrations. The first *in vivo* investigation of the subject was published only recently by Cholewa and her colleagues (1997) using isolated *Asparagus sprengeri* mesophyll cells. These are the first published *in vivo* data linking cytosolic Ca^{2+} increases, GAD stimulation, and GABA synthesis. Cold shock (an abrupt temperature reduction from 20°C to 1°C) caused a 100% increase in GABA levels within 15 min. This effect was significantly reduced by both La^{3+}, a Ca^{2+}-channel blocker and N-(6-aminohexyl)-5-chloro-1-naphthalene-sulfonamide, a CaM antagonist. GABA levels were enhanced by 61%

following a 15-min incubation with the Ca^{2+} ionophore calcimycin. A perfusion of cold buffer was applied to cells loaded with Fluo-3, a Ca^{2+}- sensitive fluorescent probe. Using a fluorescence imaging system which utilizes an arbitrary pseudo-colour scale to illustrate a broad range of Ca^{2+} concentrations, it was observed that cytosolic Ca^{2+} levels increased within 2 s of cold stress and within 25 s had already returned to resting levels. Similar treatment of cells loaded with a pH-sensitive probe demonstrated a rapid cytosolic alkalinization, ruling out the stimulation of GAD by acidic pH and concomitant increase in GABA synthesis.

Although hydrogen ion stimulation of GAD at pH 5.8 is several-fold higher than Ca^{2+}/CaM stimulation at pH 7, clearly two mechanisms of *in vitro* GAD regulation exist. Some data indicate that certain stresses lead to both cytosolic acidification and higher levels of cytosolic Ca^{2+} (Bush, 1993). The relationship between *in vivo* fluxes of the two ions are not as well understood. Although the *in vivo* data presented by Cholewa *et al.* (1997) rejects the involvement of hydrogen ions in Ca^{2+} regulation of GAD, it has been postulated that a reduction in pH leading to GABA accumulation may not in fact be independent of Ca^{2+} (Snedden and Fromm, unpublished). Recent data published by Aurisano *et al.* (1995) supports this idea. Rice roots were deprived of oxygen in the presence of either a CaM antagonist or a Ca^{2+}-channel blocker. Anoxia is one of the stresses reported to cause increases in both H^+ and Ca^{2+} levels in the cytosol (Bush, 1993). The CaM antagonist and Ca^{2+}-channel blocker both reduced GABA accumulation as compared with controls. In this case at least, it seems that hydrogen ions are insufficient to stimulate *in vivo* GAD activity; instead, an influx of

Ca^{2+} is required for the anoxic stimulation of GAD. The relationship between H^+ and Ca^{2+} regulation of GAD *in vivo* may not parallel *in vitro* data. More research is necessary to elucidate the contributions of H^+ and Ca^{2+} to the activation of the *in vivo* enzyme.

2.1.4. Possible roles of GABA

In plants, the function of GABA accumulation is less clear than the mechanism of GABA accumulation. Several hypotheses exist to explain the role of GABA accumulation.

2.1.4.1. A remedy for cytosolic acidification

L-glu decarboxylation by GAD both consumes a proton and is optimized at an acidic pH. Furthermore, permeant weak acids and other treatments resulting in a decreased cytosolic pH (like hypoxia) stimulate GABA synthesis (Bown and Shelp, 1989; Crawford *et al.*, 1994; Carroll *et al.*, 1994). These data, taken together, suggest that GABA synthesis may serve to rectify acidification of the cytosol to a more neutral pH.

2.1.4.2. Nitrogen storage and transport

L-glu is decarboxylated, i.e., GABA accumulates at a higher rate when alternative metabolic processes involving L-glu are less favorable or when a plant is under stress. For example, L-glu is preferentially converted to GABA when

-L-glu to L-gln conversion is inhibited,

-cellular requirements for L-glu and L-gln are low,

-or during periods of increased proteolysis (Bown and Shelp, 1997). These

data support the notion of GABA as a temporary nitrogen storage compound.

Due to the presence of GABA in the xylem fluid of *A. sprengeri* (Chung et al., 1992; Parsons and Baker, 1996) as well as its efflux from cells (Chung *et al.*, 1992), it has also been suggested that GABA may serve as a transport compound in plants, supplying developing tissues with nitrogen. However, long term xylem transport seems unlikely to be a response to rapid and transient GABA accumulation.

2.1.4.3. A modulator of plant development

Evidence supports the role of GABA in the developmental regulation of plant morphology. Being found in virtually all plant tissues examined, GAD is one of the most abundant soluble Ca^{2+}/CaM binding proteins in plants (Baum *et al.*, 1993). The level of GAD is regulated by transcription and post-transcriptional modification during development (Chen *et al.*, 1994). GAD possesses an autoinhibitory domain that blocks its activity in the absence of Ca^{2+}/CaM. An experiment with transgenic tobacco plants expressing a mutant GAD which lacked an autoinhibitory domain demonstrated higher GABA levels, lower L-glu levels and reduced stem elongation (Baum *et al.*, 1996). These data indicate that GABA may be involved in the regulation of stem elongation. Documentation of GABA accumulation and its subsequent efflux also supports this idea. Extracellular GABA may serve as an intercellular messenger to induce systemic effects on the growth and development of a plant. However, plasma-membrane receptors for GABA (corresponding to $GABA_A$ and $GABA_B$ receptors in animal cells), necessary to mediate the external signal into a cellular response, have not been identified in plants (Bown and Shelp, 1997). Very recent work shows that exogenous GABA invokes ethylene biosynthesis (Kathiresan *et al.*, 1997). Thus the effects of GABA on the anatomy of the plant may occur via signal transduction leading

to the production of the plant hormone, ethylene.

2.1.4.4. Plant defense against predators

In animal systems, GABA acts as an inhibitory neurotransmitter. Hyperpolarization (due to Cl^- influx) results when GABA binds to a GABA-gated Cl^- channel in the plasma membrane of a neuron. Subsequent neural activity is inhibited because depolarization will fail to reach the threshold value necessary to initiate an action potential.

Feeding activity by phytophagous insects entails mechanical manipulation and damage. This leads to rapid GABA accumulation and concomitant ingestion by the predator. A study by Ramputh and Bown (1996) demonstrated that simulated phytophagous activity involving mechanical damage resulted in 2 μmol GABA g^{-1} fresh weight soybean leaf within 2 min. This represents a 10- to 25-fold increase in GABA levels. This level of GABA in the diets of *Christoneura rosaceana* (oblique-banded leaf roller) larvae reduced growth rates, delayed pupal development and decreased larval survival as compared with control larvae. GABA ingested by insects is not limited by a blood-brain barrier and may contact GABA-gated Cl^- channels at neuromuscular junctions. These data suggest that ingested GABA may block neuromuscular activity, inhibiting larval growth and development.

2.2. Plant phosphoinositide signal transduction

Phosphoinositide (PI) signal transduction has been well characterized in animal systems. According to the animal paradigm of PI signal transduction, phosphatidylinositol-4,5-bisphosphate (PIP_2), naturally occurring in the phospholipid bilayer of the plasma membrane, is cleaved by the enzyme phospholipase C (PLC).

PLC activity is often stimulated by a heterotrimeric GTP-binding protein which has been activated by a signal-receptor complex. The products of PIP_2 hydrolysis, inositol-1,4,5-trisphosphate (IP_3) and diacylglycerol (DAG), serve to open intracellular Ca^{2+} channels and activate protein kinase C (PKC), respectively. These are involved in initiating the cellular response i.e., the modulation of the activities of other enzymes in the short term as well as the long-term regulation of gene expression. Most of the structural and enzymic elements of the PI signal transduction pathway necessary for operation appear to be present in plants and have been implicated in the induction of plant cellular responses (Boss, 1989; Einspahr and Thompson, 1990; Coté and Crain, 1993).

2.2.1. G protein involvement

Broadly speaking, heterotrimeric GTP-binding proteins, commonly called G proteins, can be stimulating (G_S) or inhibiting (G_i). They are composed of three subunits: $G\alpha$, $G\beta$, $G\gamma$. The catalytic cycle of G protein function in animal systems has been established (Millner and Causier, 1996). When binding GDP, the $G\alpha$ subunit is inactive and is associated with the $G\beta\gamma$ complex and an integral receptor protein. Upon activation of the receptor due to ligand binding, the subunit undergoes an allosteric change which promotes the exchange of GDP for GTP and the dissociation from $G\beta\gamma$. In this active conformation, the $G\alpha$-GTP regulates the activity of specific effector molecules; in the PI signal transduction system, PLC is activated. Activation continues until the intrinsic GTPase activity of the $G\alpha$ subunit hydrolyzes the GTP to GDP. This results in the reassociation of $G\alpha$ and $G\beta\gamma$ and restores the trimer for the resumption of the cycle. Each step of signal transduction contributes to the

amplification of the signal and the many steps involved allow for fine-tuning of the response.

Until the cloning of a putative Gα subunit gene from *Arabidopsis* (Ma *et al.*, 1990), the isolation of cDNAs encoding a tomato Gα subunit (Ma *et al.*, 1991) and Gβ subunits from *Arabidopsis* and maize (Weiss *et al.*, 1994), the argument for the existence of G proteins in plants was based on circumstantial evidence. This evidence included

-the binding of GTP analogues to membrane preparations,

-cholera and pertussis toxins mediating ADP-ribosylation of specific proteins, and

-isolating proteins of an expected molecular weight with an antibody raised against a mammalian Gα subunit (Terryn *et al.*, 1993).

Further experimental evidence implicating receptor-linked G protein signal transduction in plants was gained by using GTP and GTP analogues. In one study, membranes isolated from *Acer pseudoplatanus* cell suspension cultures were labelled with [^{3}H]-inositol (Dillenschneider *et al.*, 1986). Following treatment of membrane preparations with GTP analogues, soluble phosphoinositol derivatives were released in a dose-dependent manner. Maximal stimulation was caused by GTPγS, a nonhydrolyzable guanine nucleotide derivative. In addition, 100 μM GTPγS stimulated phospholipase activity in *Dunaliella salina* membranes in the presence of free Ca^{2+} (Einspahr *et al.*, 1989). This was also measured by the release of radiolabelled inositol phosphate derivatives, over 80% of which were recovered as [^{3}H] IP_3. This product distribution specifically supports PLC stimulation via G protein activation.

Taken together, this evidence demonstrates G protein involvement in the PI signal transduction pathway in plants.

2.2.2. Products of PIP_2 hydrolysis

2.2.2.1. Inositol-1,4,5-trisphosphate

Inositol-1,4,5-trisphosphate (IP_3) is a water-soluble sugar. In animal cells, IP_3 initiates Ca^{2+} release from internal stores by the binding of one or more IP_3 molecules to an IP_3-receptor on the membrane of a Ca^{2+}-storage vesicle. A Ca^{2+} channel linked to the receptor opens and Ca^{2+} flows down its electrochemical gradient into the cytosol. Ca^{2+} is released primarily from the endoplasmic reticulum and possibly the nucleus of animal cells (Berridge and Irvine, 1989).

Plant IP_3 was first positively identified in the green alga, *Chlamydomonas reinhardtii* (Coté and Crain, 1993). A compound isolated from *C. reinhardtii* comigrated with authentic IP_3 on HPLC. It also bound with high-affinity to an IP_3-receptor-protein. Related inositol phosphates either did not comigrate with authentic IP_3 or displayed lower affinity binding with the receptor.

A growing body of evidence supports a role for IP_3 as a second messenger in plant signal transduction systems. Increases in intracellular IP_3 concentrations have been demonstrated in response to non-killing freezing temperatures, lowered tissue water potential, and the phytohormone abscisic acid in *Brassica napus* plants (Smolenska-Sym and Kacperska, 1996). Photolysis of caged IP_3 caused an increase in cytosolic Ca^{2+} in guard cells of *Commelina communis* (Gilroy *et al.*, 1990) and in pollen tubes of *Papaver rhoeas* (Franklin-Tong *et al.*, 1996). These elevations in

cytosolic Ca2+ were followed by stomatal closure and tube growth inhibition, respectively. In addition, IP_3 application has been shown to cause the release of Ca^{2+} from red beet microsomes (Brosnan and Sanders, 1990). Furthermore, in *Samanea saman* pulvini, transient IP_3 accumulation precedes K^+ channel closure in response to blue light and darkness (Kim *et al.*, 1996). K^+-channel closure was inhibited by neomycin, an inhibitor of phosphoinositide hydrolysis. These data infer that IP_3 is an intracellular messenger inducing Ca^{2+} increases and physiological responses in plant cells.

The mechanism of IP_3-induced Ca^{2+} release has also been under investigation. Analogous to animal systems, IP_3 caused the opening of Ca^{2+} channels in isolated red beet tonoplast vesicles as measured by patch-clamping (Alexandre *et al.*, 1990). IP_3-induced Ca^{2+} release from red beet microsomes was inhibited by heparin, a glycosaminoglycan used to competitively inhibit IP_3-receptor binding in animal systems (Brosnan and Sanders, 1990). Heparin microinjected in pollen tubes of *P. rhoeas* inhibited Ca^{2+} release induced by photolysis of caged IP_3 (Franklin-Tong *et al.*, 1996). Stimulation of pollen tube growth also resulted. Inhibition of IP_3-induced Ca^{2+} release by heparin implicates the presence of an IP_3 receptor in plants. Recently, a high-affinity binding site for IP_3 was identified in a membrane vesicle preparation from *Chenopodium rubrum* ($K_d \cong 142 \pm 17$ nM) (Scanlon *et al.*, 1996). Binding of [^{3}H] IP_3 was found to be Ca^{2+}-dependent, totally displacable by

cold IP_3, and inhibited by heparin. Although this novel plant IP_3-binding site requires further characterization, all of the evidence suggests that the mechanism of IP_3-induced Ca^{2+} release is conserved between plant and animal systems.

The location of stored Ca^{2+} involved in IP_3-induced Ca^{2+} release in plants is another question. Only IP_3-induced Ca^{2+} release from the vacuole has been established. The vacuole is the largest compartment of the cell, occupying up to 90% of the cell's volume and containing millimolar concentrations of Ca^{2+}. Canut and colleagues (1990) separated membrane vesicles isolated from carrot microsomal fractions. Each membrane fraction was identified by both electron microscopy and marker enzyme activities. With pure plasma membrane, pure tonoplast, and mixed mitochondria/endoplasmic reticulum/Golgi body fractions, IP_3 initiated Ca^{2+} release from the tonoplast fraction alone. However, only 40% of vacuolar Ca^{2+} was released by IP_3. While other organelles cannot be ruled out as targets of IP_3-induced Ca^{2+} release, it can be concluded that the vacuole contains the vast majority of Ca^{2+} released in reponse to IP_3, even though less than half of the mobile vacuolar Ca^{2+} can be accessed in this manner.

2.2.2.2. Diacylglycerol

The second product of PIP_2 cleavage, diacylglycerol (DAG), remains membrane-bound. In animal systems, DAG serves to activate membrane-bound Ca^{2+}- and phospholipid-dependent protein kinase C (PKC). DAG enhances the

affinity of the kinase for Ca^{2+} so that resting levels of Ca^{2+} are sufficient to activate the kinase (Boss, 1989). Evidence supporting this component of the plant PI signal transduction system is scanty at best and conflicting at worst.

There is evidence that DAG affects the physiology of plant cells. Several reports demonstrate that DAG or DAG analogues in concert with phorbol esters (compounds that mimic DAG activation of PKC in animal cells) or phosphatidylserine initiate ATP-dependent protein phosphorylation (Schafer et al., 1985; Elliott and Skinner, 1986; Oláh and Kiss, 1986). In addition, synthetic DAGs are reported to hyperpolarize guard cells and open stomata (Lee and Assmann, 1991). The latter is inhibited by protein kinase inhibitor H-7.

Researchers have encountered difficulty in accurately determining levels of DAG that may be involved in PI signal transduction. This is due to the presence of multiple pools of DAG in the various cell membranes (Einspahr and Thompson, 1990). Furthermore, rapid hydrolysis of DAG by lipases or conversion to phosphatidic acid may destroy the possibility of accurate measurement of plasma-membrane-bound DAG. Rapid and large increases in phosphatidic acid in *Dunaliella salina* have been measured following hypoosmotic shock (Einspahr et al., 1988). Because concurrent decreases in PIP and PIP_2 levels were also observed, it is possible that these increases correspond to rapid conversion of a large pool of newly synthesized DAG to phosphatidic acid (Einspahr and Thompson, 1990).

2.2.3. Influence of IP_3 and DAG

2.2.3.1. Protein kinase C

One important piece of evidence that is missing in the plant PI signal transduction pathway is that of an animal protein kinase C analogue. Calcium- and

phospholipid-dependent protein kinases have been identified in wheat, zucchini and in oat root plasma membranes (Boss, 1989). However, besides sharing no structural or sequence similarity to the animal PKC, they are not stimulated by DAG (Coté and Crain, 1993). Thus, whether or not the DAG arm of the PI signal transduction pathway exists in plants remains speculative.

2.2.3.2. Cytosolic Ca^{2+} increase

2.2.3.2.1. Ca^{2+} homeostasis

Ca^{2+} is a ubiquitous second messenger in animal and plant systems. Its role in signal transduction is facilitated by the homeostatic mechanisms that maintain a steep electrochemical gradient for Ca^{2+} across both the plasma membrane and other internal membranes. In plant cells, for instance, the nonstressed cytosolic Ca^{2+} concentration is approximately 10 nM, while in the apoplast and inside the vacuole its concentration is approximately 1 mM (Bush, 1995). In plants, transport proteins responsible for regulating the cytosolic Ca^{2+} concentration include,

a) P-type Ca^{2+}-ATPases in the plasma membrane and the tonoplast,

b) Ca^{2+}/nH^{+} antiporters in the tonoplast, and

c) Ca^{2+} channels in the plasma membrane and the tonoplast.

While the former two proteins transport Ca^{2+} against its electrochemical gradient to keep cytosolic Ca^{2+} low, the opening of the latter allows the spontaneous flow of Ca^{2+} into the cytosol. Thus, Ca^{2+} homeostasis is achieved by a balance of these activities which may be compared to a "pump" and "leak" combination (Bush, 1993).

When an elevation in cytosolic Ca^{2+} due to a "leak" is sensed, a feedback mechanism alerts the "pump," which sets out to restore cytosolic Ca^{2+} to resting levels.

An electrical gradient for Ca^{2+} also exists across the plasma membrane and tonoplast ($\Delta\psi_{PM}$ = -120 mV; $\Delta\psi_{TONOPLAST}$ = -90 mV). The cytosol is negatively charged, whereas the apoplast and vacuole are positively charged. The Ca^{2+} concentration gradient across these membranes generates only a small portion of the electrical gradient. The majority of the electrical gradient is the result of a steep H^+ gradient, sustained by an electrogenic H^+-ATPase. This proton pump actively maintains a resting cytosolic pH of ≅ 7.2 and a pH of ≅ 5.5 in the apoplast and in the vacuole.

2.2.2.3.2. Ca^{2+} perturbation

Transduction of a signal is often mediated by an influx of Ca^{2+} into the cytosol following the opening of Ca^{2+} channels in the plasma membrane and/or tonoplast (Bush, 1995). In PI signal transduction, the intracellular messenger, IP_3, triggers Ca^{2+} release from the vacuole. The increase in cytosolic Ca^{2+} ions is involved in regulation of subsequent cellular processes. Ca^{2+} increases must be transient as high Ca^{2+} concentrations are toxic to the cell. Ca^{2+} pumps and antiporters function to reduce Ca^{2+} levels rapidly.

There are 3 main types of Ca^{2+} channels: voltage-gated, ligand-gated and

stretch-activated (Bush, 1995). All three types exist in the plasma membrane of plants, while only the former 2 types are found in the tonoplast.

Previously, experimental evidence suggested that extracellular and intracellular pools of Ca^{2+} might be mobilized separately. Knight and colleagues (1992) used transgenic tobacco plants expressing aequorin, a Ca^{2+}-dependent chemiluminescent protein, and various Ca^{2+}-channel blockers to demonstrate that although cold temperatures induced Ca^{2+} influx from outside the cell, wind movements induced internal Ca^{2+} release. However, further experimental data on cold-induced Ca^{2+} influx indicated that both extra- and intracellular pools of Ca^{2+} were mobilized (Knight *et al.*, 1996).

Increased cytosolic Ca^{2+} has been observed in plants in response to the following stimuli: touch, low temperature, red light, auxin, yeast elicitors, gibberellic acid, cytokinin, abscisic acid, hypoxia, salinity, wind and gravity (as reviewed by Gilroy *et al.*, 1993 and Bush, 1995). Although the model presented for Ca^{2+} involvement in signal transduction is simple, the phenomenon is very complex (Trewavas *et al.*, 1996). Oscillations in cytosolic Ca^{2+} suggest that positive feedback is involved such that Ca^{2+} can induce further Ca^{2+} release (Ward and Schroeder, 1994) or even IP_3 production by activating PLC. Furthermore, due to the low diffusability of Ca^{2+} in the cytosol (Speksnijder *et al.*, 1989), increases in cytosolic Ca^{2+} are highly localized, allowing specific regulation of Ca^{2+} targets. A variety of stimuli may generate specialized cellular responses by altering the magnitude, duration, kinetics and spatial

distribution of the Ca^{2+} increases used in the transduction (Berridge, 1993).

2.2.2.3.3. Ca^{2+} targets

Cytosolic Ca^{2+} increases mediate cellular responses by binding to Ca^{2+}-sensitive proteins, i.e., Ca^{2+}-binding proteins which have K_ds in the nanomolar range. Ca^{2+} binds to many target proteins and enzymes, such as calmodulin, protein kinases and protein phosphatases, ion transporters, cytoskeletal proteins and lipases (Bush, 1993). These then change the activities of effector proteins, which include cytoskeletal proteins, lipid binding proteins, metabolic enzymes and ion transporters.

2.2.2.3.4. Ca^{2+} as a messenger in PI signal transduction

In order to validate the involvement of Ca^{2+} in PI signal transduction, a target protein and/or cellular response must be associated with a stimulus inducing a change in cytosolic Ca^{2+}. Cytosolic Ca^{2+} increases, induced by photolysis of caged IP_3, mediated stomatal closure in *C. communis* guard cells (Gilroy *et al.*, 1990). In addition, the propagation of a wave of cytosolic Ca^{2+} initiated by IP_3 inhibited growth in *P. rhoeas* pollen tubes (Franklin-Tong *et al.*, 1996). Furthermore, a G protein activator, mastoparan, stimulated IP_3 production and IP_3-induced Ca^{2+} release in the pollen tubes. Thus, there is evidence for PI signal transduction in the regulation of pollen tube growth and probably in stomatal closure. It is likely that PI signal transduction inducing increased cytosolic Ca^{2+} is involved in the physiological responses of plant cells to other stimuli.

2.3. Mastoparan

2.3.1. Structure and function

Mastoparan (MP) [Ile-Asn-Leu-Lys-Ala-Leu-Ala-Ala-Leu-Ala-Lys-Lys-Ile-Leu-NH_2], is an amphiphilic, cationic tetradecapeptide isolated from wasp venom. MP and other similar peptides were isolated from wasp venom on the basis of their ability to cause secretion from mast cells (Higashijima *et al.*, 1990). Physiological concentrations of MP which stimulate secretion range from 1-50 μM (Ross and Higashijima, 1994).

It is believed that MP-induced secretion results from interaction of MP with a G protein. MP stimulation of G proteins is well documented in animal cells (Higashijima *et al.*, 1988, 1990). Although MP exists as a random coil in aqueous solution, it takes on an α-helical conformation upon binding to a phospholipid membrane (Higashijima *et al.*, 1983). This conformational change is due, in large part, to hydrophobic interactions between the aliphatic side chains of MP and the hydrophobic interior region of the lipid bilayer. When bound to a plasma membrane in this fashion, MP presents three positive charges (Lys side chains) on the cytoplasmic face of the membrane, mimicking an activated (ligand-bound) G-protein-coupled receptor complex (White *et al.*, 1993). Although MP bears no sequence similarity with a G-protein-coupled receptor domain, it shows structural similarity to regions of the third cytoplasmic domain of the receptor (Higashijima and Ross, 1991). As an activated-receptor mimic, MP binds to a Gα subunit. This accelerates the exchange of GDP for GTP, thereby activating the G protein. MP selectively activates Go and Gi proteins, accelerating nucleotide exchange approximately 30-fold (Ross and Higashijima, 1994). MP activation of G proteins is inhibited by pertussis toxin. G proteins that are

subject to MP activation (Higashijima *et al.*, 1990). MP also interacts with low molecular mass G proteins rho/rac, blocking ADP-ribosylation of these proteins (Koch *et al.*, 1991).

MP has been shown to possess numerous biological activities. In addition to its ability to cause histamine release from mast cells (Raynor *et al.*, 1991), MP causes mast cell degranulation, activates phospholipase A_2 and inhibits PKC, Na^+-K^+ ATPase and Ca^{2+}/CaM-dependent protein kinase (Raynor *et al.*, 1991). One study reports MP activation of phosphoinositide-specific PLC (Okano *et al.*, 1985) while another cites MP inhibition of PI-specific PLC activity (Drøbak and Watkins, 1994). MP also intercalates in the lipid bilayer of liposomes and binds to CaM with a high affinity (Kd = 0.3 nM). Furthermore, high concentrations of amphipathic polypeptides such as MP are cytolytic. Hence, MP's cellular mode of action may reflect more than one site of action.

2.3.2. Mastoparan stimulation of phosphoinositide signal transduction

MP has been implicated in PI signal transduction presumably via G protein activation. Application of 13.5 μM MP to rat peritoneal mast cells caused secretion of histamine within 5 s (Okano *et al.*, 1985). In addition, transient breakdown of [^{32}P] PIP_2 and transient production of [^{3}H] IP_3 were measured after 10 s in [^{32}P]-orthophosphate-prelabeled cells and [^{3}H]-inositol-prelabeled cells, respectively. However, if PI signal transduction leads to histamine release, an increase in IP_3 would be expected to precede the cellular response. However, overall these data suggest that PI metabolism is involved, in some capacity, in mast cell secretion.

MP appears to invoke PI signal transduction in plants also. Blue light and

darkness cause IP_3 increases that lead to the opening and closure of K^+ channels, in *Samanea saman* pulvinar extensor and flexor protoplasts, respectively (Kim *et al.*, 1996). Similarly, 10 μM MP causes IP_3 increases and regulates K^+ channel opening and closure at the appropriate times in the appropriate cell types. A blue-light-activated G protein has been demonstrated previously (Warpeha *et al.*, 1991). These data implicate G protein activation and PLC-catalyzed production of IP_3 in the regulation of K^+ fluxes in response to blue light and darkness in these cells.

Enhanced PLC activity has also been measured in wheat root microsomes in response to 25 μM MP (Jones and Kochian, 1995). In carrot cells labelled with [^{3}H] inositol, greater than 70% of radiolabelled PIP and PIP_2 was lost in response to 10 or 25 μM MP or Mas7, an active MP analogue (Cho *et al.*, 1995). Losses occurred in less than one minute. Three- to 4-fold increases in IP_2 and IP_3 were measured simultaneously. Mas17, the inactive analogue, had no effect on PIP_2 hydrolysis *in vivo*. Although Mas7 was able to stimulate PLC activity *in vivo*, it did not stimulate PLC in isolated plasma membranes. In fact, concentrations of Mas7 greater than 10 μM inhibited PLC activity *in vitro*. These data suggest that an important membrane component was lost in the isolation process. In another study utilizing cultured carrot cells, MP stimulated a rapid increase in IP_3 levels in a dose-dependent manner (Drøbak and Watkins, 1994). Maximal IP_3 was observed within 2-4 minutes in response to 24 μM MP.

Mas7 microinjected into staminal hairs of *Setcreasea purpurea* induced an increase in Ca^{2+} (visualized by calcium green dextran 10,000) and closure of plasmodesmata (Tucker and Boss, 1996). Both effects were transient and were not

inducible by Mas17. IP_3 microinjection caused the same effects. Collectively, the data support the role of MP (at concentrations between 10 and 25 μM) as a G protein activator and stimulator of PI signal transduction in intact plant cells.

2.4. The hypersensitive response

2.4.1. Background of plant defense

Plants are exposed regularly to potentially pathogenic microorganisms and yet remain uninfected the majority of the time (Boller, 1989). This is due to the fact that plant cells have a highly complex and effective array of defense techniques. In fact, in contrast to mammalian systems in which only certain cells are responsible for the defense of the organism, every plant cell is equipped for pathogen resistance with both constitutive and inducible defenses. Most inducible biochemical defenses require transcriptional activation of plant defense genes. Some plant defense mechanisms reinforce barriers to invasion while other "defenses" seem to be aimed at destroying the invader. Examples of inducible defenses include the formation of antimicrobial compounds called phytoalexins, the induction of lytic enzymes like chitinases and glucanases, the fortification of the cell wall by production of hydroxyproline-rich glycoproteins (Boller, 1989; Scheel and Parker, 1990). A notable inducible defense is the hypersensitive response (HR), that is, necrosis of cells in the area of pathogen infection. The HR may serve to prevent the spread of the pathogen by limiting the availability of nutrients to biotrophic pathogens.

Plant resistance mechanisms are evoked primarily in response to endogenous (plant-derived) or exogenous (pathogen-derived) molecules called elicitors (Boller, 1989). Originally, the term elicitor referred to compounds that induced phytoalexin biosynthesis but now it is applied to any substance that elicits a general defense response (Scheel and Parker, 1990).

The gene-for-gene hypothesis proposed by Flor (1942) predicts the molecular basis for plant resistance against pathogens. According to Flor, a defense response is initiated when a pathogen expressing the product of an avirulence (*avr*) gene is recognized by a plant expressing the product of a reciprocal resistance (R) gene. Plant defense mechanisms (like the HR) keep the pathogen in check and infection does not occur.

Presumably, R genes code for a specific receptor and *avr* genes encode some type of elicitor (Dong, 1995). Sequence analysis of an R gene cloned from tomato shows that the putative receptor contains a serine/threonine protein kinase domain. This piece of evidence indicates a role for signal transduction in the elicitation of plant defense responses.

A biochemical interpretation of the gene-for-gene hypothesis was expressed by Knogge (1996) as "the interaction of a race-specific pathogen elicitor with either a cultivar-specific plant receptor or alternatively with a cultivar-specific signal transduction compound." Thus, triggering of resistance mechanisms requires race- and cultivar-specificity.

2.4.2. Characteristics of the hypersensitive response

Many reports on the nature of the hypersensitive response indicate that components of the response include:

-Ca^{2+}, K^{+}, and anion fluxes

-changes in external pH

-perturbed membrane potential

-production of active oxygen species

-cell death

Each of these HR components will be discussed with respect to the current model as

well as to their relevant interactions with the other components.

2.4.2.1. Ion fluxes

Ion fluxes in the HR have been established as rapidly occurring events (Smith, 1996). Most commonly reported are Ca^{2+} influx and changed H^+ translocation, often accompanied by K^+ and anion effluxes. Resulting depolarization of the plasma membrane was often observed, although in one case, elicitor-induced hyperpolarization was observed (Gelli and Blumwald, 1996).

It is difficult to distinguish channel-mediated ion fluxes and ion fluxes due to the disruption of the plasma membrane. Each are driven by established gradients. While ion flow through channel proteins is driven by an electrochemical gradient, electrolyte leakage is driven only by concentration gradients. Electrolyte leakage is commonly assayed with a conductivity bridge. As electrolytes leak from disrupted cells, the conductivity of the cell medium increases. Electrolyte leakage due to the loss of plasma membrane integrity would result in the same fluxes (Ca^{2+} influx, K^+ and anion effluxes) as are mediated by passive diffusion through open ion channels.

2.4.2.1.1. Ca^{2+} influx

Many reports demonstrate the requirement for external Ca^{2+} for elicitation of defense responses, including induction of defense gene transcription, phytoalexin formation and accumulation of extracellular H_2O_2 (Boller, 1989; Scheel and Parker, 1990; Schwacke and Hager, 1992; Ebel and Cosio, 1994; Salzer, 1996). Often measurements of Ca^{2+} influx are accompanied by almost concurrent K^+ efflux, H^+

influx and anion (usually Cl^-) efflux (Ebel and Cosio, 1994; Benhamou, 1996; Dangl *et al.*, 1996; Nürnberger *et al.*, 1997). Although ion fluxes are known to be some of the earliest responses, occurring within seconds of elicitor application, the order and the triggering mechanisms for each of these ion fluxes are not well established and may differ in different systems.

The mechanism of Ca^{2+} influx is likely due to the opening of Ca^{2+} channels in the plasma membrane. For example, in cultured tomato cells at least, elicitor-induced hyperpolarization of the plasma membrane causes the opening of voltage-dependent Ca^{2+} channels (Gelli and Blumwald, 1997). The omission of external Ca^{2+} plus the presence of 1 mM EDTA eliminated cell death in a putative hypersensitive response in asparagus mesophyll cells as well as reducing the extent of medium alkalinization (Wong, 1997). However, the lack of external Ca^{2+} was unable to inhibit O_2 uptake, an indirect measurement of the oxidative burst. Ca^{2+} influx from internal stores may be necessary to invoke this component of the HR. It is not clear if Ca^{2+} release from internal stores plays a significant role in the elicitation of the HR.

The function of the often rapid and transient influx of Ca^{2+} has not been established. Its role may be two-fold. In addition to activating Ca^{2+} target proteins, influx contributes to the depolarization of the plasma membrane which may trigger other events.

Another complicating factor is the Ca^{2+} influx induced by active oxygen species which are typically understood to be formed downstream of Ca^{2+} influx in the defense pathway (Levine *et al.*, 1994, 1996). H_2O_2 application to transgenic tobacco

seedlings expressing aequorin resulted in an elevation in cytosolic Ca^{2+} and a reduction in superoxide dismutase (SOD) activity (Price *et al.*, 1994). The Ca^{2+} channel blocker La^{3+} inhibited this reduction in SOD activity, suggesting that external Ca^{2+} influx is involved in the response. In addition, the plant plasmalemma Ca^{2+}-ATPase is highly sensitive to oxidative stress (Price *et al.*, 1996). Inhibition of the Ca^{2+}-ATPase by active oxygen species would also cause an increased cytosolic Ca^{2+} concentration. Delayed cytosolic Ca^{2+} increases support the involvement of alternate or feedback pathways in Ca^{2+} signaling in defense elicitation. This correlates with recent evidence demonstrating that time-dependent oscillations and waves of Ca^{2+} are a part of the highly complex manner in which Ca^{2+} acts as a second messenger (Trewavas *et al.*, 1996).

2.4.2.1.2. K^+ efflux

A change in plant cell plasma membrane permeability to K^+ ions has been documented in the current literature (Mathieu *et al.*, 1991; Bach *et al.*, 1993; Ebel and Cosio, 1994; Benhamou, 1996; Salzer *et al.*, 1996; Nürnberger *et al.*, 1997). Typically, K^+ efflux from cells has been reported.

In elicited tobacco cells (Mathieu *et al.*, 1991) and elicited carrot protoplasts (Bach *et al.*, 1993), rapid K^+ efflux concomitant with Ca^{2+} influx occurred. It is possible that K^+ efflux serves a function in the regulation of the membrane potential. Mathieu and colleagues (1991) have suggested that depolarization may induce K^+

efflux, perhaps by opening voltage-gated plasma-membrane K^+ channels. In this way, K^+ efflux may serve to compensate for other ion fluxes (like Ca^{2+} influx) which lead to depolarization. However, the possibility remains that a component of K^+ efflux results from membrane disintegration.

2.4.2.1.3. Anion efflux

Anion efflux is often mentioned in the context of the aforementioned elicitor-generated ion fluxes (Ebel and Cosio, 1994; Benhamou, 1996; Dangl *et al.*, 1996; Salzer *et al.*, 1996; Nürnberger *et al.*, 1997). Information regarding the significance of anion (usually Cl^- ion) efflux is even more limited than information on the significance of K^+ efflux. Schroeder and Hagiwara (1989) and Hedrich and colleagues (1990) both demonstrated that increases in cytosolic Ca^{2+} activate voltage-dependent anion channels in guard cells. The opening of anion channels most likely facilitates anion efflux and anion channel opening in the HR may be sensitive to depolarization resulting from rapid Ca^{2+} influx. Using anion channel blockers, it was found that phytoalexin synthesis, the production of active oxygen species, and defense gene transcription are dependent on anion efflux (Dangl *et al.*, 1996).

2.4.2.2. Changes in external pH

Typically, fungal elicitation of plant cells has resulted in the alkalinization of the external medium (Boller, 1989; Mathieu *et al.*, 1991; Felix *et al.*, 1993; Ebel and Cosio, 1994; Granado *et al.*, 1995; Dangl *et al.*, 1996; Salzer *et al.*, 1996). Nürnberger and colleagues (1997) report that the alkalinization of the medium they observed is due to

H^+ influx. In addition to medium alkalinization, Mathieu and colleagues (1991) measured an acidification of the cytosol in tobacco cells in response to an endogenous oligogalacturonide elicitor. It is also possible that alkalinization of the cell medium may be a result of Ca^{2+}-inhibition of the plasma membrane ATPase (Kinoshita *et al.*, 1995).

In contrast, there is also evidence to support acidification of the extracellular medium of certain elicited cells. The basis for the toxicity of one *avr* gene product appears to be indirect stimulation of the plasma membrane H^+-ATPase (Wevelsiep *et al.*, 1993). However, it induces necrosis in host plants in a nonspecific manner and at concentrations higher than those normally required for elicitor activity. Thus, it is unlikely that the acidification of the medium and alkalinization of the cytosol is the physiological result of elicitation. More convincing evidence for acidification of the apoplast was provided using suspension-cultured tomato cells (Vera-Estrella *et al.*, 1994a). In this study, it was demonstrated that elicitation stimulated G-protein-mediated dephosphorylation of the plasma membrane H^+-ATPase. Dephosphorylation resulted in pump stimulation which led to acidification of the external medium and hyperpolarization of the plasma membrane. [This hyperpolarization led to plasma-membrane Ca^{2+} channel opening (see section 7.2.1.1. Ca^{2+} influx)].

Thus, although elicitor-induced pH changes in the external medium and even in the cytosol are well documented phenomena, the direction of the change and the mechanism responsible have not been clearly established. They may vary between elicitors and host plants in a complex manner typifying biological systems in general.

2.4.2.3. Perturbation of plasma membrane electrical potential

Another early event characteristic of the elicitation of plant defense including the HR is a perturbation of the resting potential of the plasma membrane, usually depolarization (Pavlovkin et al., 1986; Boller, 1989; Mathieu *et al.*, 1991; Doke *et al.*, 1996). Because a membrane potential is achieved by ion (charge) separation, membrane depolarization/hyperpolarization are inextricably linked with ion fluxes. Each of the fluxes described previously affects the magnitude of the membrane potential. In an unstressed cell, the cytosol possesses a net negative charge while the apoplast is positively charged. Thus, Ca^{2+} and H^+ influxes and anion efflux contribute to membrane depolarization, while K^+ efflux generates a higher potential (hyperpolarization).

Stomatal closure involves complex ion fluxes which lead to depolarization similar to those observed in the HR. Plasma-membrane depolarization in guard cells may result from three redundant mechanisms involving Ca^{2+} (Chasan, 1995): Ca^{2+} influx, Ca^{2+} activation of anion channels, and Ca^{2+} inhibition of the H^+-ATPase. These three mechanisms may be necessary to cause sufficient depolarization for the activation of voltage-dependent outward K^+ channels. This guard cell model explains the early ion fluxes occurring in the HR. It may be that these mechanisms are conserved between cellular responses like stomatal closure and defense responses like the HR.

Hyperpolarization of the plasma membrane due to an elicitor-stimulated H^+-ATPase in tomato cells is in conflict with data demonstrating membrane depolarization (Xing *et al.*, 1996). However, it does support the general involvement of rapid membrane potential changes in response to elicitation of plant cell defenses.

2.4.2.4. The oxidative burst

Active oxygen species (AOS) (including $O_2^{\cdot -}$, H_2O_2, $OH^{\cdot}$) are produced routinely in side reactions of metabolism. Plants possess antioxidative enzymes (superoxide dismutase, catalase, peroxidases) which normally protect the cellular environment from oxidative damage caused by these species. However, under stress conditions (for example, imminent pathogen infection), antioxidant protective mechanisms are overridden by the unusually rapid formation of high levels of active oxygen species. This is known as the oxidative burst (Sutherland, 1991; Mehdy, 1994, 1996; Bolwell *et al.*, 1995; Doke, 1996; Hammond-Kosack and Jones, 1996).

The oxidative burst has been the focus of much interest for over a decade. It is characterized by increased O_2 uptake (Robertson *et al.*, 1995; Bolwell *et al.*, 1995; Smith, 1996) and the accumulation of the various AOS (Sutherland, 1991; Legendre *et al.*, 1993a, 1993b; Foyer *et al.*, 1994; Low and Merida, 1996). The oxidative burst has been observed in various species of monocotyledonous and dicotyledonous plants in response to fungal, bacterial and viral pathogens (Mehdy, 1996). In addition, it has been demonstrated to be a critical factor in the HR (Doke, 1983). Although the oxidative burst is typically denoted as an early response to pathogen attack, occurring within seconds (Legendre *et al.*, 1992) and minutes (Kauss and Jeblick, 1995; Nürnberger *et al.*, 1997), the formation of AOS has been reported as late as 1-4 h (Doke, 1983, Levine *et al.*, 1994). Recently, a model for the oxidative burst has been proposed which includes two temporally distinct stages of AOS production, one early and the second later (Low and Merida, 1996).

Early evidence suggested that the oxidative burst was involved in a 2-phase plant response (Chai and Doke, 1987). The first step involved the formation of AOS

(specifically $O_2^{\cdot -}$) and characterized both compatible and incompatible pathogen plant reactions. In contrast, the second step was Ca^{2+}-dependent, occurred only in incompatible interactions and led to hypersensitive cell death. This model has never been conclusively established or falsified. It is not clear what allows incompatible interactions to result in the HR, what prohibits the HR in compatible plant-pathogen interactions and what the role of AOS, if any, is in uniting the two phases.

The first report of superoxide anion production as a part of the HR involved an incompatible interaction between *Phytophthora infestans* and potato tubers (Doke, 1983). Recent studies seem to indicate that some plant cells possess an NADPH oxidase that reduces molecular O_2 to $O_2^{\cdot -}$ (Auh and Murphy, 1995; Doke *et al.*, 1996; Nürnberger *et al.*, 1997). Analogies have been made between the plant oxidative burst via the putative NAD(P)H oxidase and the mammalian phagocyte NADH oxidase (Sutherland, 1991; Robertson *et al.*, 1995; Doke *et al.*, 1996; Mehdy, 1996; Low and Merida, 1996). In elicited parsley cells, inhibitors of the mammalian NADPH oxidase blocked phytoalexin formation (Jabs *et al.*, 1997). In addition, SOD inhibited phytoalexin formation in a dose-dependent manner. Superoxide rather than H_2O_2 was shown to be essential and sufficient to initiate hypersensitive cell death in *Arabidopsis* "lesion simulating disease resistance" (*lsd*) mutants (Jabs *et al.*, 1996). These data indicate an indispensable role for $O_2^{\cdot -}$ in the oxidative burst.

Other studies of the oxidative burst do not support a role for $O_2^{\cdot -}$. Bolwell and colleagues (1995) have demonstrated that in cultured French bean cells, H_2O_2 seems to be directly produced by a CN^--sensitive cell wall peroxidase. The oxidative burst in

these cells was dependent on external alkalinization to pH 7.0 - 7.2. The use of catalase, superoxide dismutase as well as hydrogen peroxide scavengers supported this hypothesis. Similarly, there is no evidence for the presence of superoxide in the oxidative burst in elicited soybean cultured cells (Levine *et al.*, 1994).

There is evidence to support a third mechanism for H_2O_2 production in plants . Plant oxalate oxidase with H_2O_2-forming ability was discovered in incompatible interactions between barley and powdery mildew (Zhang *et al.*, 1995). No consensus exists regarding the mechanism of the oxidative burst in plants.

Whatever the enzymic mechanisms producing active oxygen species, various reactions exist which allow for their interconversion. The superoxide anion, formed by the one-electron reduction of O_2 by a putative plasma membrane NADPH oxidase, may be dismutated either enzymically or nonenzymically. In aqueous solution, the superoxide anion radical exists in acid/base equilibrium with its protonated form, known as the hydroperoxyl radical $HO_2^{\cdot}$ (equation 1).

$$H^+ + O_2^{\cdot -} \text{ <---> } HO_2^{\cdot} \qquad pK_a = 4.8 \qquad (1)$$

This species may disappear by spontaneous dismutation (equation 2).

$$HO_2^{\cdot} + HO_2^{\cdot} \text{ ---> } H_2O_2 + O_2 \qquad (2)$$

The decay of $O_2^{\cdot -}$ is pH-dependent and at pH 6.5 (typical of the plant cell wall), the $t_{1/2}$ of $O_2^{\cdot -}$ is 0.5 s (Sutherland, 1991). Most aerobic cells constitutively express superoxide dismutases that convert superoxide to H_2O_2 at a rate of 10^9 $M^{-1} \cdot s^{-1}$

(equation 3). It has been postulated that removal of $O_2^{\cdot -}$ enzymically is 10^{10} times faster than spontaneous dismutation of $O_2^{\cdot -}$ (Sutherland, 1991).

$$2O_2^{\cdot -} + 2H^+ \text{ <---> } H_2O_2 + O_2 \qquad (3)$$

Superoxide and H_2O_2 undergo reactions catalyzed by Fe^{3+}, known as a metal-catalyzed Haber-Weiss reaction or a "Fenton-type" reaction (Cadenas, 1989) (equations 4-6).

a) $Fe^{3+} + O_2^{\cdot -} \text{ ---> } Fe^{2+} + O_2 \qquad (4)$

b) $Fe^{2+} + H_2O_2 \text{ ---> } Fe^{3+} + OH^{\cdot} + OH^- \qquad (5)$

overall: $O_2^{\cdot -} + H_2O_2 \text{ ---> } OH^{\cdot} + OH^- + O_2 \qquad (6)$

Specific reactivities of AOS with cellular components have been demonstrated. $O_2^{\cdot -}$ reacts with proteins possessing Fe-S_4 clusters and heme groups, while H_2O_2 oxidizes thiol groups of proteins or glutathione (Mehdy, 1994). Of all the AOS, H_2O_2 is the most toxic to photosynthesis (Kaiser, 1979; Foyer *et al.*, 1994). However, in comparison with the hydroperoxyl and hydroxyl radicals, $O_2^{\cdot -}$ and H_2O_2 are only moderately reactive. Hydroperoxyl radicals, being less polar than superoxide, are more likely to cross the lipid bilayer as does H_2O_2. Unlike $O_2^{\cdot -}$, these radicals can attack lipids directly. The result may be irreversible membrane damage and the formation of lipid peroxide signal molecules. The hydroxyl radical is exceedingly

destructive and may cause the initiation of a chain of lipid peroxidation reactions, the inactivation of enzymes and the degradation of nucleic acids (Mehdy, 1994).

The formation of AOS in incompatible plant-pathogen interactions may serve a variety of functions. AOS have been postulated to defend the host plant cell by initiating lignin polymerization reactions for cell wall reinforcement. AOS produced in response to fungal elicitation also cause crosslinking of hydroxyproline and proline glycoproteins in the cell wall also for structural fortification (Smith, 1996). Although the effect would be dependent on the sensitivitiy of the pathogen, AOS may be toxic to microbial pathogens at physiological concentrations (Smith, 1996).

The production of AOS may alter the redox balance of the cell with far-reaching effects. It has been suggested that the post-oxidative-burst cellular redox state may contribute to the stability of defense gene mRNAs (Mehdy et al., 1994) or, more speculatively, regulate redox-sensitive protein kinases and phosphatases as found in mammalian systems (Mehdy, 1996).

A large amount of evidence indicates a signalling role for AOS, specifically H_2O_2. Cytosolic Ca^{2+} increases in response to H_2O_2 have been documented in tobacco seedlings (Price *et al.*, 1994) and in *C. communis* guard cells (McAinsh *et al.*, 1996). In addition, H_2O_2 upregulates benzoic acid-2-hydrolase, an enzyme involved in the biosynthesis of salicylic acid. Salicylic acid is involved in the induction of systemic acquired resistance. The accumulation of H_2O_2 during elicitation of soybean cultured cells is essential for the stimulation of phytoalexin production (Apostol *et al.*, 1989). AOS may also coordinate the induction of defense gene expression (Levine *et al.*, 1994; Smith, 1996; Nürnberger *et al.*, 1997). H_2O_2 is produced in response to a variety of non-pathogen related stresses such as UV radiation, chilling and mechanical perturbation. Based on the above evidence, it seems likely that H_2O_2

plays a general role in the transduction of a variety of external signals as well as a specific role in the oxidative burst in plant-pathogen interactions.

2.4.2.5. Cell death

One noteworthy difference between mammalian "oxidative bursts" of phagocytes and those of hypersensitively responding plant cells is that in the plant HR, the host cell(s) die(s) (Sutherland, 1991; Low and Merida, 1996). This is adaptive, for in plants, this localized cell death is beneficial to the entire organism.

The agent of cell death is a complicated question because there seem to be multiple factors contributing to necrosis. Postulated causes of cell death include:

1. lipid peroxidation. Self-perpetuating peroxidation of lipids may lead to extensive membrane damage (Keppler and Novacky, 1987; Doke and Ohashi, 1988; Rogers *et al.*,1988; Ádám *et al.*, 1989; Peever and Higgins, 1989). Concomitant loss of electrolytes and membrane integrity may not be reparable. Although the $OH^{\cdot}$ and $HO_2^{\cdot}$ radicals seem to be the best candidates for membrane damage, H_2O_2 has also been observed to cause the death of cells as assessed with Evan's blue dye (Levine *et al.*, 1994).

2. NADPH depletion. If NADPH is the source of reducing equivalents for the production of AOS, the pool of NADPH may be rapidly exhausted, leaving the cell without a vital resource for maintaining normal cellular operations (Mehdy, 1996).

3. the cell's inability to restore steady state conditions. Large fluxes of ions down their gradients involving the loss of membrane potential diminish the cell's store of electrical energy. In addition, high levels of Ca^{2+} may not be reduced quickly enough to avoid deleterious effects of extended Ca^{2+}-stimulated activities on the cell

(Price *et al.*, 1996).

2.4.3. Signal transduction in the hypersensitive response

Certain components of the PI signal transduction pathway have been implicated in the development of a plant HR. G protein participation in the oxidative burst has been suggested on the basis of data gleaned through experiments utilizing G protein antibodies and various G protein activators (Legendre *et al.*, 1992; 1993a, 1993b). Fungal elicitors were shown to stimulate inositol phospholipid metabolism *in vivo* in cultured tobacco cells (Kamada and Muto, 1994a) and *in vitro* in pea plasma membranes (Toyoda *et al.*, 1992). Cultured spruce cells exhibit an oxidative burst that is both Ca^{2+}-dependent and phosphorylation-dependent (Schwacke and Hager, 1992). Farmer and colleagues (1991) reported that the fungal elicitor α-1,4-D-polygalacturonic acid stimulated the *in vitro* phosphorylation of a 34-kD plasma-membrane-bound protein. Kinase inhibitors, K252a and staurosporine both blocked inositol phospholipid turnover in cultured tobacco cells treated with a fungal elicitor isolated from *Phytophthora nicotianae* (Kamada and Muto, 1994b). Furthermore, Xing and colleagues (1996) showed that Ca^{2+}-dependent protein kinases were involved in the regulation of the tomato plasma membrane H^+-ATPase in an incompatible plant-pathogen interaction. Collectively, the data suggest that the elicitation of the HR by a fungal pathogen entails G proteins and the PI signal transduction pathway.

3. Materials and Methods

3.1. Materials

3.1.1. Chemicals

	Supplier
calcium sulfate	Fisher
2-(n-morpholino)ethanesulphonic acid (MES)	Sigma
Evan's blue	Sigma
monopotassium phosphate	BDH
dipotassum phosphate	Caledon
tetrapotassium pyrophosphate	Sigma
chloroform	BDH
methanol	BDH
glycerol	Mallinckrodt
gabase	Sigma
α-ketoglutaric acid (α-KG), monosodium salt	Sigma
4-aminobutyric acid (GABA)	Sigma
ß-nicotinamide adenine dinucleotide phosphate (NADP+), sodium salt	Sigma
sulfuric acid	BDH
sodium hydroxide solution	BDH
potassium chloride	BDH
mastoparan (isolated from *Vespula lewisii*)	Sigma/Bachem
Mas17	Sigma/Bachem
staurosporine	Calbiochem
n-butyric acid	Sigma
L-glutamic acid	Sigma
buffer salt, pH 6.86	Fisher Scientific
standard HCl, 0.1 N	BDH
potassium ferricyanide	BDH
luminol	Sigma
hydrogen peroxide, 30%	Caledon
potassium hydrogen carbonate	BDH

sodium dithionite	Sigma
catalase, bovine erythrocyte	Boehringer Mannheim
superoxide dismutase	Calbiochem
nigericin	Sigma

3.1.2. Plant material

Asparagus sprengeri Regel ferns were grown in a mixture of sphagnum peatmoss and vermiculite perlite (Complete Sunshine Mix, supplier: JVK, St. Catharines, ON). They received natural sunlight in a biologically controlled greenhouse (no chemical pesticides used). The plants were watered on alternate days and fertilized every two weeks in the summer and once monthly in the winter (N:P:K of 24:7:15).

3.2. Methods

3.2.1. Cell isolation

The cell isolation procedure followed was first developed and described by Colman *et al.* (1979). Three to five glossy and dark green shoots from *Asparagus sprengeri* Regel ferns were selected and cut at pot level. Their cladophylls were stripped and collected in a Buchner funnel. Following a thorough rinse with tap water to dislodge surface contaminants and debris, excess water was drained by vacuum suction. The cladophylls were sliced into 0.5 cm sections with a razor to expose the mesoderm layer. Cladophyll sections were placed into a beaker containing 100 - 150 ml of 1 mM $CaSO_4$, pH 5.5. The beaker was placed in a sealed chamber for 4 - 5 min of vacuum infiltration. This removed air from the spaces between the mesophyll cells so that when the vacuum was turned off, the cladophyll sections sank to the bottom of the beaker. The cladophyll sections were resuspended in fresh $CaSO_4$ in a mortar (just enough to cover) and a pestle was used to gently push mesophyll cells into the

medium. When the $CaSO_4$ became dark green with suspended cells, it was removed by Pasteur pipette and filtered through two layers of cheesecloth to remove larger plant particles. The filtrate was collected in 30-ml Corex tubes. Fresh medium was added to the cladophyll sections and the process was repeated until enough cells had been isolated for a particular experiment. The Corex tubes containing the cell suspension were spun in an IEC clinical centrifuge for 2 - 3 min at 550 × g. The supernatant was decanted and the cell pellet was resuspended in approximately 10 ml of fresh $CaSO_4$ per tube. The concentration of cells (in 10^6 cells/ml) was determined using a haemocytometer and a light microscope. Damage was also assessed at the same time with Evan's blue dye (see Section 3.2.2.1.).

3.2.2. Cell viability determination

Cell viability was assessed primarily with the Evan's blue dye (Kanai and Edwards, 1973; Levine *et al.*, 1994) and secondarily with fluorescein diacetate (Huang *et al.*, 1986; Withers, 1985) to provide complementary data. The Evan's blue viability test is a dye-exclusion test, i.e., intact cells exclude the dye. On the other hand, the fluorescein diacetate test is a dye-inclusion test -- fluorescein diacetate is taken up by living cells.

3.2.2.1. The Evan's blue viability test

Evan's blue dye allows one to visualize mesophyll cells that have been disrupted (Colman *et al.*, 1979) as well as protoplasts that have been broken (Kanai and Edwards, 1973). The test has been applied to cells from a large number of species from a variety of families to distinguish between "living" cells and "dead" cells (Gaff and Okong'o-ogola, 1971). Cells with broken (thus depolarized) plasmalemmas

take up the negatively charged dye [Figure 5.1(A)] and appear blue, while intact cells appear green under a light microscope.

Fifty μl of 2.5% Evan's blue dye (Colman *et al.*, 1979) was mixed with about 1 ml of cell suspension. After 20 min of incubation under ambient conditions, the percentage of blue cells in each suspension was assessed in a counting chamber under a light microscope. Twenty or forty secondary squares were normally counted with a minimum of 100 cells being observed. The total number of blue cells was divided by the total number of cells to give a percentage of nonviable cells. Cell suspensions having greater than 25% nonviable cells were not used for experiments.

3.2.2.2. The fluorescein diacetate viability test

Fluorescein fluoresces yellow-green light when irradiated with UV light. Fluorescein diacetate (FDA) [Figure 5.1(B)] is a nonfluorescent diester that fluoresces yellow-green when the acetate groups are removed. The plasma membrane is permeable to FDA and in viable cells, esterases cleave the diacetate, leaving the non-permeant, anionic, fluorescent fluorescein "trapped" in the cytosol. In nonviable cells, fluorescein is not retained in the cytosol (Rotman and Papermaster, 1966).

FDA tests of were always employed in conjunction with Evan's blue. One hundred μl of refrigerated FDA stock solution (0.5% (w/v) FDA in acetone) was diluted with 5 ml of the suspension medium (5 mM MES, 1 mM $CaSO_4$, pH 6.0). The diluted FDA was kept on ice and used within one hour. One drop of cell suspension incubated with Evan's blue was placed on a slide and then a drop of diluted FDA on top of this. A cover slip was then carefully placed on top of this. The slide was immediately viewed under the bright field of a Wild Leitz fluorescent microscope (with attached camera) to observe blue cells and to locate areas with a random distribution of cells. After a 2 - 5 min development period healthy cells were observed, fluorescing

yellow-green under UV illumination. Non-fluorescent (nonviable) cells were still observable due to faint autofluorescence. Counting of cells and assessment of damage could not be conducted as normally done with Evan's blue because secondary squares of the haemocytometer could not be observed under dark field and also FDA fluorescence is short-lived due to photobleaching. To acquire qualitative and quantitative data regarding the complementarity of the two vital stains, photographs were taken of the same fields of view under both bright and dark fields, slides were developed and cells counted from the slides. Kodak EKTACHROME Elite 400 film was used to produce the colour slides.

3.2.3. Cell incubations

A. sprengeri mesophyll cells were isolated, suspended in 1 mM $CaSO_4$, pH 5.5 and counted (including damage assessment) as described in Section 3.2.1. Twenty million cells were centrifuged at 550 × g for 2 - 3 min and the supernatant was discarded. The cell pellet was resuspended in 5 ml 5 mM MES, 1 mM $CaSO_4$ pH 6.0. (For some experiments, a smaller volume of cell suspension was used and for other experiments, a less concentrated cell suspension was used). This suspension was preincubated at 22°C for 5 min with gentle stirring with a magnetic stirring bar (usually 3 mm × 1mm). At incubation time 0, various volumes of chemicals were added to achieve the desired final concentrations. Cold shock (transfer of suspension into a beaker of ice at 1°C) was also applied at time 0. Appropriate solvent additions were made to the control suspensions. Incubation and gentle stirring continued for 16 min (Allen, 1995) after which the suspensions were centrifuged for 2 - 3 min at 550 × g. All concentrations quoted in the Results section are final concentrations after dilution with

the cell medium.

3.2.4. Extraction of intracellular and extracellular GABA

Intracellular and extracellular GABA was extracted according to the procedure outlined by Crawford *et al.* (1994). At the end of the incubation period, the cell suspension was spun immediately for five minutes at 800 × g. The supernatant was the cell-free medium and contained the extracellular fraction of GABA. It was decanted and set aside to be dried down later.

Two and a half ml of hot methanol was added to the cell pellet. The tube was stoppered and shaken vigorously and intermittently. After 30 min, the tubes were centrifuged for five min at 1950 × g. The supernatant was decanted into a clean tube to which 5 ml of chloroform had been added. The pellet was discarded. After 20 min of intermittent shaking of the methanol/chloroform mixture, 2.5 ml of distilled water was added. Intermittent shaking continued for 15 more min. Then the tubes were centrifuged at 2800 × g for 10 min in order to separate the higher density organic phase from the lower density aqueous phase. The aqueous phase contained the intracellular GABA fraction. Four of the five ml of the aqueous phase were transferred to a clean tube to be dried down in a heated water bath under a stream of air. Thus, determination of the GABA in the residue in the tube would account for four fifths of the GABA present in the cells.

3.2.5. GABA determination

GABA was determined using a commercially available coupled-enzyme assay system known as Gabase (Sigma, St. Louis, MO) as described by Crawford *et al.* (1994). The assay is based on two reactions:

i) GABA + α-ketoglutarate --> L-glutamate + succinic semialdehyde

ii) succinic semialdehyde + $NADP^+$ --> succinate + NADPH

The first reaction is catalyzed by GABA: glutamate transaminase and the second by succinic semialdehyde dehydrogenase. NADPH absorbs 340 nm radiation and the conversion of $NADP^+$ to NADPH can be determined spectrophotometrically. In this way, unknown GABA samples can be determined by measuring the change in absorbance at 340 nm (ΔA_{340}).

Lyophilized sample GABA was dissolved in 500 μl of 0.1 M potassium pyrophosphate buffer, pH 8.6 by vortexing. Samples were transferred to microcentrifuge tubes and were spun in a Fisher microcentrifuge (Model 235B) for about 1 min at 10,000 - 15,000 × g to pellet any residual particulate material that might interfere with the spectrophotometric assay.

Plastic disposable one-millilitre cuvettes were used for the assay. The contents of each cuvette included:

650 μl 0.1 M potassium pyrophosphate buffer, pH 8.6

150 μl 0.04 M $NADP^+$, pH 7.0

50 μl gabase (reconstituted according to supplier's instructions)

100 μl GABA sample

Initial absorbance at 340 nm was read using a Beckman DU-50 spectrophotometer. Then 50 μl of 0.02 M α-ketoglutarate, pH 7.9 was added to trigger the reaction. The time course of the reaction was followed until absorbance no longer increased (usually 30 - 45 min), indicating that the limiting reagent, GABA, had been used up.

A calibration graph was prepared by measuring the ΔA_{340} spectrophotometrically with known amounts of GABA (see Appendix I). A linear relationship was found to exist between ΔA_{340} and 0 - 20 nanomoles of GABA per cuvette. Using the equation for the standard curve/line and the ΔA_{340} from the assay, unknown GABA quantities were able to be determined. GABA levels were expressed in nanomoles per million cells.

3.2.6. PAM fluorometer measurements

Changes in chlorophyll *a* fluorescence emission and oxygen levels were monitored simultaneously with a pulse-amplitude modulated (PAM) fluorometer (PAM 101 Chlorophyll Fluorometer, H. Walz, Effeltrich, FRG) (Schreiber *et al.*, 1986). Isolated *A. sprengeri* mesophyll cells were resuspended in 5 mM MES, 1 mM $CaSO_4$, pH 6.0. Two ml of the cell suspension was added to an oxygen electrode chamber (model DW1, Hansatech, Norfolk, UK) which rested on a stirring plate. The chamber was connected to a circulating water bath (RM6 and RMS Lauda) and an oxygen probe power supply (Armaco UM-2). The power supply (adjusted to about 65 μA) was also connected to a 486 IBM clone. The temperature of the water bath was set to 25°C. The cells were stirred with a magnetic stir bar to uniformly distribute the dissolved oxygen for accurate measurement.

Three light sources were set up around the oxygen electrode chamber. Two of these, the pulsed light source (a light-emitting diode) and the saturating flash source were supplied to the cells by fibreoptics and were controlled by the PAM control unit. The other light source, a halogen lamp, was adjusted to provide light with an intensity of 400 $\mu E \cdot m^{-2} \cdot s^{-1}$ to the cells. This light was called actinic light (AL) because its

purpose was to drive photosynthesis. The pulsed light, also known as the measuring beam, illuminated the cells at a frequency of 1.6 KHz at a low intensity (approximately 0.02 $\mu E \cdot m^{-2} \cdot s^{-1}$). This weak pulse was not sufficient to drive photosynthesis but could evoke fluorescence emission which was measured and recorded on the computer. The saturating flash delivered 6,000 $\mu E \cdot m^{-2} \cdot s^{-1}$ for 500 ms. The interval between flashes was 30 s. The IBM clone was equipped with custom software for displaying and manipulating fluorescence and oxygen data (Electronics Shop, Brock University). Data were accumulated at the rate of 5 points per s.

Before each experiment, 10 μl of 100 mM $KHCO_3$ (final concentration 500 μM) was added to the cell suspension to prevent the cells from depleting the carbon available for photosynthesis. The oxygen electrode chamber was covered with a black cloth. After a 5 min period of dark adaptation, the measuring beam (MB) was turned on and background fluorescence, F_o, was measured (Figure 3.1). This point defines time 0. The F_o fluorescence level represents a situation in which all PSII reaction centres are "open," that is, Q_A, the primary electron acceptor of PSII, is oxidized (Schreiber *et al.*, 1986). The cells were still essentially in the dark and the oxygen concentration was slowly decreasing due to respiration. After respiration and a baseline fluorescence measurement were established, regular saturating flashes (SF) were introduced (Figure 3.1). Because these flashes saturated photosystem II for 500 ms, maximal fluorescence (F_m) was given off. F_m represents a situation in which all the PSII reaction centres are "closed," that is, Q_A is reduced (Schreiber *et al.*, 1986). Thus, every 30 s, when a saturating flash was applied to the cells, a spike of fluorescence was observed. This change in fluorescence is called the variable fluorescence ($F_v = F_m - F_o$). Because these flashes were so short, there was no

Figure 3.1: Sample of Pulse-Amplitude Modulated Chlorophyll *a* Fluorescence Yield and O_2 Measurements from a Suspension of Isolated Asparagus Mesophyll Cells

(MB = measuring beam; Fo = background fluorescence; Fv = variable fluorescence; Fm = maximal fluorescence; SF = saturating flash; AL = actinic light).

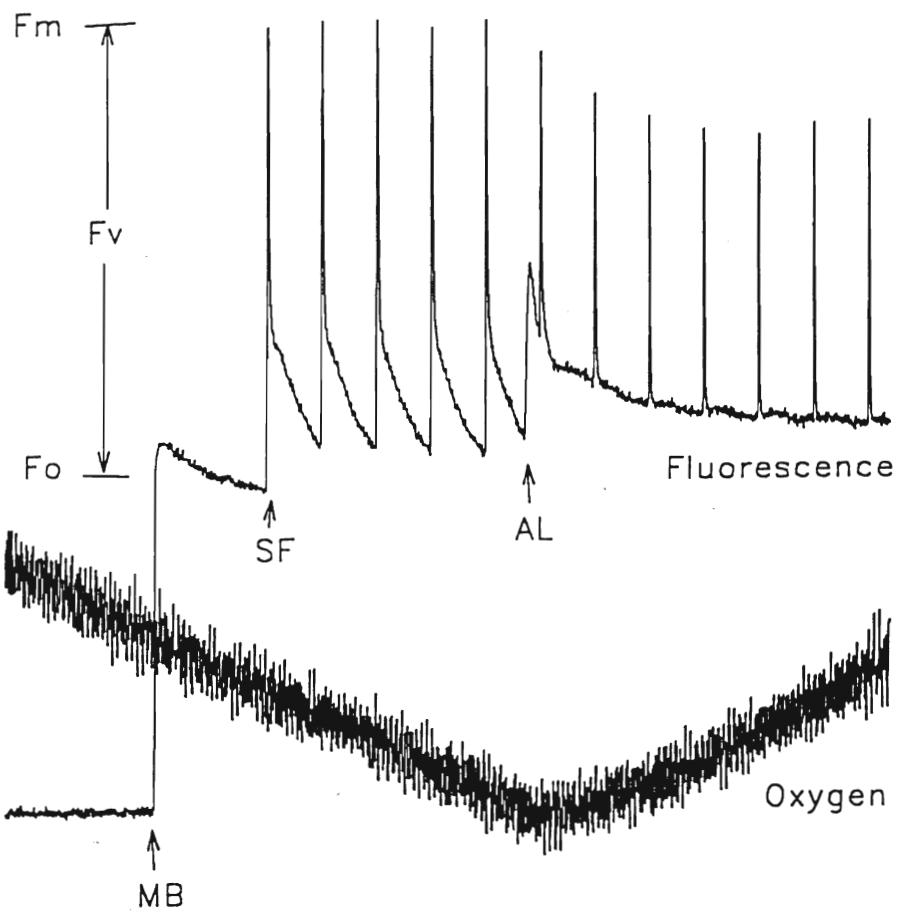

observable increase in the oxygen concentration. After approximately 3 saturating flashes, the actinic light (AL) was turned on, simultaneous with the removal of the black cloth (Figure 3.1). Fluorescence increased suddenly and then diminished to a steady state level over approximately 2 min. Oxygen levels began to rise due to photosynthetic oxygen evolution. Once fluorescence reached a steady level, the chemical of interest was added to the cell suspension. Fluorescence and oxygen measurements were continued until they stopped changing. Photochemistry is one source of chlorophyll fluorescence quenching (Schreiber *et al.*, 1986). Photochemical quenching, q_P, at any given point in time, is equal to the ratio of Fv/Fm, where F_m is the maximal fluorescence level *at that particular point in time.* An increase in photochemical quenching denotes an oxidation of Q_A, while a decrease in photochemical quenching indicates reduction of Q_A. Decreases in fluorescence levels evoked by saturating flashes (F_m) represent increases in *non*photochemical quenching (q_N) because at this point, all Q_A molecules have been saturated with electrons (Schreiber *et al.*, 1986).

Each day a PAM experiment was conducted, the oxygen electrode was calibrated. Water was saturated with air by bubbling with a transfer pipette and the oxygen level was measured. A spatula-tip of sodium dithionite crystals was added and immediately, the oxygen level plummeted. All of the dissolved oxygen was consumed in the following reaction.

$$Na_2S_2O_4 + O_2 + H_2O \text{ ---> } NaHSO_4 + NaHSO_3$$

Because air-saturated water at 25°C contains 253 μM O_2 (DW1 DW2/2 manual, Hansatech, Norfolk, UK), the difference in the oxygen level due to the dithionite addition can be equated to 253 μM O_2. In this way, changes in experimental O_2 levels were converted to μM O_2. Given the volume of the cell suspension, moles of oxygen

evolved could be calculated. Rates of O_2 consumption were calculated (Section 4.10. and Table 4.1) using a value of 0.042 mg chl/10^6 asparagus mesophyll cells (Bown, 1982). O_2 consumption rates were expressed in units of μmol O_2/mg chl/hr.

3.2.7. Alkalinization of the medium

Alkalinization measurements were carried out following a procedure similar to those outlined by Bown and Crawford (1988) and Felix *et al.* (1993). A PHM 64 research pH meter was connected to a REC 61 Servograph (both Radiometer Copenhagen). The pH electrode was calibrated with a standard buffer at pH 6.86. Isolated *A. sprengeri* mesophyll cells were resuspended in 3 ml of 1 mM MES, 1 mM $CaSO_4$ or 3 ml of 1 mM $CaSO_4$ alone. The cell suspension was placed into a water-jacketed incubation chamber and the pH electrode was submerged in it. (A Heto circulating water bath system (Denmark) had been turned on in advance and was heated to 25°C). The cell suspension was stirred gently on a Corning PC-351 hot plate-stirrer. The pH was adjusted to between 4.9 and 5.1 with dilute H_2SO_4 and a stiff black cloth was draped over the apparatus carefully to eliminate light. After establishing a constant pH value on the recorder, the chemical of interest was added with a Hamilton syringe under the black cloth. pH measurements were continued until the pH stopped changing.

At this point, a back-titration was carried out to define the number of protons involved in the alkalinization of the medium. Aliquots of 0.1 N HCl were added and the moles of H^+ involved in the alkalinization were calculated. This information is more definitive than simply measuring the change in pH because it takes into consideration the buffering capacity of the system. The alkalinization was expressed as nanomoles $H^+/10^6$ cells.

3.2.8. Hydrogen peroxide determination

Hydrogen peroxide in the medium of isolated *A. sprengeri* mesophyll cells was determined by a chemiluminescent assay based on the ferricyanide-catalyzed oxidation of luminol (Warm and Laties, 1982; Schwacke and Hager, 1992). One millilitre of cell suspension (containing 4×10^6 cells) was transferred to an Eppendorf tube and was centrifuged for approximately 30 s (including acceleration and deceleration times) in a Fisher microcentrifuge (model 235B) at 13,600 × g. One hundred µl of the cell-free supernatant was added to a polystyrene disposable 3.4-ml cuvette (Clinicon, 2174-086) containing 750 µl of 50 mM KP_i buffer, pH 7.9 and 50 µl of 1.1 mM luminol (in KP_i buffer). After mixing, background chemiluminescence (CL) was measured with an LKB Wallac luminometer (model 1250, Pharmacia). Transfer to mixing took approximately 1.5 min. The reaction was triggered by the addition of 100 µl of 14 mM $K_3Fe(CN)_6$ (freshly prepared in H_20). CL was measured and the maximum signal (in mV) was recorded. Background CL was subtracted from maximum CL to give a net CL measurement.

In order to convert CL measurements in mV to hydrogen peroxide concentration, a calibration curve was prepared with H_2O_2 solutions ranging in concentration from 1×10^{-4} to 2.5×10^{-7} M (Figure 3.2). The method described was not capable of measuring H_2O_2 concentrations lower than 2.5×10^{-7} M. In addition, on the day of each experiment, standard H_2O_2 solutions were freshly prepared and CL measured for several H_2O_2 concentrations that fell within the range of the calibration curve. This helped to confirm the integrity of the stock solutions and the relevance of the calibration curve.

Figure 3.2: H_2O_2 Calibration Curve

30% (9.79 M) H_2O_2 was diluted with distilled water to give 3%, 0.03% and 0.003% H_2O_2 solutions. Aliquots of these solutions were added to cuvettes containing 748 - 840 μl of 50 mM KP_i buffer, pH 7.9 and 50 μl of luminol (1.1 mM in 50 mM KP_i, pH 7.9). The oxidation of luminol was triggered by the addition of 100 μl of 14 mM $K_3Fe(CN)_6$. Final concentrations of H_2O_2 ranged from 1×10^{-4} M to 2.5×10^{-7} M. Chemiluminescence was measured (see Section 3.2.9. Hydrogen peroxide determination) and net mV signals were plotted against H_2O_2 concentration. Each point represents the mean of three experiments.

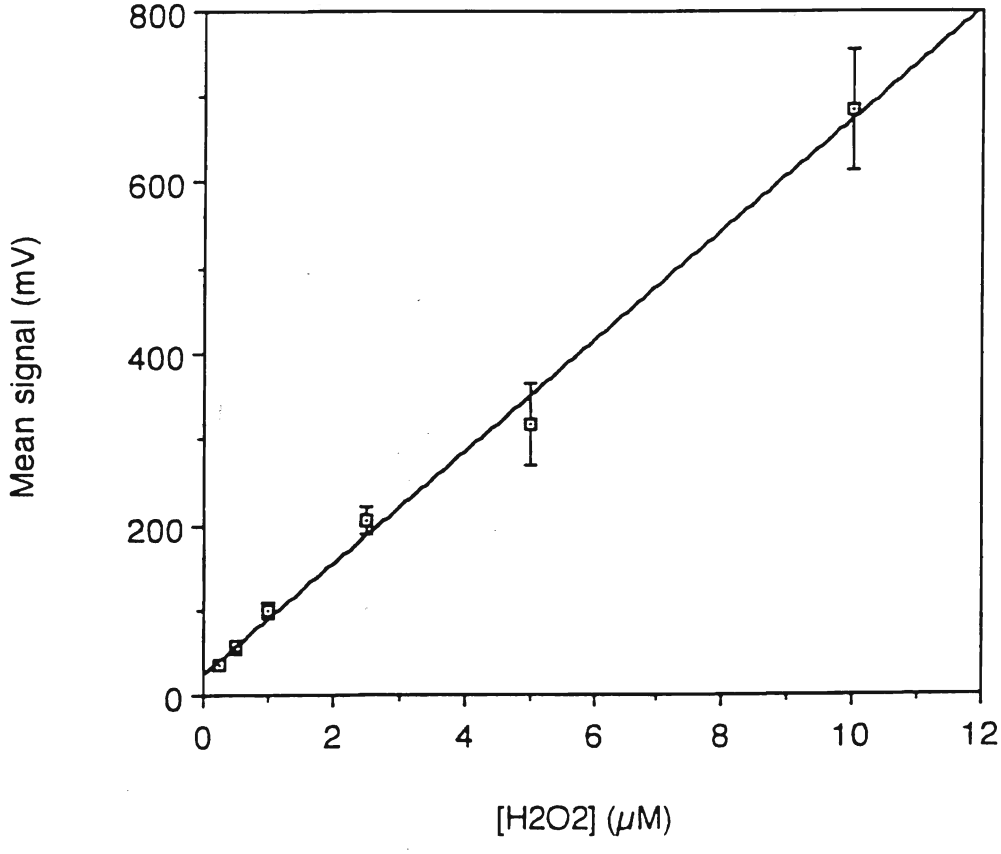

4. Results

4.1. Intracellular and extracellular GABA accumulation in response to mastoparan and Mas17

After incubating 20×10^6 cells with either 25 μM mastoparan (MP) or 25 μM Mas17 for 16 min, GABA levels inside and outside the cell were determined. GABA assays were run in duplicate for each of the experiments. GABA levels are shown in Figure 4.1. According to the Wilcoxon rank sum test, the probability that total (intra- plus extracellular) GABA levels in response to MP do not differ significantly from control total GABA levels is 0.05. Total GABA levels in response to Mas17 are not significantly different from control levels. In addition, Wilcoxon rank sum analysis of intracellular GABA and extracellular GABA indicates that there is a significantly higher % of the total GABA outside the cells treated with MP (82.6 ± 6.6%; standard error, n = 6) than there is outside of control cells (44.6 ± 7.7%, n = 6) or those treated with the inactive MP analogue, Mas17 (39.7 ± 14.0%, n = 3) (P = 0.05).

Figure 4.1: Intracellular and Extracellular GABA Accumulation in Response to Mastoparan and Mas17

Three batches of 20×10^6 cells were each resuspended in 5 ml of 5 mM MES, 1 mM $CaSO_4$, pH 6.0. Twenty-five μM MP and 25 μM Mas17 were added to 2 cell suspensions, respectively. No additions were made to the control suspension. After a 16-min incubation period, intracellular and extracellular GABA was extracted and determined with the gabase assay. GABA values shown represent the mean of 6 (MP) and 3 (Mas17) experiments. Standard error bars are included.

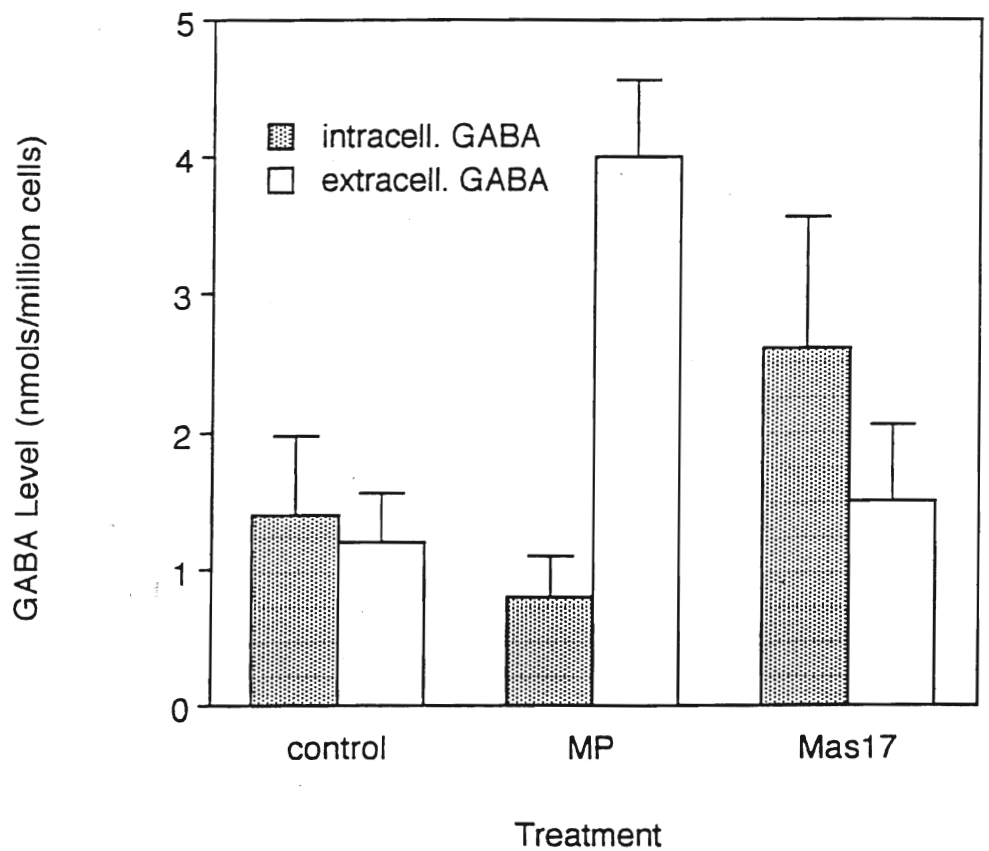

4.2. Cell Viability in Response to Treatments Stimulating GABA Accumulation

Suspensions of 20×10^6 cells were incubated for 16 min with various treatments previously shown to stimulate GABA accumulation in asparagus mesophyll cells. These treatments include MP (Mas17 control), arachidonic acid, butyrate, L-glutamate, abscisic acid and cold temperature shock (1°C). After a 16-min incubation, cell viability was assessed with Evan's blue dye. Cell viability data is expressed as % of nonviable cells. Only MP and AA caused an increase in the % of nonviable cells as compared to the control. The Wilcoxon rank sum test indicates that the probability of both MP-reduced viability and AA-reduced viability not being significantly different from control viability is 0.05.

Figure 4.2: Cell Viability in Response to Treatments Stimulating GABA Accumulation

Eight batches of 20×10^6 cells were resuspended in 5 ml of 5 mM MES, 1 mM $CaSO_4$, pH 6.0. Each batch was incubated for 36 min with one of the seven treatments applied [25 μM MP, 25 μM Mas17, 2.8 mM arachidonic acid, 5 mM butyrate, 5 mM L-glutamate, 100 μM abscisic acid, cold shock (1°C)]. No additions were made to the control suspension. Evan's blue dye was added after the first 16 min of incubation. Cell viability was assessed under a light microscope following incubation. Percent viability values represent the mean of at least 3 experiments (exceptions: control, MP and butyrate where n = 17, 6 and 4, respectively). Standard errors bars are shown.

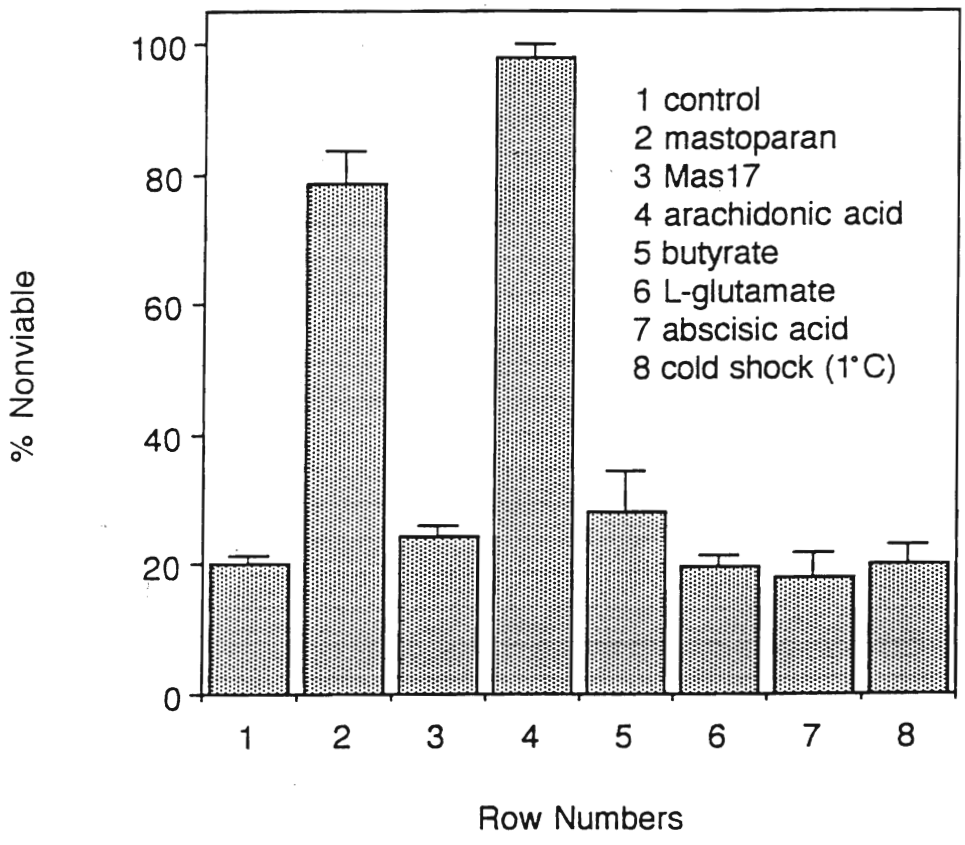

4.3. Cell viability assayed with Evan's blue dye and fluorescein diacetate

Suspensions of 10×10^6 cells were incubated for 16 min with or without MP. In order to confirm cell viability determinations with Evan's blue dye, cell viability was assessed with Evan's blue in conjunction with fluorescein diacetate. Photographs were taken of the same cells under bright and dark fields in order to confirm the complementarity of the 2 tests. The Evan's blue and fluorescein diacetate viability tests identified the same cells as nonviable (Figure 4.3a) and gave the same percentage of nonviable cells (Figure 4.3b).

Figure 4.3a: Individual Cell Viability Assayed with Evan's Blue Dye and Fluorescein Diacetate

Two batches of 10×10^6 cells were resuspended in 5 mM MES, 1 mM $CaSO_4$, pH 6.0. These suspensions were incubated for 16 min with and without 25 μM MP, respectively. Cells were then incubated with fluorescein diacetate in conjunction with Evan's blue. Seven pairs of photographs were taken of the same fields of view under both bright and dark fields. These four photographs represent control cells under (A) bright and (B) dark fields; and MP-treated cells under (C) bright and (D) dark fields.

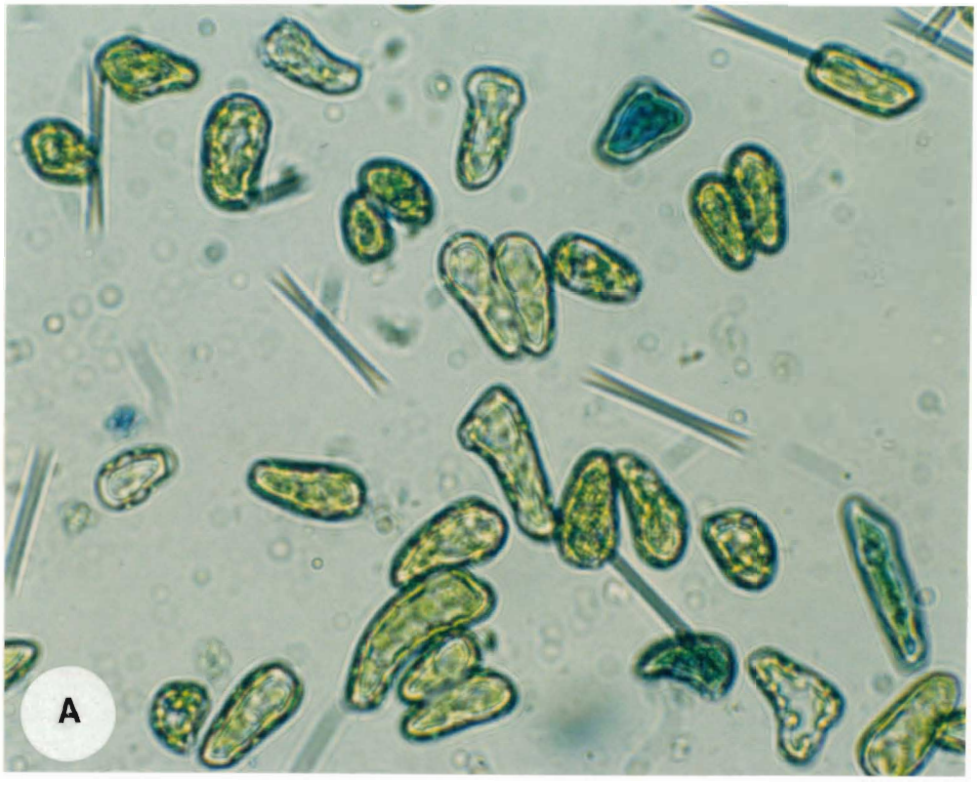
A

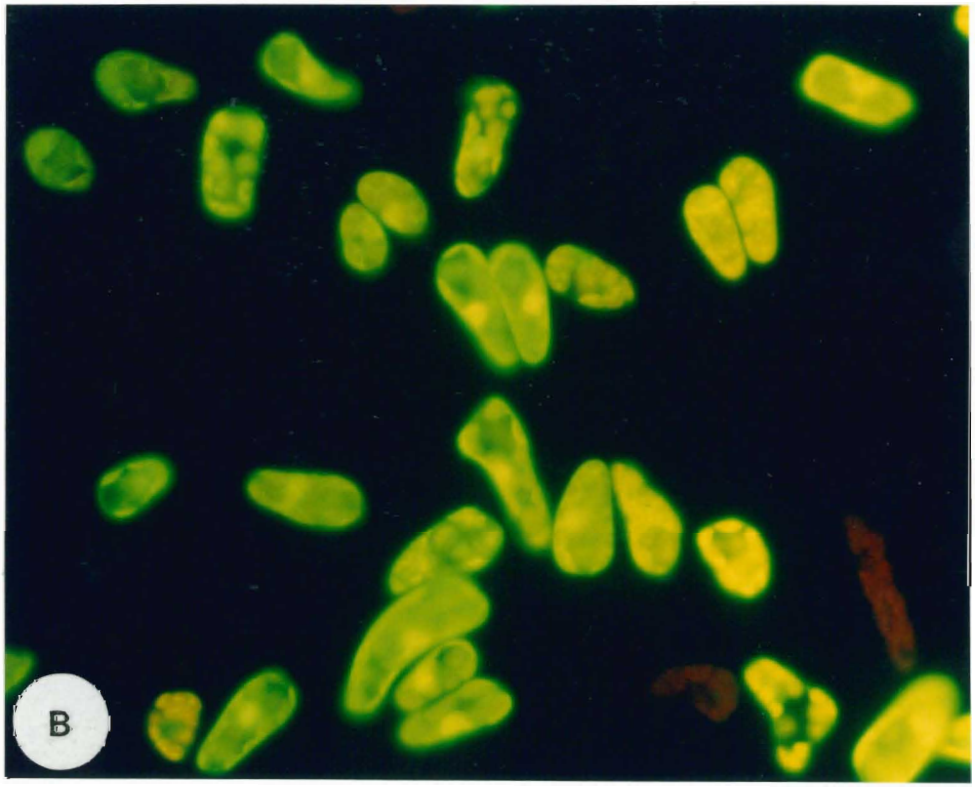
B


C

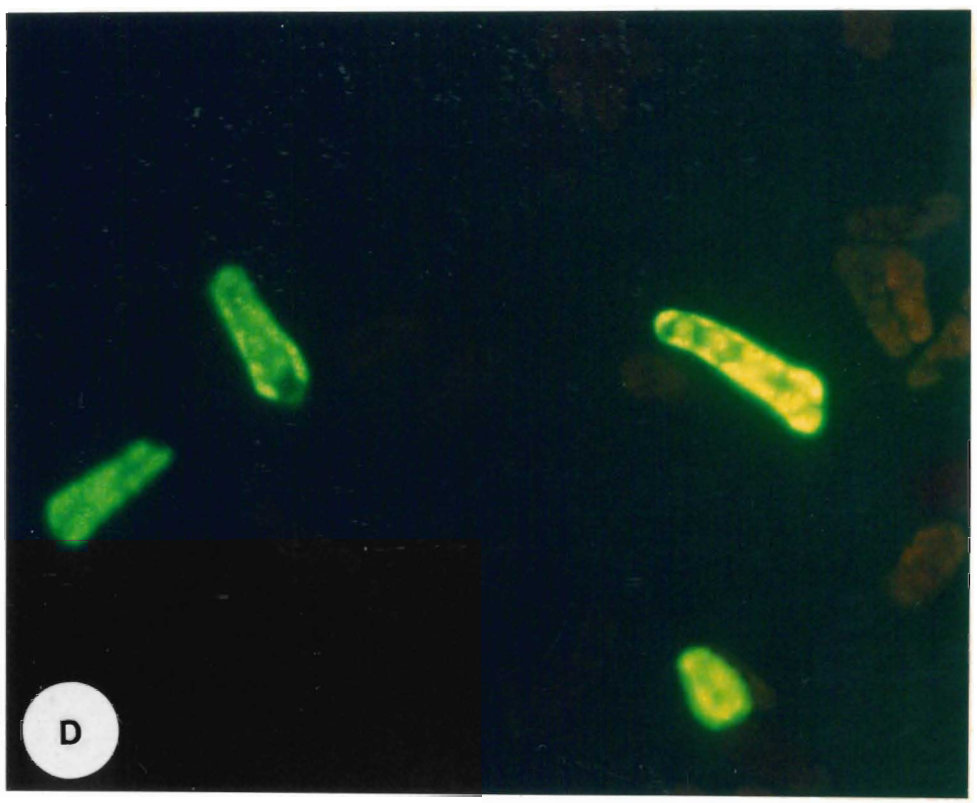
D

Figure 4.3b: Populational Cell Viability Assayed with Evan's Blue Dye and Fluorescein Diacetate

The total number of cells in the photographs described in Figure 4.3a were counted. Nonviable cells [the blue cells in bright field photographs and the cells not fluorescing bright yellow in dark field photographs] were also counted. The percentages of nonviable cells assessed with Evan's blue (EB) and fluorescein diacetate (FDA) are shown. Approximately 250 control cells and 100 MP-treated cells were assessed from 4 cell preparations.

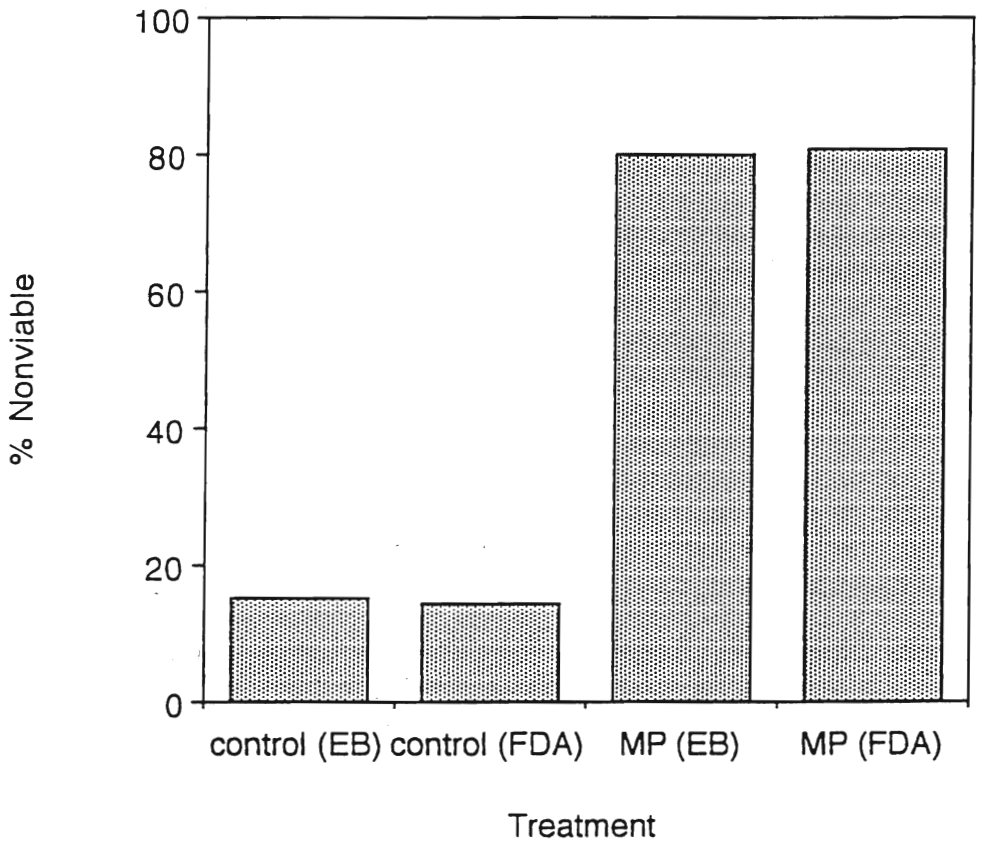

4.4. Cell viability as a function of MP concentration

Cell suspensions of 6×10^6 cells/ml were incubated for 16 min with these concentrations of MP: 0 μM, 0.25 μM, 2.5 μM and 25 μM. Cell viability after incubation with 0.25 μM MP and 2.5 μM MP did not differ significantly from the control level of cell viability (0 μM MP). However, incubation with 25 μM MP resulted in a significantly higher % of nonviable cells than the control % of nonviable cells ($P = 0.05$ according to the Wilcoxon rank sum test). Thus, it appears that the threshold concentration of MP causing increased nonviability lies between 2.5 μM and 25 μM.

Figure 4.4: Cell Viability as a Function of Mastoparan Concentration

Four batches of 12×10^6 cells were resuspended in 2 ml of 5 mM MES, 1 mM $CaSO_4$, pH 6.0. Aliquots of 0.338 mM MP were added to each suspension to give final concentrations of 25, 2.5 0.25 and 0 μM MP. After 36 min of incubation, damage was assessed with Evan's blue dye. Percent damage values represent the mean of three experiments. Standard errors bars are shown.

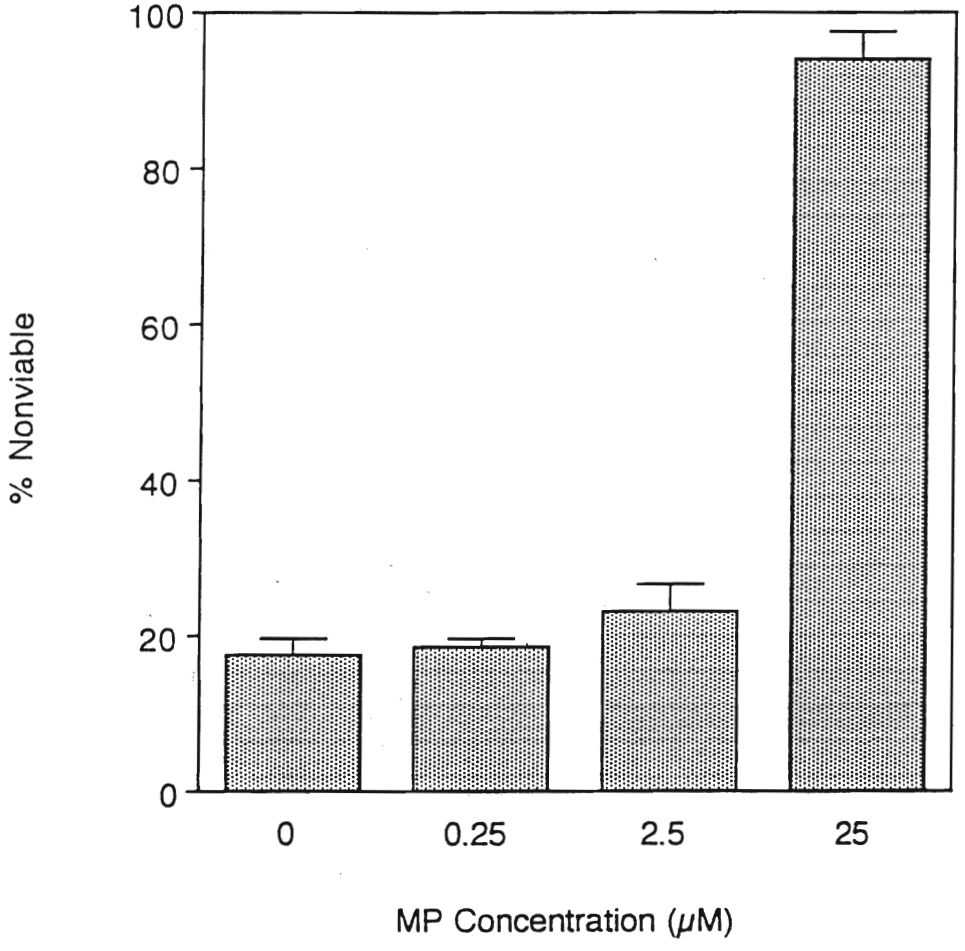

4.5. The effect of MP and Mas17 on the pH of the medium

The loss of cell viability is indicative of the HR as are rapid changes in the pH of the cell suspension medium. Cells (4.5×10^6) were suspended in 3 ml of 1 mM $CaSO_4$ and the pH of the suspension was adjusted to between 4.9 and 5.0. The addition of 13.2 μM MP caused a rapid alkalinization of 0.85 pH units (Figure 4.5A). Back-titration with 0.1 N HCl revealed that the pH change was equivalent to 270 nmols/10^6 cells. Mas17 addition (13.2 μM) did not result in alkalinization (Figure 4.5B). Alkalinization in response to MP was reproducible and cell-dependent. It was also pH-dependent. When the initial pH was 5.9, only a slight alkalinization was observed, and when the initial pH was 7, no alkalinization occurred in response to MP. Repeat additions of 13.2 μM MP after approximately 4-5 min did not result in further alkalinization of the medium. Back-titrations in 5 experiments gave a mean medium alkalinization value of 270 ± 23 nmols $H^+/10^6$ cells.

Figure 4.5: The Effect of Mastoparan and Mas17 on the pH of the Medium

In both experiments A and B, 4.5×10^6 cells were resuspended in 3 ml of 1 mM $CaSO_4$. The pHs of the cell suspensions were adjusted to between 4.9 and 5.0 (exact pHs are shown on the figure). The cell suspensions were kept at 25.0-25.5°C in the dark. Continuous pH measurements were begun. The chart speed was 30 s/cm. In A, the addition of 13.2 μM MP and two aliquots of 0.1 N HCl (for back-titration) are indicated by arrows. In B, the addition of 13.2 μM Mas17 is indicated by an arrow.

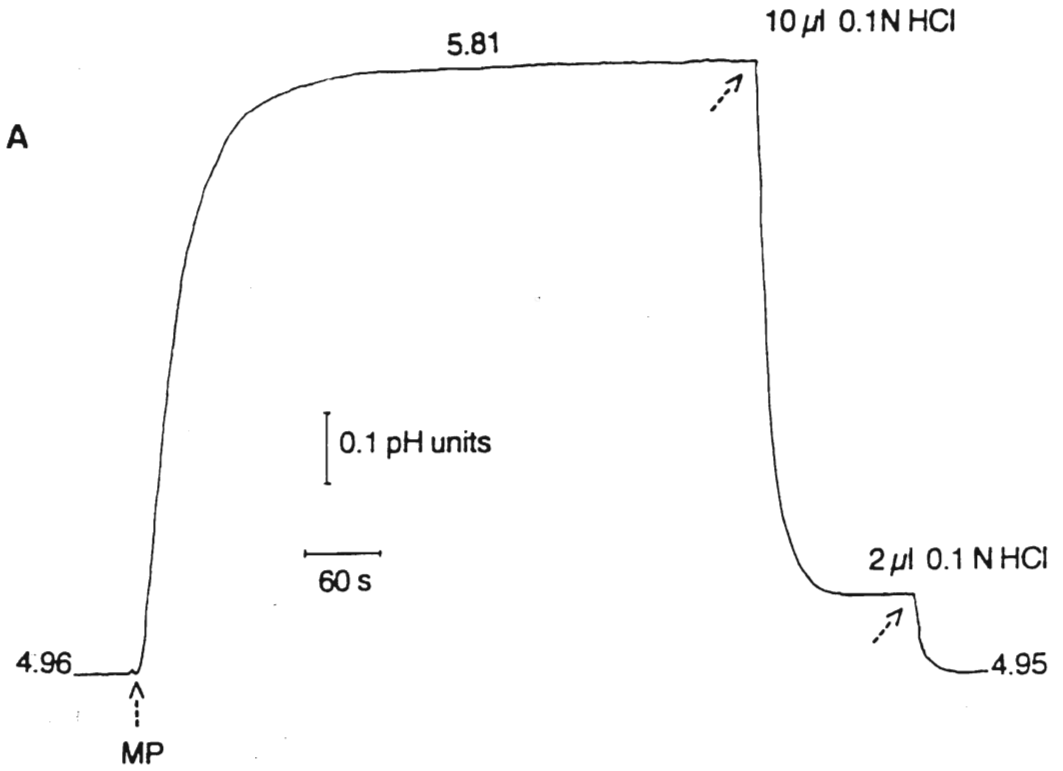

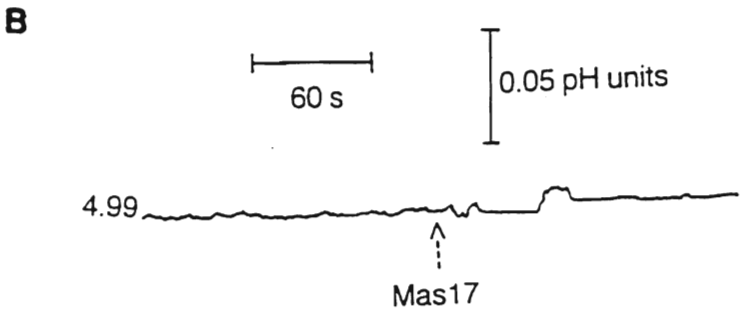

4.6. The effect of ferricyanide on chlorophyll *a* fluorescence yield and oxygen consumption in the light

The loss of cell viability in response to MP was suggestive of the hypersensitive response. Because the hypersensitive response involves reduction at the plasma membrane, the idea behind this experiment involved providing an artificial oxidizing agent in the cell medium.

A PAM fluorometer was used to measure the oxygen and chlorophyll *a* fluorescence yield of a cell suspension (1.5×10^6 cells/ml) in the light (800 $\mu E \cdot m^{-2} \cdot s^{-1}$). Upon addition of 1 mM $K_3Fe(CN)_6$, photochemical quenching increased. This increase corresponds to the oxidation of the Q_A pool. In addition to increased photochemical quenching, the first addition of $Fe(CN)_6^{3-}$ resulted in an increase in the rate of O_2 evolution. Subsequent additions of $Fe(CN)_6^{3-}$ did not stimulate further photochemical quenching or accelerated O_2 evolution. This effect of $Fe(CN)_6^{3-}$ was observed 5 times. [The decline in O_2 evolution is believed to be merely coincidental to the fourth $Fe(CN)_6^{3-}$ addition and due to the depletion of C_i. In other trials, in which 500 μM $KHCO_3$ had been added prior to the experiment, O_2 evolution did not level off.]

Figure 4.6: The Effect of Ferricyanide on Chlorophyll *a* Fluorescence and Oxygen Consumption in the Light

Three million cells were resuspended in 2 ml of 5 mM MES, 1 mM $CaSO_4$, pH 6.0. Oxygen and chlorophyll *a* fluorescence measurements with the PAM fluorometer were begun after 5 min of dark adaptation. The intensity of the actinic light was 800 $\mu E \cdot m^{-2} \cdot s^{-1}$. At time = 237 s, 1 mM $K_3Fe(CN)_6$ was added. This ferricyanide addition was repeated at times 296 s, 373 s and 450 s.

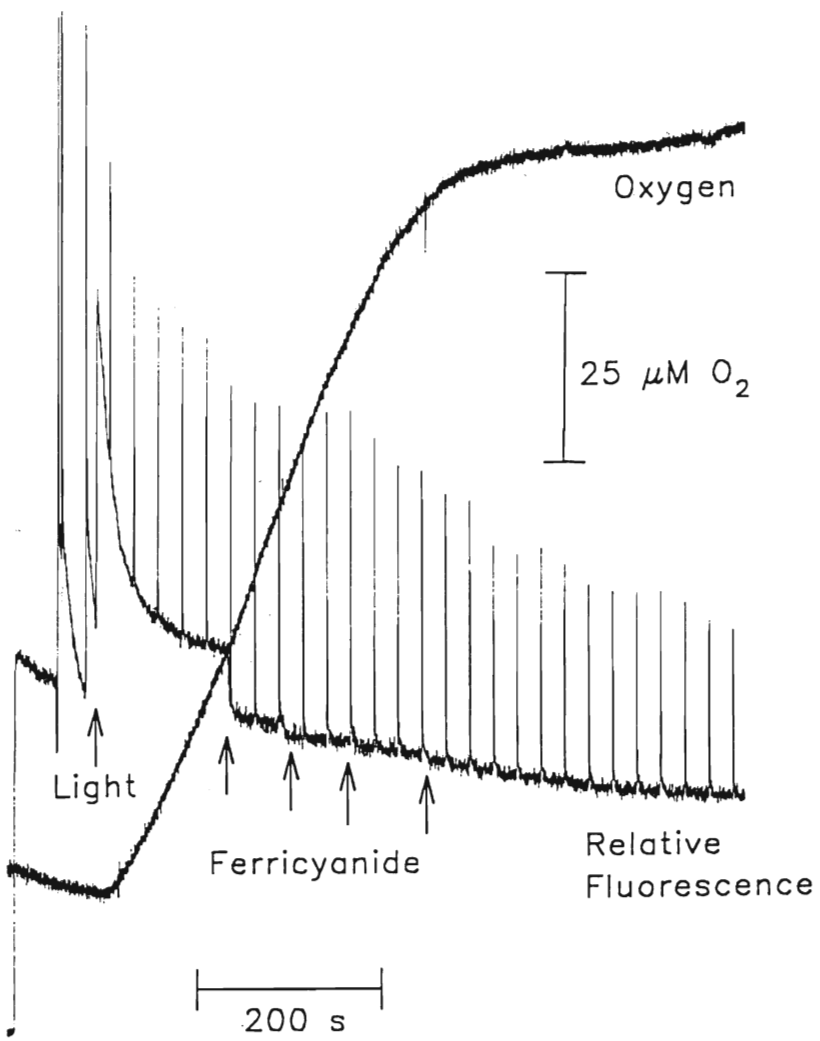

4.7. The effect of MP on chlorophyll *a* fluorescence yield and oxygen consumption in the light

One of the characteristics of the hypersensitive response is the production of active oxygen species at the plasma membrane. With this in mind, oxygen and chl *a* fluorescence yield were monitored in a suspension containing 1.35×10^6 cells/ml. The actinic light source provided 800 $\mu E \cdot m^{-2} \cdot s^{-1}$. The addition of 6.6 μM MP was followed by a short burst of O_2 production which was followed by a rapid and large consumption of O_2. These were accompanied by a transient increase in photochemical quenching corresponding to the oxidation of Q_A. In addition, a large nonphotochemical quenching of F_m occurred and, following O_2 uptake, no further O_2 evolution was detected. These phenomena were observed about 25 times in response to MP. The addition of 6.6 μM Mas17 did not cause any of these effects.

The effect of MP on oxygen levels and chl *a* fluorescence is cell-dependent. The addition of 0.18 μM catalase 10 s before and 10 s after MP addition did not diminish the rate of O_2 consumption (see Appendix II.1.). The addition of sodium dithionite crystals following the O_2 consumption caused a further reduction in O_2 concentration 3 out of 4 times (see Appendix II.2.). Nonphotochemical quenching (as well as photochemical quenching and O_2 consumption) in response to MP were still observed in experiments with additions of 6.7 μM nigericin (a protonophore) 1 min before or 15 s after MP addition (see Appendix II.3.).

Figure 4.7: The Effect of Mastoparan on Chlorophyll *a* Fluorescence and Oxygen Consumption in the Light

Cells (2.7×10^{6}) were resuspended in 2 ml of 5 mM MES, 1 mM CaSO4, pH 6.0. Oxygen and chl *a* fluorescence measurements were begun after 5 min of dark adaptation. Saturating flashes were applied at 20 s intervals. The intensity of the actinic light was 800 $\mu E \cdot m^{-2} \cdot s^{-1}$. At time = 270 s, 6.6 μM MP was added.

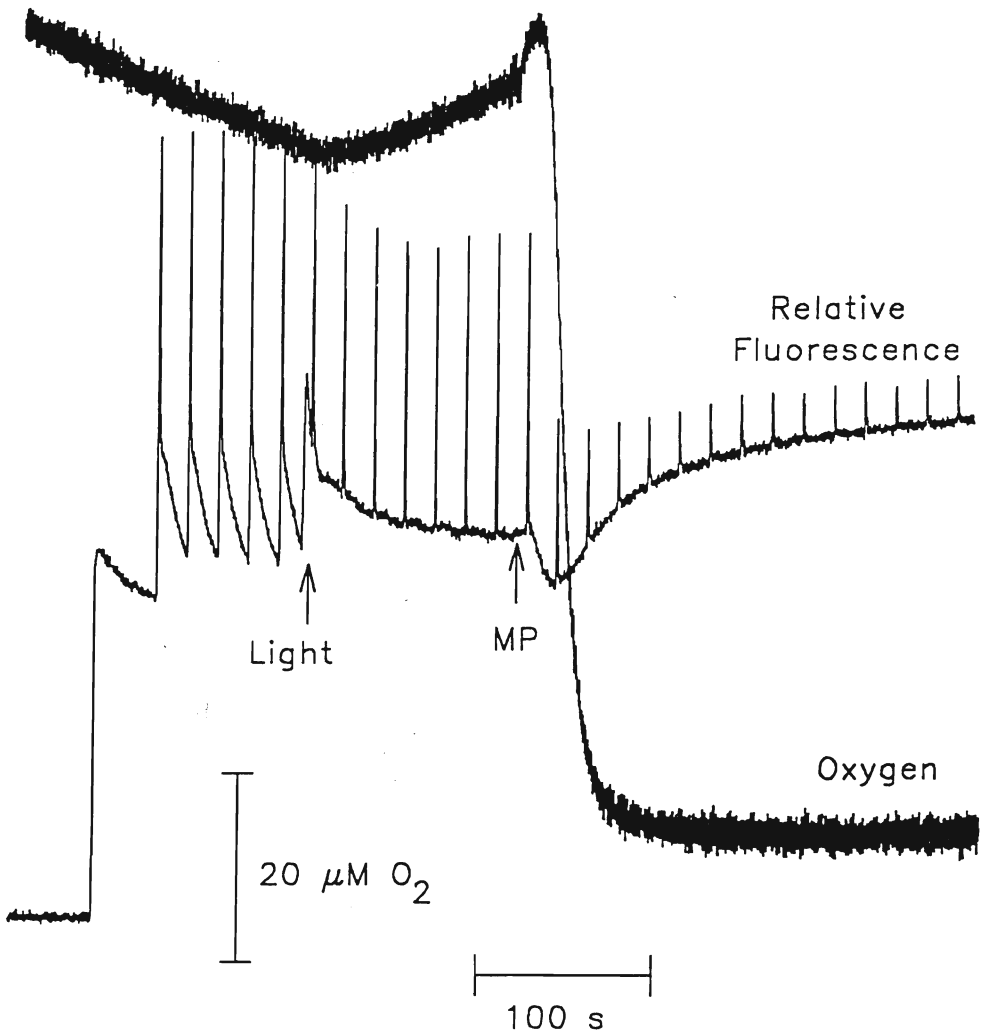

4.8. The effect of MP on chlorophyll *a* fluorescence yield and oxygen consumption in the dark

MP (6.6 μM) was added to a suspension containing 1.5×10^6 cells/ml. Oxygen and chl *a* fluorescence measurements were made with the PAM fluorometer in the absence of actinic light. The transient burst of O_2 production followed by the abrupt decrease in O_2 concentration characteristic of the response to MP in the light were also observed in the dark. Large nonphotochemical quenching of F_m as well as photochemical quenching (oxidation of Q_A) also occurred as in the light. However the subsequent reversal of photochemical quenching, indicating re-reduction of Q_A, was absent. Thus, re-reduction of Q_A appears to be light-driven.

Figure 4.8: The Effect of Mastoparan on Chlorophyll *a* Fluorescence and Oxygen Consumption in the Dark

Three million cells were resuspended in 2 ml of 5 mM MES, 1 mM $CaSO_4$, pH 6.0. Oxygen and chl *a* fluorescence measurements were begun after 5 min of dark adaptation. The actinic light was not used. At time = 104 s, 6.6 μM MP was added.

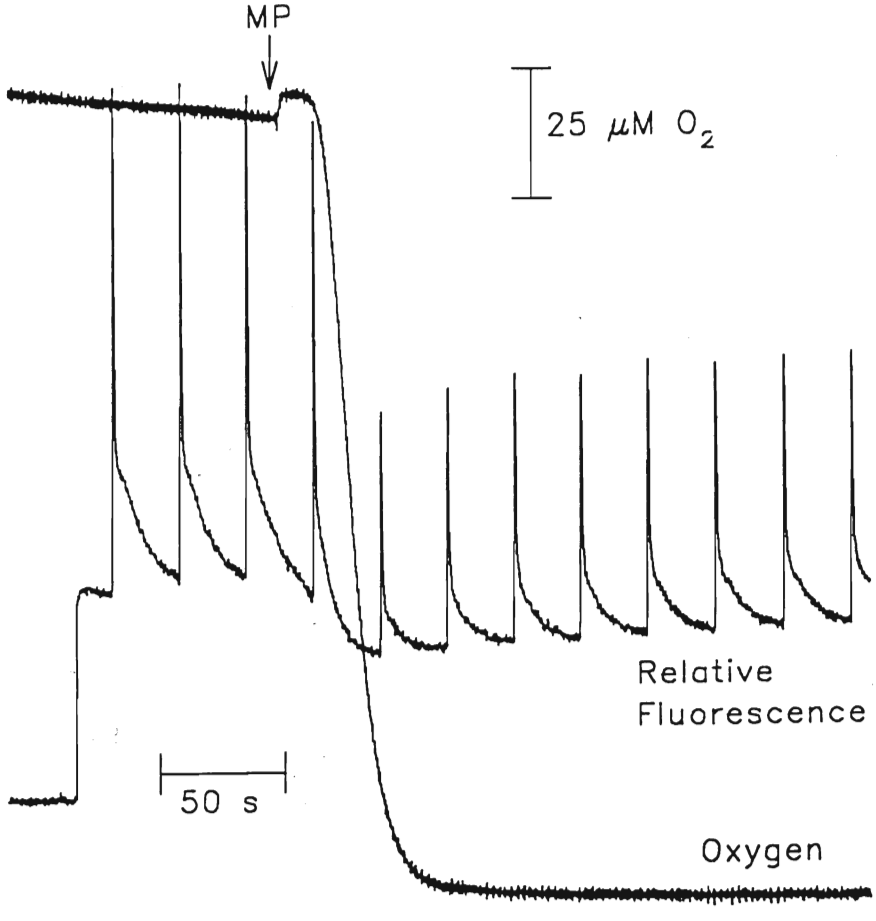

4.9. The effect of MP on oxygen consumption in the light and in the dark

Photosynthetic oxygen evolution and respiratory oxygen consumption were monitored with cell suspensions (1.5×10^6 cells/ml) in the light and in the dark, respectively. Upon addition of 13.2 μM MP, rapid O_2 consumption was measured. Rates of O_2 consumption (μmol O_2/mg chl/ hr) and net O_2 consumption (μmol O_2) were calculated. Both rates of O_2 consumption and net O_2 consumption were significantly higher in the light than in the dark ($P = 0.05$ according to the Wilcoxon rank sum test).

Table 4.1: The Effect of Mastoparan on Oxygen Consumption in the Light and in the Dark

Three million cells were resuspended in 2 ml of 5 mM MES, 1 mM $CaSO_4$, pH 6.0. Oxygen measurements were begun after 5 min of dark adaptation. The intensity of the actinic light was 400 $\mu E \cdot m^{-2} \cdot s^{-1}$. After photosynthetic oxygen evolution was established, 13.2 μM MP was added and the subsequent oxygen consumption was measured. This experiment was also conducted in the dark (no actinic light). Both light and dark experiments were repeated 3 times. The mean rate of oxygen consumption after MP addition and the mean net oxygen consumption are shown. Standard error values are included.

Condition	Initial Rate of O2 Consumption (μmol O2/mg chl/hr)	Net O2 Consumption (μmol)
Light	105 ± 1.7	240 ± 1.6
Dark	85 ± 1.7	150 ± 12

4.10. The effect of mastoparan concentration on oxygen consumption

Five concentrations of MP ranging from 0.66 μM to 6.6 μM were applied to cell suspensions containing 1.5×10^6 cells/ml. These experiments were carried out under 400 $\mu E \cdot m^{-2} \cdot s^{-1}$ actinic light. Oxygen levels and chl *a* fluorescence were monitored with the PAM fluorometer. Figure 4.9 shows the corresponding oxygen traces superimposed with MP addition defining time = 0. No net O_2 consumption occurred in response to 0.66 μM and 1.65 μM MP, although the latter showed a decreased rate of photosynthetic O_2 evolution compared to the former. The three higher MP concentrations (3.3 μM, 4.65 μM, 6.6 μM) each caused net O_2 consumption in a dose-dependent manner (121nmols O_2, 199 nmols O_2, 244 nmols O_2, respectively). Initial rates of O_2 consumption for each concentration (0.66 μM, 1.65 μM, 3.3 μM 4.65 μM, 6.6 μM) were calculated to be -10.8, -1.2, 45.1, 84.0, 129.1 μmol O_2/mg chl/hr, respectively. [Chl *a* fluorescence in response to these MP concentrations also exhibits a dose-dependence, with the largest effects (as in Figure 4.9) resulting from the highest concentrations of MP (data not shown)]. The threshold MP concentration for the stimulation of rapid and transient O_2 uptake lies between 1.65 μM and 3.3 μM. The threshold MP concentration for increasing the nonviability of cells fell between 2.5 μM and 25 μM (Figure 4.4). These threshold concentration ranges overlap, allowing the possibility of a single mechanism which results in both an oxidative burst and increased cell nonviability.

Figure 4.9: The Effect of Mastoparan Concentration on Oxygen Consumption

This figure shows oxygen measurements compiled from 5 PAM experiments. In each experiment, 3×10^6 cells were resuspended in 2 ml of 5 mM MES, 1 mM $CaSO_4$, pH 6.0. Oxygen and chl *a* fluorescence (not shown) measurements were begun after 5 min of dark adaptation. The intensity of the actinic light was 400 $\mu E \cdot m^{-2} \cdot s^{-1}$. At time = 0, aliquots of MP were added to give the concentrations indicated.

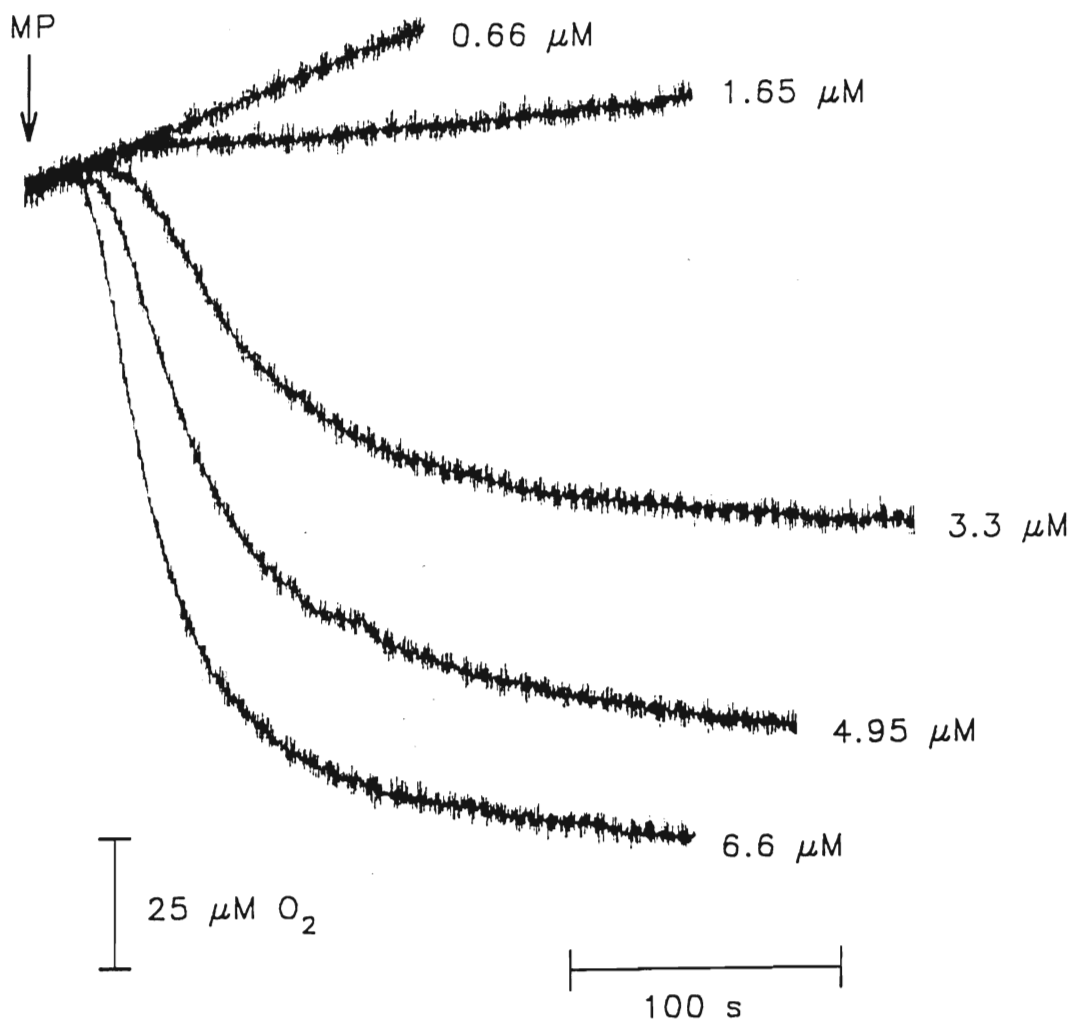

4.11. The effect of hydrogen peroxide on chlorophyll *a* fluorescence yield and oxygen production

Oxygen and chl *a* fluorescence yield of a cell suspension containing 1.5×10^6 cells/ml were monitored with a PAM fluorometer in the light. When 240 μM H_2O_2 was added, O_2 production was temporarily enhanced and nonphotochemical quenching increased. After approximately 200 s, O_2 evolution ceased. The effect of H_2O_2 on oxygen and chl *a* fluorescence was reproducible. It was determined that the enhanced O_2 production was cell-dependent and that increased nonphotochemical quenching was light-dependent. Related experiments showed that H_2O_2 (0.5, 5 and 50 mM) does not increase the % of nonviable cells within 36 min of incubation (see Appendix II.4.) and that incubation with 2 mM H_2O_2 for 16 min does not induce GABA accumulation (see Appendix II.5.).

The idea that the consumed O_2 was converted not to H_2O_2 but rather to the superoxide anion ($O_2^{\cdot -}$) was also examined. Perhaps increased nonviability was largely due to this anion radical. Fifty units of superoxide dismutase (SOD) was added to cell suspensions incubated with 25 μM MP. The % of nonviable cells in response to MP plus SOD was no different than the % of nonviable cells in response to MP alone (see Appendix II.6.).

Figure 4.10: The Effect of H_2O_2 on Chlorophyll *a* Fluorescence and Oxygen Production

Three million cells were resuspended in 2 ml of 5 mM MES, 1 mM $CaSO_4$, pH 6.0. Oxygen and chl *a* fluorescence measurements were begun after 5 min of dark adaptation. The intensity of the actinic light was 100 $\mu E \cdot m^{-2} \cdot s^{-1}$. The interval between saturating flashes was reduced from 30 s to 20 s at approximately time = 300 s. At time = 471 s, 2.4×10^{-4} M H_2O_2 was added to the cell suspension.

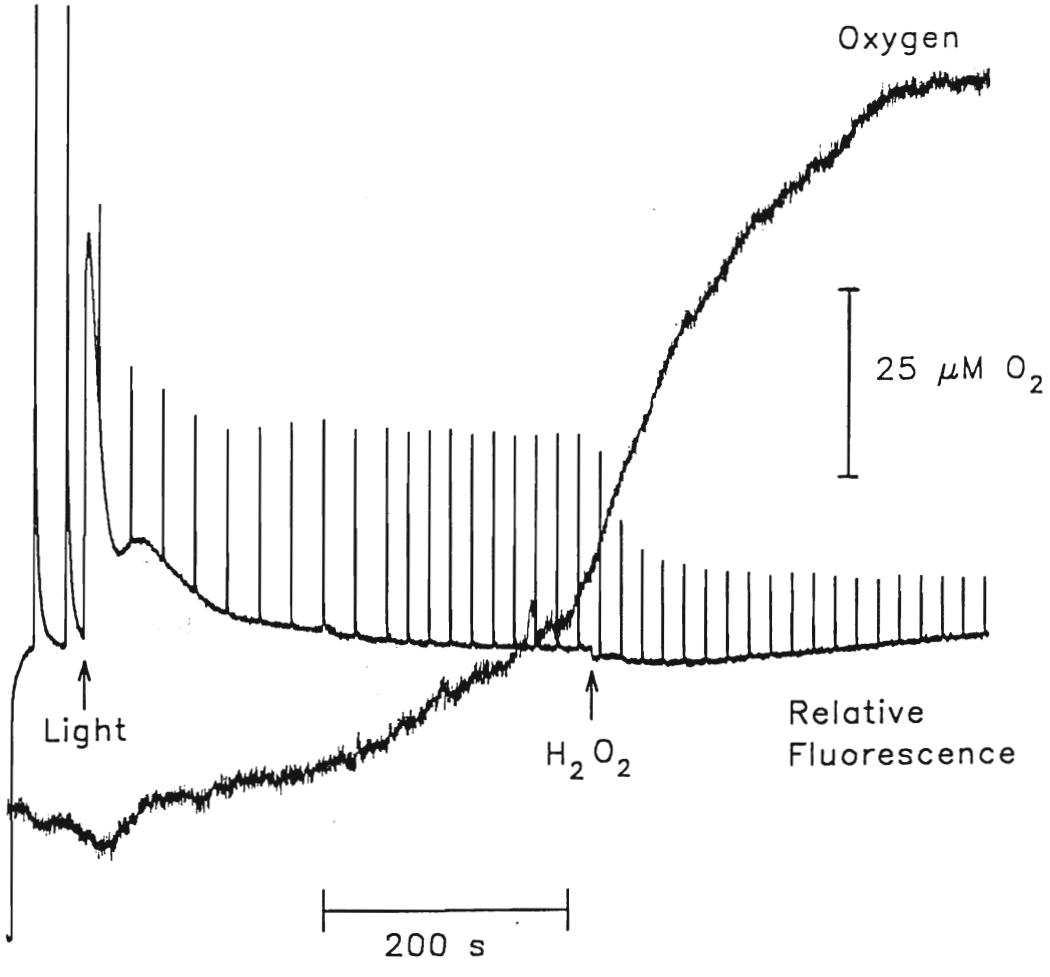

4.12. The effect of MP on hydrogen peroxide concentration

Using the chemiluminescent luminol oxidation assay, hydrogen peroxide was determined following incubation of 4×10^6 cells/ml ± 64 μM MP and ± 38.5 μM H_2O_2. MP alone did not induce net H_2O_2 production, however, the presence of MP resulted in the degradation of added H_2O_2. When H_2O_2 in the absence of MP was added to cells, 52% was recovered. Recovery was based on the chemiluminescence measurements obtained following H_2O_2 addition to cell-free medium (data not shown).

To investigate the possibility of MP-stimulated superoxide production, 112.4 units of SOD were added along with 66 μM MP. No measurable H_2O_2 was detected (see Appendix II.7.). These data do not support the hypothesis that MP stimulates superoxide production.

Table 4.2: The Effect of Mastoparan on Hydrogen Peroxide Concentration

Four batches of 4×10^6 cells were each resuspended in 1 ml of 5 mM MES, 1 mM $CaSO_4$, pH 6.0. Runs were performed consecutively. In the combinations indicated below, 38.5 μM H_2O_2 and 64 μM MP were added to the cell suspensions. When both were employed, H_2O_2 was added first and then MP within 5 s. Aliquots of the appropriate volumes of distilled water were added to the cell suspensions so that the final volumes of the suspensions were equal. After 30 s of incubation, 100-μl aliquots were removed and hydrogen peroxide was determined in 1-ml final assay volumes. The means of 3 experiments are expressed in μM H_2O_2. Standard error is included where appropriate.

	μM H_2O_2	
Treatment	+ MP	- MP
+ H2O2	< 0.25	1.91 ± 0.23
- H2O2	< 0.25	< 0.25

5. Discussion

5.1. Mastoparan induction of death of asparagus mesophyll cells

Several lines of evidence suggest that MP induces cell death. First of all, two separate visual tests of viability demonstrate loss of viability in response to MP (Figures 4.3a and 4.3b). The tests display complementarity, that is, evaluations of viability of individual cells with Evan's blue and with fluorescein diacetate are in agreement (Figure 4.3a) and viability percentages derived from populations of cells (Figure 4.3b) also concur.

The basis for each of the cell viability tests is well-documented. The Evan's blue test discriminates between viable and nonviable cells on the basis of membrane integrity. It has been used successfully to distinguish dead cells and protoplasts from a large number of plant species from several families (Gaff and Okong'o-ogola, 1971; Colman *et al.*, 1979; Huang *et al.*, 1986). The penetration of Evan's blue into dead or dying cells indicates the loss of discriminatory semi-permeability of the plasma membrane, a characteristic of living cells (Gaff and Okong'o-ogola, 1971). The normal membrane potential, negative inside, causes viable cells to repel the negatively charged dye (Figure 5.1A).

The basis of the FDA test is different. Nonpolar FDA (Figure 5.1B) enters living cells where ester groups are hydrolyzed. The polar product, fluorescein, fluoresces yellow-green when excited with UV radiation. Its polar nature traps free fluorescein in the cytosol of viable cells. Although the FDA viability test has been widely used (Rotman and Papermaster, 1966; Widholm, 1972; Huang *et al.*, 1986; Vera-Estrella *et al.*, 1992), the property of nonviability that it is testing for is not agreed upon. Rotman and Papermaster (1966) claim that the FDA test measures membrane integrity. That is, nonviable cells, having lost their semi-permeable nature, do not successfully trap fluorescein. In contrast, Huang and colleagues (1986) state that FDA is only

Figure 5.1: Chemical Structures of Evan's Blue Dye (A) and Fluorescein Diacetate (B)

(A)

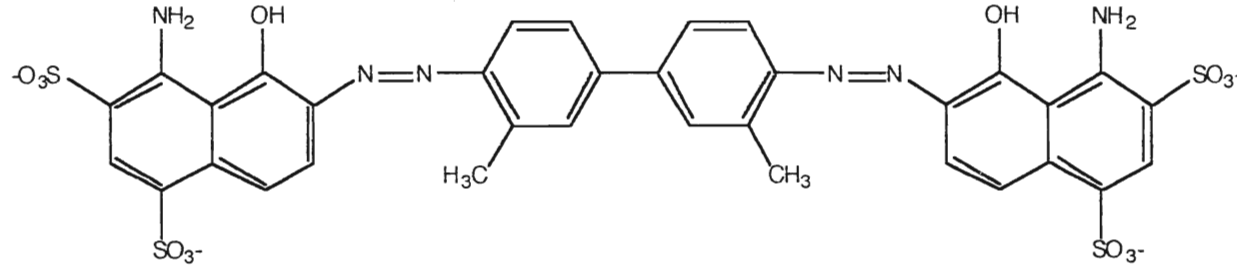

(B)

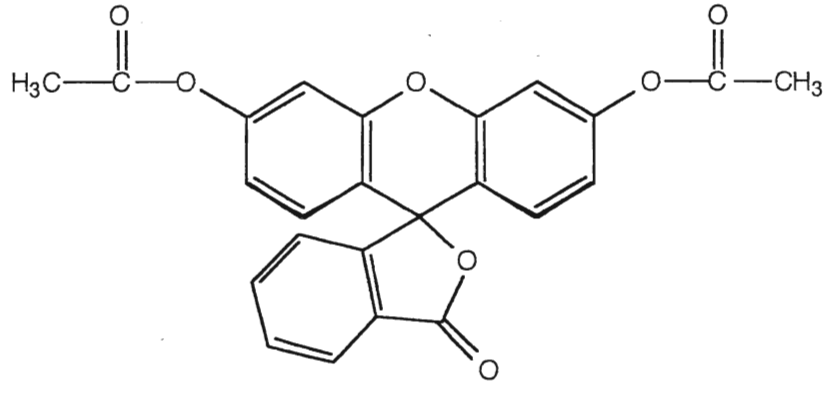

hydrolyzed in living cells, implying that FDA discriminates between cells on the basis of esterase functionality. Loss of membrane integrity and loss of esterase function may not be mutually exclusive. If a cell loses either of these functions, many other fundamentally deleterious effects are probably unavoidable.

The use of FDA (a fluorescent inclusion dye) in conjunction with a non-fluorescent exclusion dye (such as Evan's blue) to test plant cell viability has been demonstrated previously (Huang *et al.*, 1986). Double-staining with an inclusion dye and an exclusion dye is advantageous because it allows for simultaneous independent tests for living cells.

Secondly, the alkalinization of the medium following MP addition indicates the death of the cells (Figure 4.5). The alkalinization that occurs is both permanent and pH-dependent. The pH of the medium rises within 180 s to approximately 5.8 from pH 5.0. However, when the cells are incubated in medium with a pH of 5.9, the induced alkalinization is diminished approximately 90%. Furthermore, no alkalinization is observed when the initial pH of the medium is 7.0. Alkalinization due to the elicitation of cultured tomato cells by ergosterol is transient (Felix *et al.*, 1993; Granado *et al.*, 1995). In addition, alkalinization occurred after a lag period which ranged from 0.5 - 2.5 min in each instance. The mechanism of this alkalinization is not clear. It may be due to Ca^{2+} inhibition of the H^{+}-ATPase (Kinoshita *et al.*, 1995), such that the observed transient alkalinization is the result of a transient increase in Ca^{2+} resulting in temporary inhibition of the proton pump. In each of these studies, there was no indication of the HR (cell death). Inhibition of the H^{+}-ATPase may have been relieved by the action of Ca^{2+}-ATPases and Ca^{2+}/nH^{+} antiporters to lower the cytosolic Ca^{2+} concentration. The H^{+}-ATPase could then act to restore the original pH.

Alkalinization of the medium of asparagus mesophyll cells does not seem to be a requirement for the oxidative burst. Experiments in which O_2 uptake is measured were performed at pH 6.0, a pH at which alkalinization is almost negligible (data not shown). These data contrast with data generated using French bean suspension cultured cells and the fungal pathogen *Colletotrichum lindemuthianum*. Using this system, transient alkalinization of the apoplast was demonstrated to be necessary for the oxidative burst (Bolwell *et al.*, 1995). The prevention of elicited alkalinization with strong buffers and a variety of protonophores eliminated the production of H_2O_2. It was noted that in order for the oxidative burst to occur, the pH must change 0.5 - 1.0 pH units (generally in the direction of cell wall alkalinization) with the final pH being greater than 6.5. Plasma membrane damage was observed microscopically in cells producing H_2O_2. A cell wall peroxidase with a pH optimum of 7.2 was considered to be the source of H_2O_2.

Alternatively, in the present study, the permanence and pH-dependence of alkalinization correlates better with electrolyte leakage than with alkalinization due to a specific change in plasma-membrane-protein-mediated H^+ translocation. If the observed alkalinization was due to leakage of cellular electrolytes following oxidative membrane damage as per Model 5.1(**1**), the timing of these events is a complicating factor. MP-induced alkalinization of the medium occurs within about 2 s (Figure 4.5). O_2 uptake (a measure of the oxidative burst) is initiated about 15 s after MP addition and continues for approximately 1.5 min (Figure 4.7). According to Model 5.4, the oxidative burst is the cause of electrolyte leakage (via lipid peroxidative membrane damage) and should therefore precede it.

External alkalinization via perturbed H^+ translocation (either H^+ influx or

inhibited efflux via the H^+ pump) is typically a rapid response to elicitation (Mathieu *et al.*, 1991; Bach *et al.*, 1993; Felix *et al.*, 1993; Smith, 1996). However, because no causal link between medium alkalinization and the oxidative burst has been established, there is no reason to stipulate an order for the 2 events. To reconcile the data presented here regarding the timing and pH dependence of medium alkalinization, a dual mechanism is suggested: immediate alkalinization of the external medium due to H^+ influx [Model 5.1(**2a**)] and possibly Ca^{2+} inhibition of the H^+-ATPase [Model 5.1(**2b**)]. This may be transient as is observed in the literature (Felix *et al.*, 1993; Bolwell *et al.*, 1995; Granado *et al.*, 1995). Following the production of destructive AOS, lipid peroxidation would occur with concomitant electrolyte leakage causing a rise in pH [Model 5.1(**1**))] In addition, extracellular dismutation, both spontaneous or enzymic, of $O_2^{\cdot -}$ to H_2O_2 would cause alkalinization due to H^+ consumption [Model 5.1(**3a**)]. Furthermore, one of the products of the Fe^{3+}-catalyzed Fenton-type reaction between $O_2^{\cdot -}$ and H_2O_2 is OH^- [Model 5.1(**3a**)]. Thus initial medium alkalinization is due to altered H^+ translocation and later alkalinization may be attributed to a combination of membrane leakiness and interconversions of AOS.

Other data support a dual mechanism for medium alkalinization in asparagus mesophyll cells. The omission of Ca^{2+} and the presence of EDTA in the external medium of asparagus cells significantly reduced the extent of MP-stimulated medium alkalinization as well as abolishing GABA accumulation and cell death in response to MP (Wong, 1997). However, the absence of external free Ca^{2+} did not block the stimulation of the oxidative burst by MP. [Wong's data are reminiscent of the 2-phase

Model 5.1: Possible Mechanisms Leading to Alkalinization of the Medium.

(**1** leakage of Brønsted bases through disrupted membrane; **2** protein-mediated processes: **2a** H^+ influx and **2b** Ca^{2+} inhibition of the H^+-ATPase; **3** interconversions of active oxygen species: **3a** superoxide dismutation and **3b** Fe^{3+}-catalyzed Fenton reaction. (PM = plasma membrane; A^- = free Brønsted base; X^- = anion charge-balancing H^+ influx; XH_2 = generic reductant of $NADP^+$; X = product of oxidation of XH_2).

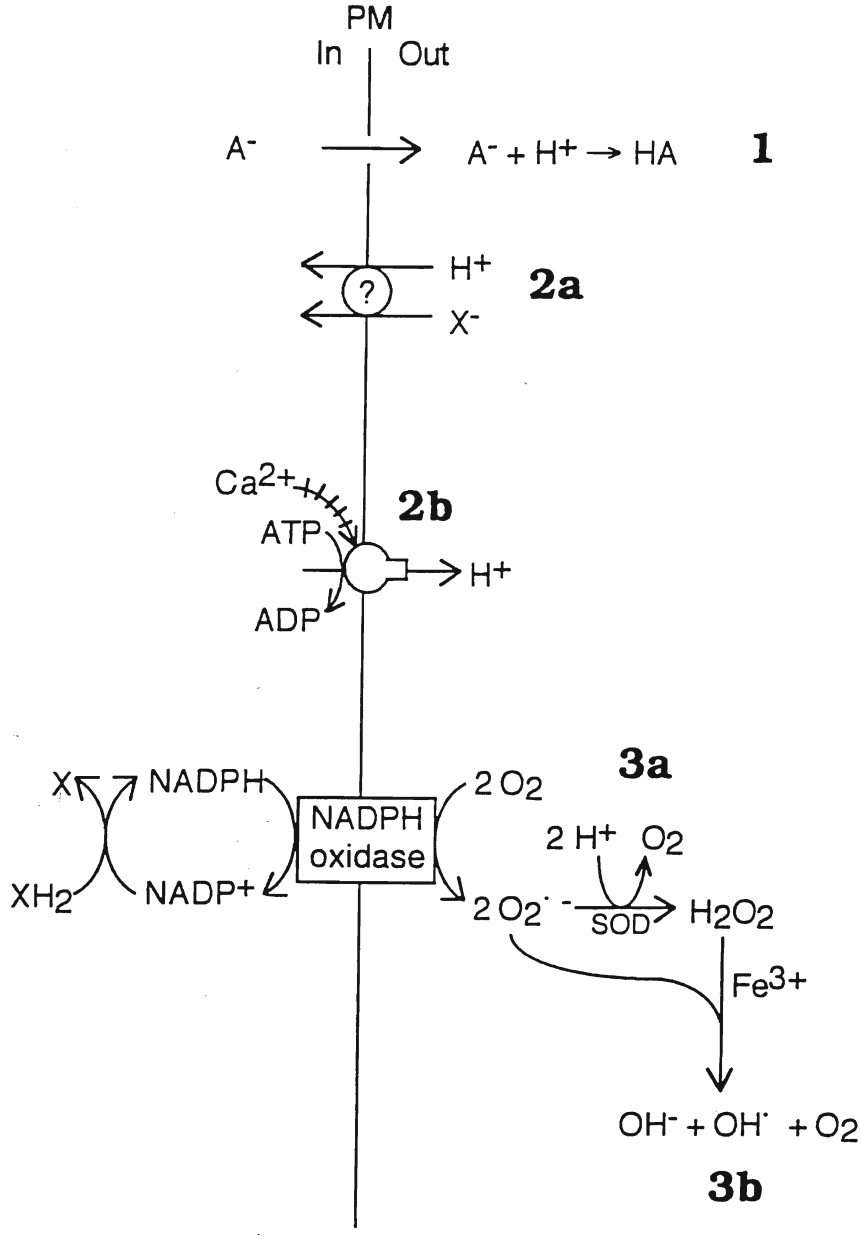

plant defense response proposed by Chai and Doke (1987) in which the first step involved an oxidative burst and occurred in both compatible and incompatible plant-pathogen interactions. The second step was Ca^{2+}-dependent, characterized only incompatible interactions and led to hypersensitive cell death]. It seems then that MP-stimulated alkalinization has Ca^{2+}-dependent and Ca^{2+}-independent components. Ca^{2+}-dependent alkalinization may be attributed to Ca^{2+} inhibition of the H^+-ATPase and other phenomena related to Ca^{2+}-dependent cell death (such as electrolyte leakage, superoxide dismutation and the aforementioned Fenton-type reaction) while Ca^{2+}-independent alkalinization is likely due to H^+ influx. The Ca^{2+}-independence of the oxidative burst and the Ca^{2+}-dependence of cell death will be discussed in detail in a later section.

The third piece of evidence indicating that MP does in fact cause the death of asparagus mesophyll cells is the loss of O_2 evolution in the light, apparent 1-2 min following MP addition (Figure 4.7). This indicates a loss of photosynthetic activity, which would be expected in dead cells. Collectively, the data indicate that MP does induce cell death in isolated asparagus mesophyll cells.

5.2. GABA accumulation as a metabolic marker for dead or dying plant cells

Using nuclear magnetic resonance spectroscopy, Roberts and colleagues (1992) demonstrated GABA accumulation in maize root tips that were dying from hypoxia. This finding became the basis for their hypothesis that GABA accumulation was a metabolic marker for dead or dying plant cells. GABA accumulation resulted from treatments that cause the death of asparagus mesophyll cells (Figure 4.2) [25 μM mastoparan (Figure 4.1) and 2.8 mM arachidonic acid (Cleve, 1995)]. However, not all treatments that cause GABA accumulation resulted in death of asparagus mesophyll cells (Figure 4.2). Treatment of asparagus cells with 5 mM L-glu at pH 5.0 resulted in an approximately 900% increase in GABA after 60 min of incubation (Crawford *et al.*,

1994). [This is believed to have occurred due to H^+/L-glu symport]. Similarly, 5 mM butyrate at pH 5.0 caused 200-300% higher GABA levels after only 15 s (Crawford *et al.*, 1994). Abscisic acid (100 μM), a plant hormone, raised GABA levels by 83% after 5 min (Cholewa, 1995). Furthermore, abrupt transfer of asparagus cells from 20°C to 1°C stimulated a 100% increase in GABA levels after 15 min (Cholewa *et al.*, 1997). In this study, the former four treatments did not result in the death of cells as assessed with Evan's blue dye (Figure 4.2). Therefore, although GABA accumulation may accompany the death of cells, the death of cells does not necessarily accompany GABA accumulation. Thus, GABA accumulation is not a distinguishing feature of dead or dying cells and cannot be used to evaluate the viability of plant cells.

5.3. MP stimulation of the oxidative burst

5.3.1. Evidence for the oxidative burst in response to MP

5.3.1.1. O_2 data

Treatment of asparagus mesophyll cells with MP results in an oxidative burst. This is indicated by the large, rapid and often exhaustive uptake of O_2 (Figures 4.7 and 4.8). This kind of O_2 uptake has been repeatedly correlated with the reduction of O2 to $O_2^{\cdot -}$ (Neubauer and Schreiber, 1988; Schreiber *et al.*, 1991; Miyake and Asada, 1992; Bolwell *et al.*, 1995; Robertson *et al.*, 1995; Smith, 1996). The oxidative burst occurs after a 15 - 20 s lag period following MP addition (Figure 4.7). The rate-limiting step is almost certainly the diffusion-controlled permeation of MP into the cell membranes (Rubinstein *et al.*, 1984). This interpretation is supported by the contrasting rapidity of the decrease in F_o when $Fe(CN)_6^{3-}$ is added (Figure 4.6). The

implied reduction of $Fe(CN)_6^{3-}$ must occur at the cell surface because $Fe(CN)_6^{3-}$ is non-permeant (Rubinstein *et al.*, 1984). Recently, complementary data generated using asparagus mesophyll cells show transient $O_2^{\cdot -}$ generation in response to Mas7, a highly active analogue of MP (MacGregor, 1997). Superoxide was detected via a light-emitting reaction with lucigenin in a luminometer. The timing of the appearance of $O_2^{\cdot -}$ (from 20 - 100 s) corresponds to the timing of O_2 uptake (Figure 4.7), confirming that O_2 is being reduced to $O_2^{\cdot -}$.

Following the large and rapid O_2 reduction, the O_2 level remains constant -- no photosynthetic O_2 evolution is observed (Figures 4.7 and 4.8). This lack of photosynthetic activity may be due to the presence of H_2O_2. H_2O_2 is the most photosynthetically damaging of the AOS (Kaiser, 1979). Photosynthetic inhibition by H_2O_2 is facilitated by its ready diffusibility through lipid bilayers (Hammond-Kosack and Jones, 1996). The IC_{50} for H_2O_2 inhibition of photosynthetic assimilation of CO_2 is 10 μM (Kaiser, 1976). H_2O_2 acts specifically to oxidize reduced thiol groups of Calvin-cycle thiol-modulated enzymes (fructose 1,6-bisphosphatase, NADP-glyceraldehyde-3-phosphate dehydrogenase, ribulose-5-phosphate kinase) (Takeda *et al.*, 1995). Inhibition of the dark reactions of photosynthesis leads to accumulation of light reaction products (NADPH and ATP) and inevitably the obstruction of electron transport, water-splitting, and thus O_2 evolution. Subsequent reduction of H_2O_2, as a result of its own oxidizing activity or ascorbate peroxidase activity, removes the source of dark reaction inhibition. The thiol groups of the inactivated enzymes can then be reduced photochemically via a thioredoxin/ferredoxin system (Takeda *et al.*, 1995).

Thus, unless the cell has suffered irreparable damage of another nature, photosynthetic activity would resume with concomitant O_2 evolution following the utilization of H_2O_2. It is postulated that photosynthetic O_2 evolution does not resume following the MP-stimulated oxidative burst due to membrane damage and the death of the cells (Figure 4.7).

5.3.1.2. Chlorophyll *a* fluorescence data

Changes in chlorophyll *a* fluorescence also corroborate MP stimulation of an oxidative burst. During the uptake of O_2 following MP addition, there is a temporary increase in photochemical fluorescence quenching, or in other words, an oxidation of Q_A. In the light, rereduction of Q_A (decreased photochemical quenching) is seen (Figure 4.7), however, in the dark, photochemical quenching is not relieved (Figure 4.8). In spinach chloroplasts, photochemical quenching has been observed in conjunction with the photoreduction of monodehydroascorbate (MDA). MDA is the primary product of the redox reaction between H_2O_2 and ascorbate catalyzed by ascorbate peroxidase (Miyake and Asada, 1992) (Figure 5.2). [Although MDA may also be reduced enzymically by NADPH in a reaction catalyzed by a reductase, this photoreduction was shown to be largely dependent on ferredoxin (Miyake and Asada, 1994)]. Quenching of chlorophyll fluorescence by H_2O_2 occurs in higher plants and certain cyanobacteria, however, H_2O_2-induced quenching does not occur in cyanobacteria which lack ascorbate peroxidase (Miyake *et al.*, 1991). Although *Euglena* cells do not possess chloroplastic ascorbate peroxidase but only the cytosolic isozyme, ascorbate-peroxidase-catalyzed H_2O_2 reduction in *Euglena* utilized a photoreductant as an electron donor as opposed to endogenous reductants (like NADPH) or respiration (Miyake *et al.*, 1991). Apparently, photoreductants generated

in the thylakoids may be utilized not only inside the chloroplast but in the cytosol, possibly even at the plasma membrane. Higher plants possess both chloroplastic and cytosolic isozymes of ascorbate peroxidase. Thus, in asparagus cells, photochemical quenching may occur due to electron flow in the reduction of H_2O_2 to H_2O in the chloroplast and/or the cytosol or even in the reduction of O_2 to $O_2^{\cdot -}$ (Figure 5.2). If

Figure 5.2: The Mehler-Peroxidase Cycle

(Fd = ferredoxin; AsA = ascorbate; MDA = monodehydroascorbate)

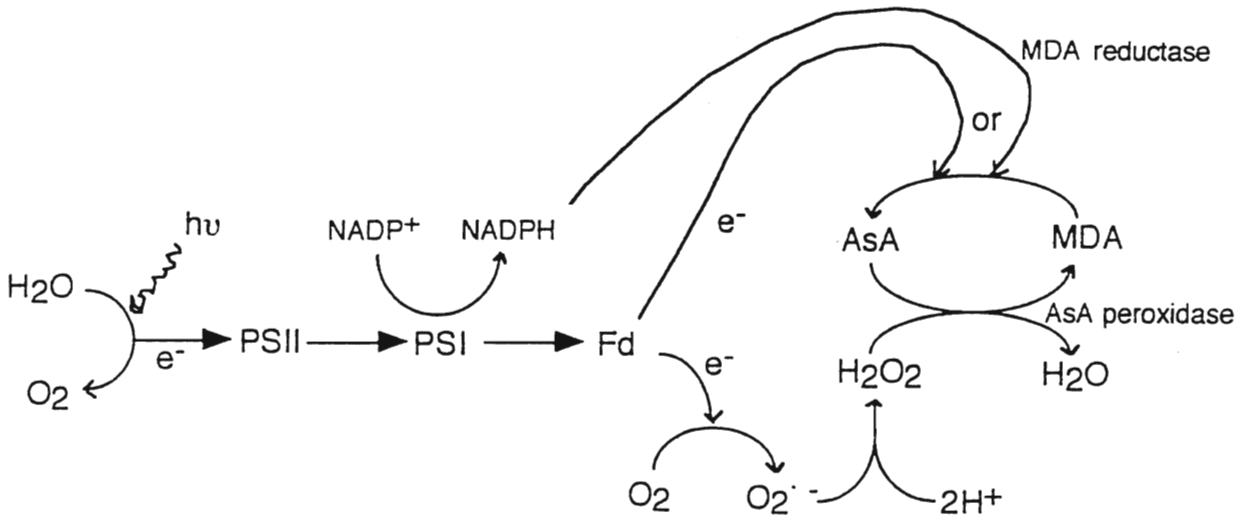

photoreductants could be used to reduce molecular oxygen at the plasma membrane, this would answer the question of the source of the reducing power required to reduce over 250 μmols of O_2 in the light, at least (Table 4.1) [See section 5.3.3. re: the source of reductant for the oxidative burst]. In the dark, only a small amount of photochemical quenching was observed (Figure 4.8). The small extent of Q_A oxidation may reflect the withdrawal of the few electrons remaining in the PSII in the dark to fuel the reduction of

O_2 or H_2O_2. The result would be a fully oxidized electron transport system. Rereduction of Q_A is light-driven; thus it occurs in the light but not in the dark.

The nonphotochemical component of chlorophyll *a* fluorescence is also affected by MP. After a lag period similar to that of O_2 uptake, increased nonphotochemical quenching was observed in the light (Figure 4.7) and in the dark (Figure 4.8). Most nonphotochemical quenching is caused by "energization" of thylakoid membranes which results from the formation of a pH gradient. It is therefore termed "energy-dependent" quenching (Neubauer and Schreiber, 1988; Schreiber *et al.*, 1991). Some stromal alkalinization and lumen acidification normally occur due to the proton pumping associated with photosynthetic electron transport. Thus, in the light, a degree of nonphotochemical quenching is observed. Nonphotochemical quenching due to ΔpH formation may be relieved by the protonophore nigericin. MP-induced nonphotochemical quenching was not relieved by the addition of nigericin (see Appendix II.3.), indicating that it is not a result of a pH gradient across thylakoid membranes. Although H_2O_2 induces light-dependent nonphotochemical quenching in spinach chloroplasts (Schreiber *et al.*, 1991), MP-stimulated nonphotochemical quenching is light-independent and should not be attributed to H_2O_2. In this case, because nonphotochemical quenching occurs concurrently with lost photosynthetic activity, it is ascribed to the death of the cells (Figure 4.2).

5.3.2. The mechanism of the MP-stimulated oxidative burst

A controversy exists regarding the enzyme responsible for the reduction of O_2 during the oxidative burst. Data gleaned from certain experimental systems indicate a plasma membrane NADPH oxidase which reduces O_2 to $O_2^{\cdot -}$ (Vianello and Macrì,

1989; Auh and Murphy, 1995; Doke *et al.*, 1996; Nürnberger *et al.*, 1997). Other data favour a cell-wall peroxidase which reduces O_2 directly to H_2O_2 (Bolwell *et al.*, 1995). The signal transduction paradigm for the activation of the cell-wall peroxidase in the oxidative burst is very weak. Extracellular alkalinization has been suggested to activate the putative peroxidase which has a pH optimum of 7.2 (Bolwell *et al.*, 1995). On the other hand, many components of a G protein-mediated signal transduction pathway have been implicated in the activation of a plant plasmalemma oxidase (Legendre *et al.*, 1992, 1993a, 1993b; Schwacke and Hager, 1992; Morré *et al.*, 1993; Vera-Estrella *et al.*, 1994b; Munnik *et al.*, 1995). For example, guanine nucleotides and MP both stimulated NADH oxidase activity in soybean hypocotyl plasma membranes (Morré *et al.*, 1993). In tomato cells, the non-hydrolyzable GTP analogue GTPγS and MP each stimulated dephosphorylation of NADH oxidase and ascorbate peroxidase, causing activation and inhibition of enzyme activity, respectively (Vera-Estrella *et al.*, 1994b). The same alterations in enzyme activity were also observed in an incompatible interaction between these cells and a race-specific elicitor. The MP-stimulated generation of $O_2^{\cdot -}$ in asparagus mesophyll cells (MacGregor, 1997) (see section 5.3.1.1. O_2 data) indicate that an NAD(P)H oxidase is responsible for the oxidative burst in the plant system under investigation here.

Several possible G protein-mediated signal transduction pathways may be initiated by MP and lead to the oxidative burst (Model 5.2). Certain pathways are Ca^{2+}-dependent, while others are Ca^{2+}-independent. As shown in Model 5.2(A), MP may induce Ca^{2+} influx by G protein activation of plasma membrane Ca^{2+} channels (Brown and Birnbaumer, 1990; Fairley-Grenot and Assmann, 1991) or by G-protein-stimulated PI signal transduction (IP_3) (Drobak and Watkins, 1994; Cho *et al.*, 1995;

Jones and Kochian, 1995; Kim *et al.*, 1996; Tucker and Boss, 1996). There is also the possibility that MP activates PLC directly (Okano *et al.*, 1985). Increased cytosolic Ca^{2+} activates many Ca^{2+}-dependent enzymes (Bush, 1993; Smith, 1996) including Ca^{2+}/CaM-regulated GAD (synthesizing GABA) and Ca^{2+}-dependent protein kinases. Activation of NADPH oxidase by a Ca^{2+}-stimulated protein kinase stimulates the reduction of O_2 to $O_2^{\cdot -}$ with the concomitant oxidation of NADPH (Vianello and Macrì, 1989; Doke *et al.*, 1996).

A recent paper provides compelling evidence for Ca^{2+}/CaM involvement in the oxidative burst (Harding *et al.*, 1997). This study utilizes transgenic tobacco cells expressing a mutant calmodulin which cannot be post-transcriptionally methylated. A result of this mutation is hyperactivity of a calmodulin-dependent NAD kinase, which phosphorylates NAD^+ to form $NADP^+$. When exposed to stimuli that elicit defense responses, a larger and more rapid oxidative burst was observed with these mutant cells than with cells possessing a negative control construct. At a time coinciding with the production of H_2O_2, the mutant cells also possess 4-fold higher levels of NADPH than the control cells. These data indicate a mechanism by which cytosolic Ca^{2+} increases may initiate the oxidative burst by stimulating Ca^{2+}/CaM-dependent $NADP^+$ production [Model 5.2(A)].

There is also evidence for MP-stimulated Ca^{2+}-independent signal transduction which leads to an oxidative burst. Although extracellular free Ca^{2+} was essential for GABA accumulation and cell death and allowed alkalinization of the medium to a greater extent, it was not required for the oxidative burst in asparagus

Model 5.2: Possible Signal Transduction Pathways Initiated by Mastoparan Leading to the Oxidative Burst: (A) Ca^{2+}-dependent pathways; (B) Ca^{2+}-independent pathways. [PM = plasma membrane; G = G protein; PLC = phospholipase C; kinase = Ca^{2+}-dependent protein kinase; GAD = glutamate decarboxylase; P = phosphate; XH_2 = generic reductant of $NADP^+$ (X = oxidized form of XH_2); CaM = calmodulin; PLA_2 = phospholipase A_2].

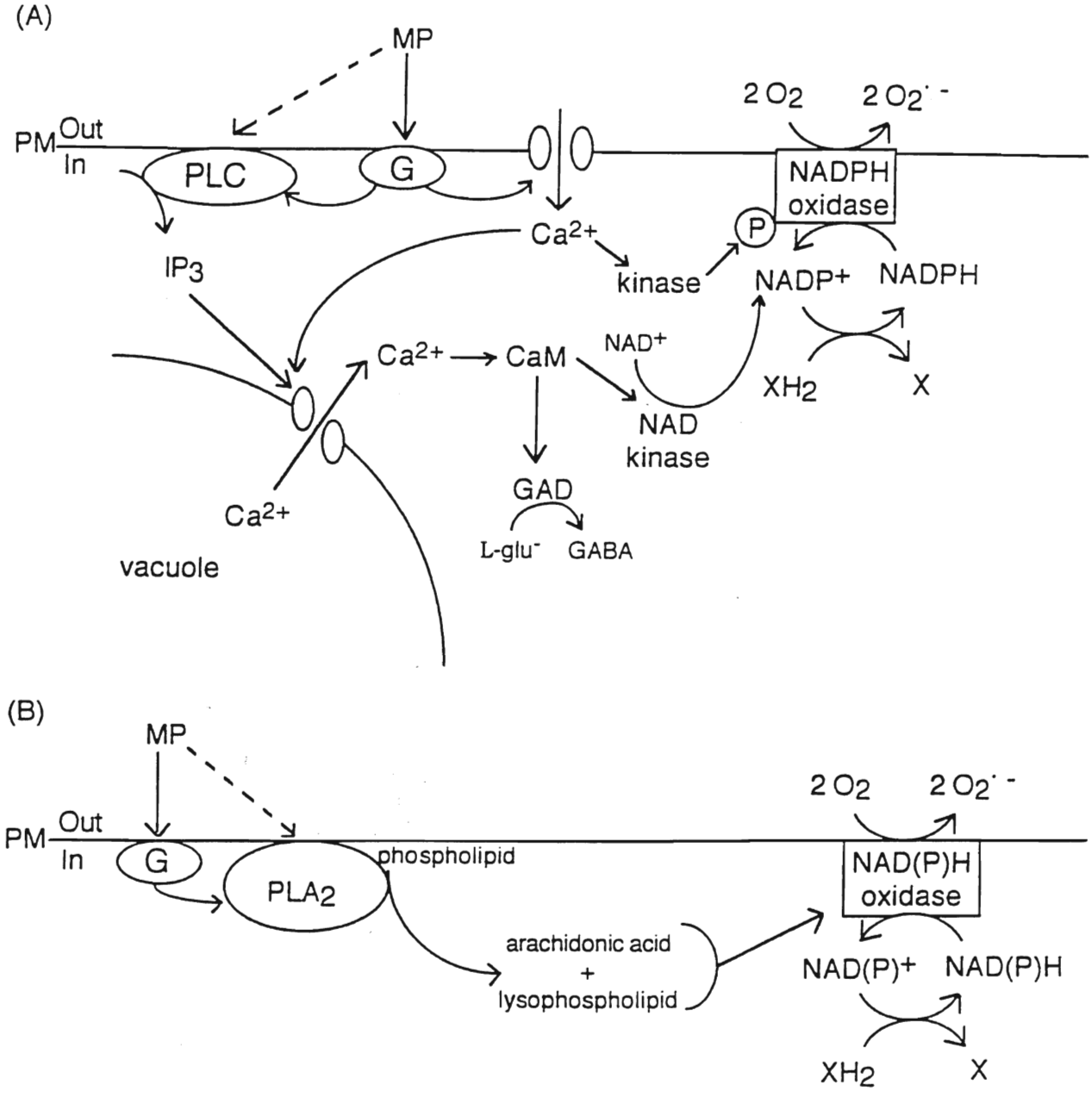

cells (Wong, 1997). Perhaps internal Ca^{2+} is involved in this "Ca^{2+}-independent" signal transduction. Alternatively, there are signal transduction pathways which lead to the reduction of O_2 that do not involve intracellular or extracellular Ca^{2+}. MP may stimulate phospholipase A_2 (PLA_2) directly (Argiolas and Pisano, 1983; Scherer, 1992) or via a G protein (Axelrod, 1990; Fischer *et al.*, 1993) [Model 5.2(B)]. Plant defense elicitors, mastoparan and auxins have been shown to activate plant PLA_2 *in vivo* and *in vitro* (Scherer and André, 1989; Scherer, 1992; Chandra *et al.*, 1996). Activation of PLA_2 leads to the hydrolysis of a phospholipid, yielding a free fatty acid (usually arachidonic acid in mammalian cells) and a lysophospholipid as products (Chandra *et al.*, 1996). Arachidonic acid in conjunction with lysophospholipids stimulated soybean plasma membrane NADH oxidase activity (Brightman *et al.*, 1991). Arachidonic acid is a fungal elicitor whose mode of action is unknown. In cultured fibroblast cells, MP stimulated arachidonic acid release and did not initiate phosphinositide signal transduction (Gil *et al.*, 1991). Arachidonic acid release in response to MP was blocked by prior treatment with pertussis toxin, indicating that the response was mediated by a pertussis-toxin-sensitive G protein in these cells. In a previous study, arachidonic acid application to isolated asparagus mesophyll cells caused GABA accumulation and cell death (Cleve, 1995). The mechanism by which arachidonic acid stimulated these effects is not clear: it may have acted via a receptor-linked G protein or by direct stimulation of an NAD(P)H oxidase, leading to the oxidative burst and subsequent cell death [Model 5.2(B)].

Another Ca^{2+}-independent pathway by which MP may initiate the oxidative burst (not shown) involves a third phospholipase, phospholipase D (PLD). Like PLA_2, PLD hydrolyzes phospholipids. Its product, phosphatidic acid (PA), however, is

different. MP and other G protein activators have been demonstrated to stimulate PLD signalling in higher plants and green algae (Munnik *et al.*, 1995). In *Chlamydomonas* cells, G protein activation by MP caused the formation of PA (Munnik *et al.*, 1996) which was then converted to DAG pyrophosphate. In human neutrophils, PA and DAG activate a plasma membrane NADPH oxidase in concert (Qualliotine-Mann *et al.*, 1993). Although this activation was observed in an animal system, it may prove to be an additional way in which the oxidative burst in plants parallels the human neutrophil oxidative burst.

The synergistic activation of the NADPH oxidase by PA and DAG suggests that PLD and PLC may be activated together in G protein-mediated signal transduction. The paradigm for the induction of the oxidative burst in human neutrophils is highly complicated as "second-messenger products from the receptor-activated phospholipases A_2, C, and D are now known to induce NADPH oxidase activation" (Qualliotine-Mann *et al.*, 1993) in cell-free systems, at least. It is very likely that the corresponding signal transduction in plants has a similar level of complexity.

5.3.3. The source of reducing power for the MP-stimulated oxidative burst

In order for 3 million cells to reduce approximately 200 μmol of O_2 to H_2O (Table 4.1), 400 μmols of NADPH (or 800 μmols of electrons) would be required. With a volume of 4.7 p*L*/asparagus cell (Snedden *et al.*,1992), the concentration of NADPH in each cell would have to be 28 mM. This concentration is much higher than occurs physiologically. Clearly, another source of reducing equivalents must be drawn upon. The recent paper by Harding and colleagues (1997) demonstrated that the oxidative burst was enhanced by the activation of NAD kinase which converted NAD^+ to $NADP^+$. The oxidation of other metabolites may be coupled to the reduction of $NADP^+$

(Model 5.3). Possible metabolites include glucose-6-phosphate and 6-phosphogluconate [intermediates of the pentose phosphate pathway (cytosol)], malate and triose phosphates exported from the chloroplast (Goodwin and Mercer, 1983). There are cytosolic enzymes or enzyme pathways which oxidize these metabolites with concomitant reduction of $NADP^+$ to NADPH. Plant cells may even stop reductive metabolic processes and upregulate oxidative processes in order to fuel the reduction of O_2 or to replenish reducing power following the oxidative burst if the cell has not died in the process. For example, in spinach chloroplasts, H_2O_2 reversibly inhibits the Calvin cycle (a process that consumes 3 ATP and 2 NADPH for each molecule of CO_2 that is fixed) and activates the oxidative pentose phosphate pathway which produces reducing power (Kaiser, 1979). In fact, H_2O_2 stimulates the formation of 6-phosphogluconate by greater than 1000%. This increase is ascribed to the activation of glucose-6-phosphate dehydrogenase which involves the production of NADPH. Reducing power is not only necessary for the reduction of O_2 but may also be required for the reduction (scavenging) of H_2O_2 and oxidized intermediates of the Mehler peroxidase pathway. It is not an unreasonable response for a microbially challenged plant cell to use up all of its chemical energy supply to fuel an oxidative burst which will lead to its death and the overall survival of the host plant.

5.3.4. The role of light in the MP-stimulated oxidative burst

The oxidation of Q_A following $Fe(CN)_6^{3-}$ addition to an asparagus cell suspension (Figure 4.6) indicates that chloroplast redox activities and plasma membrane redox activities are coupled. Plant cells are impermeable to $Fe(CN)_6^{3-}$ (Rubinstein *et al.*, 1984) and reducing equivalents generated by photosynthesis can

be used to reduce extracellular oxidizing agents. The reduction of ferricyanide may be catalyzed by the integral plasma membrane redox enzyme NADH-ferricyanide oxidoreductase (Rubinstein *et al.*, 1984; Morré *et al.*, 1988). However, the increased rate of O_2 evolution following $Fe(CN)_6^{3-}$ addition suggests that the redox enzyme responsible may be one that normally reduces O_2 at the cell surface. A likely candidate is the plasma membrane NADPH oxidase. A novel application arising from this study is the use of PAM chlorophyll fluorometry in monitoring plasma membrane redox reactions.

The reduction of exogenous $Fe(CN)_6^{3-}$ by plasma membrane redox systems has been demonstrated previously at the surface of oat root cells (Rubinstein *et al.*, 1984), in asparagus mesophyll cell suspensions (Neufeld and Bown, 1987), in soybean plasma membrane vesicles and excised soybean hypocotyls (Morré *et al.*, 1988), and in suspension-cultured tomato cells (Vera-Estrella *et al.*, 1994b). The reduction of $Fe(CN)_6^{3-}$ by asparagus cells was demonstrated to be tightly coupled with medium acidification (Neufeld and Bown, 1987). Although $Fe(CN)_6^{3-}$ reduction and acidification of the medium occurred in the absence of light, both processes were enhanced 1400 - 1600% when the cell suspension was illuminated. Thus, the reduction of $Fe(CN)_6^{3-}$ at the plasma membrane of asparagus mesophyll cells is light-stimulated but not light-dependent.

Light-stimulation of the reduction of $Fe(CN)_6^{3-}$ at the plasma membrane suggests a role for light in other plasma membrane redox processes. In this study, the data indicate that light does, in fact, enhance MP-stimulated O_2 uptake and hence the

oxidative burst (Table 4.1). Light caused an increased rate of O_2 uptake and a larger net O_2 consumption. The idea of light involvement in the hypersensitive response is not new. Peever and Higgins (1989) observed that although lipoxygenase activity and lipid peroxidation appeared to be light-independent, necrosis in tomato leaf tissue induced by incompatible fungal elicitation was delayed in the dark. In addition, photosynthesis has been directly implicated in plant defense (Peterson and Aylor, 1995). When *Phaseolus vulgaris* leaves were infected with an obligate biotrophic fungus, intense chlorophyll fluorescence monitored with video imaging was induced at centres where lesions developed 3 - 4 days later. Thus, reduction in the photochemical utilization of light seems to be involved in stages of plant defense preceding the HR.

Light-stimulation of the oxidative burst in asparagus cells (Table 4.1) implies the involvement of reducing equivalents generated by photosynthesis. Although NADPH is the main reductant produced in photosynthesis, there is no evidence for NADPH export from the chloroplast. In order for photosynthetically derived reducing equivalents to be available for the reduction of O_2 at the plasma membrane, they must leave the chloroplast. Reducing equivalents may leave the chloroplast via the phosphoglycerate(PGA)/dihydroxyacetone phosphate (DHAP) (triose phosphate) shuttle and/or the malate/oxaloacetate (OAA) shuttle (Model 5.3) (Heber, 1974). Once in the cytosol, DHAP can be oxidized with the concomitant reduction of OAA to malate in a 2-step enzyme-catalyzed process (Goodwin and Mercer, 1983). Malic enzyme generates NADPH while converting malate into pyruvate. Thus, photosynthesis may enhance the rate of the oxidative burst by replenishing the NADPH pool for the plasma membrane NADPH oxidase (Model 5.3).

Model 5.3: The Mechanism of Light Enhancement of the Oxidative Burst

(PM = plasma membrane; OAA = oxaloacetate; DHAP = dihydroxyacetone phosphate; PGA = 3-phosphoglycerate).

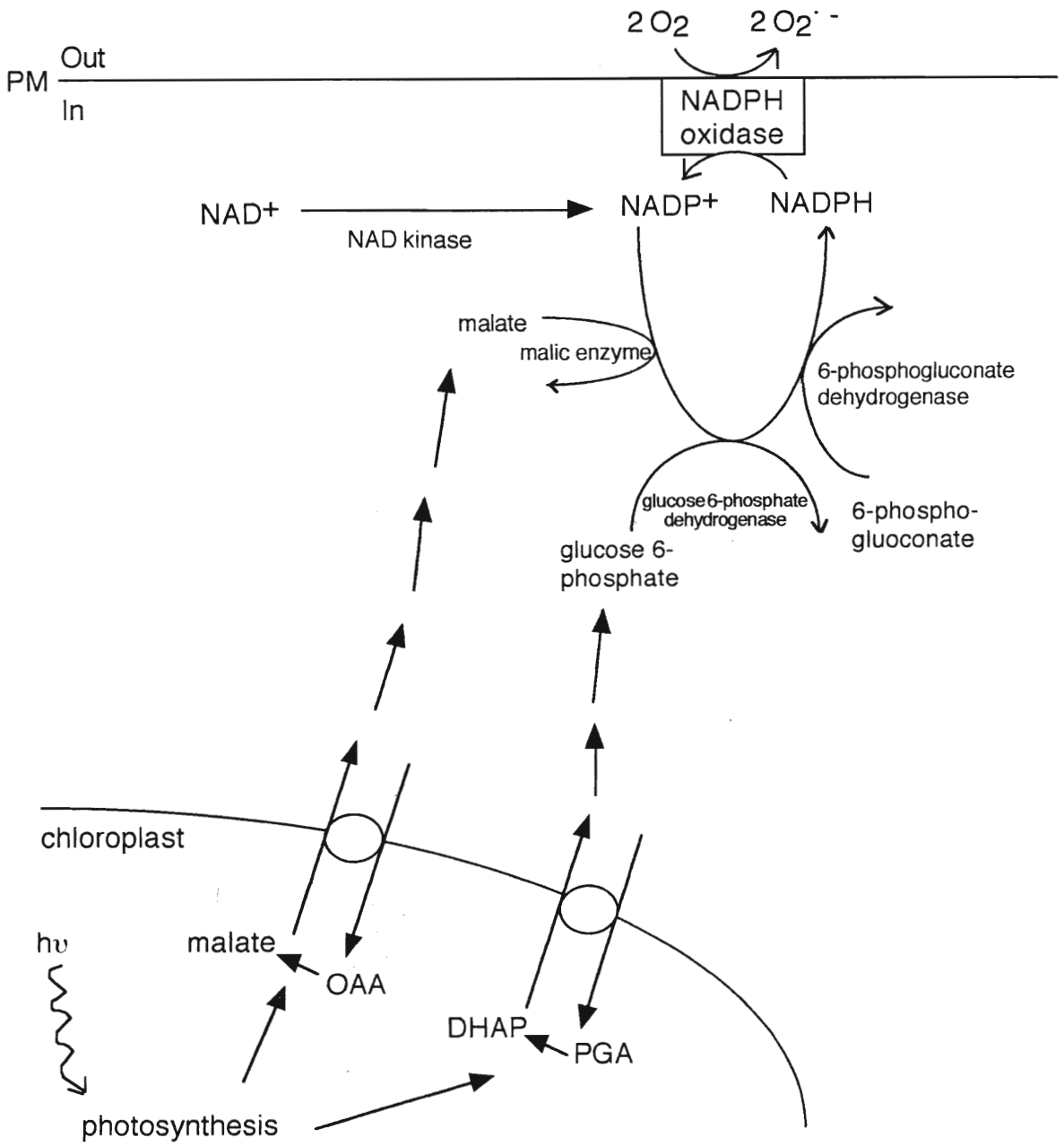

5.4. The effects of H_2O_2 on chlorophyll *a* fluorescence and O_2 concentration

Although H_2O_2 did not affect asparagus cell viability (see Appendix II.4.), H_2O_2 did have an effect on the cells. H_2O_2 stimulation of light-independent O_2 evolution (Figure 4.11) suggests that H_2O_2 is being reduced to H_2O by ascorbate peroxidase with concomitant production of O_2 (Model 5.4). Non-assimilatory O_2 evolution is characteristic of ascorbate peroxidase activity (Neubauer and Schreiber, 1988; Miyake and Asada, 1992). It lasts only until H_2O_2 is consumed. This correlates well with the temporary nature of the H_2O_2-stimulated O_2 evolution observed in Figure 4.10. After this non-photosynthetic O_2 evolution tapered off, no photosynthetic O_2 evolution occurred. This observation is consistent with the photosynthetic toxicity of H_2O_2 (see section 5.3.1.1. O_2 data).

Hydrogen peroxide caused light-dependent nonphotochemical quenching of chlorophyll *a* fluorescence (Figure 4.11). Schreiber and colleagues (1991) reported the same phenomenon in spinach chloroplasts. This nonphotochemical quenching was attributed to O_2-dependent nonassimilatory electron flow resulting in the reduction of H_2O_2 and the formation of a ΔpH. In the dark, there is neither assimilatory nor nonassimilatory electron flow, thus there is no ΔpH produced and no nonphotochemical quenching.

5.5. MP stimulation of the HR

Characteristics of the HR are ion fluxes (Ca^{2+} influx, K^+ and anion effluxes), changes in the pH of the medium, membrane depolarization, the oxidative burst (O_2 uptake and reduction to form AOS) and cell death.

In asparagus mesophyll cells, MP induces cell death (Figure 4.2); alkalinization of the medium (Figure 4.5); O_2 uptake, a measure of the oxidative burst (Neubauer and Schreiber, 1988; Schreiber *et al.*, 1991; Miyake and Asada, 1992; Vera-Estrella *et al.*, 1992; Robertson *et al.*, 1995; Chandra *et al.*, 1996; Harding *et al.*, 1997)(Figure 4.7); and concurrent $O_2^{\cdot -}$ generation (MacGregor, 1997). The preponderance of the evidence indicates that MP is inducing the HR in the cells being studied.

5.6. The mechanism of MP-stimulated cell death

The formation of $O_2^{\cdot -}$ leads to the generation of the other AOS through reactions shown in Model 5.4. Spontaneous (not shown) or superoxide dismutase-catalyzed dismutation of $O_2^{\cdot -}$ produces H_2O_2 (Sutherland, 1991). H_2O_2 may be reduced to water by ascorbate/ascorbate peroxidase with O_2 as a byproduct. [The reduction of H_2O_2 by catalase is not shown in Model 5.4. This is due to the fact that, in leaf cells, catalase is almost exclusively localized in peroxisomes (Asada, 1992); thus in the presence of other more proximal scavenging enzymes, H_2O_2 is unlikely to diffuse into peroxisomes for scavenging by catalase.] H_2O_2 also reacts with $O_2^{\cdot -}$ in an Fe^{3+}-catalyzed Fenton reaction to produce the most destructive AOS, $OH^{\cdot}$. [Iron is a contaminant of the $CaSO_4$ salt used in the cell suspension medium]. Hydroxyl radicals initiate a chain reaction of lipid peroxidation (Mehdy, 1994). Extensive membrane damage and electrolyte leakage lead ultimately to the death of the cell

Model 5.4: The Oxidative Burst and Cell Death: Possible Mechanisms

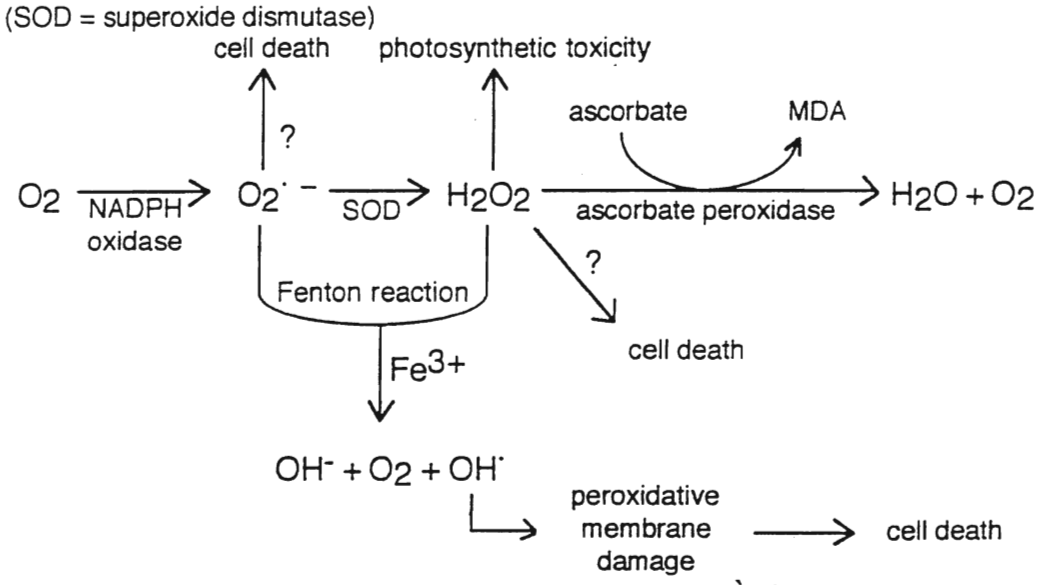

(Keppler and Novacky, 1987; Rogers *et al.*, 1988; Àdàm *et al.*, 1989; Peever and Higgins, 1989).

Cell death has also been documented in response to both $O_2^{\cdot -}$ and H_2O_2 independently although the mechanisms by which they lead to cell death are not known. The superoxide anion radical was necessary and sufficient to cause cell death in *Arabidopsis lsd1* ("lesion simulating disease resistance") mutants, while H_2O_2 failed to induce necrotic lesions in this mutant (Jabs *et al.*, 1996). In contrast, treatment of soybean cultured cells with 6 - 8 mM H_2O_2 induced their death (Levine *et al.*, 1994). The latter is in opposition to the data generated in this study where H_2O_2 (0.5 mM - 50 mM) failed to cause asparagus cell death (data not shown). The inability of SOD to inhibit MP-stimulated cell death also suggests that $O_2^{\cdot -}$ is not causing the death of these cells (see Appendix II.6.). The data indicate a mechanism in which MP stimulates cell death via the $OH^{\cdot}$ radical as described. According to this mechanism,

$O_2^{\cdot -}$ is essential for hypersensitive cell death, however cell death is dependent on its dismutation to H_2O_2 allowing the production of $OH^{\cdot}$. The observed inhibition of ascorbate peroxidase activity in an incompatible plant-pathogen interaction may serve to ensure the presence of H_2O_2 for the Fenton reaction (Vera-Estrella *et al.*, 1994). The MP-stimulated consumption of H_2O_2 (Table 4.2.) is readily explained by this hypothetical mechanism. In the experiment where MP alone is added to the cells, MP initiates the oxidative burst reactions as described above and H_2O_2 is used up in reaction with $O_2^{\cdot -}$. When MP is added to the cell suspension containing exogenous H_2O_2, the same reaction sequence occurs and even the extra H_2O_2 is spent in the Fenton reaction. H_2O_2 remains in the suspension and is able to be measured only in the absence of MP-stimulated $O_2^{\cdot -}$.

An alternative mechanism for MP-stimulated cell death involves the activity of lipid peroxidative enzymes called lipoxygenases. H2O2 activation of PLA2 leads to the activation of lipoxygenase activity (Doke et al., 1996). Furthermore, elicitors from *Cladosporium fulvum* induced electrolyte leakage, lipoxygenase activity and lipid peroxidation in tomato leaf tissue (Peever and Higgins, 1989). However, lipoxygenase activity was not investigated in this study.

5.7. MP as a G protein activator

Regarding signal transduction pathways, Legendre and colleagues (1993) aptly comment that the

"Identification of specific components in a signal transduction pathway should

> ideally be performed with multiple perturbants of a single component of an uncomplicated section of the transduction pathway. Failure to employ highly specific reagents can obviously lead to perturbations not related to the target protein...Failure to select a short, uncomplicated section of the pathway...not only enhances the probability of nonspecific perturbations within the pathway but also increases the likelihood of perturbing parallel, interacting (cross-talking) pathways."

This study attempts to evaluate the role of G proteins in signal transduction leading to the HR in asparagus mesophyll cells. Although MP is known to act in various capacities there are many studies in which the mode of action of MP seems to be to stimulate G proteins. However, as more research on signal transduction is performed, it seems that there are no "short, uncomplicated" sections, as is commonly observed in biological systems.

Since the mechanism of G protein activation and the putative MP/G protein binding site has been established in animal cells (Higashijima *et al.*, 1990; Higashijima and Ross, 1991), researchers have been using MP with plant cells in an attempt to activate analogous plant G proteins (Legendre *et al.*, 1992, 1993a, 1993b; Vera-Estrella *et al.*, 1994a, 1994b; Cho *et al.*, 1995; Kauss and Jeblick, 1995, 1996).

A variety of evidence supports the specific action of MP in G protein activation. First of all, Mas17, an inactive synthetic analogue of MP provides a helpful control to distinguish nonspecific effects of amphipathic peptides from the specific effects of MP (Figures 4.1, 4.2, 4.5, 4.7). Mas17, also a tetradecapeptide, differs from MP by 2 amino acids (Leu^6 --> Lys and Ile^{13} --> Leu). Only the Leu^6 --> Lys substitution eliminates the activity of MP, as Mas7, a highly active synthetic MP analogue, shares the same amino acid as Mas17 at position 13 (Leu). The critical amino acid substitution at position 6 in Mas17 is believed to decrease the tendency of α-helix formation upon association with lipid bilayers (White *et al.*, 1993). Several studies have shown that while MP effects a

cellular response similar to a fungal elicitor (the oxidative burst, phosphoinositide turnover, phospholipase A stimulation), Mas17 did not (Legendre *et al.*, 1993a, 1993b; Chandra *et al.*, 1996; Kauss and Jeblick, 1996). The absolute requirement for a certain amino acid at position 6 suggests that MP is participating in a specific interaction, likely with a G protein causing GDP/GTP exchange.

As anticipated by their amino acid sequences, MP and Mas17 are able to enter lipid bilayers. After 2 - 5 min of incubation with MP and Mas17 tagged with fluorescent labels, fluorescence was localized inside cultured carrot cells, even in endomembranes (Cho *et al.*, 1995). Although no fluorescence was detected in either starch granules or the nucleus, small vacuoles showed fluorescence after about 10 min. MP entry into the cell is required for it to mimic the cytosolic domain of the receptor, thereby activating a G protein.

The low concentrations of MP used to elicit a defense response also support the specific activation of G proteins. In this study, MP concentrations used to achieve a cellular response ranged from 3.3 μM to 25 μM (Figures 4.1, 4.2, 4.3, 4.4, 4.5, 4.7, 4.8, 4.9, Table 4.1, exception Table 4.2: 64 μM). The threshold concentration of MP required to initiate net O_2 uptake lies between 1.65 μM and 3.3 μM (Figure 4.9) and the threshold concentration causing both cell death and GABA accumulation lies between 2.5 μM and 25 μM (Figure 4.4; Allen, 1995). Nonspecific effects of amphiphilic peptides (often relying on membrane disruption) typically require ≥100 μM (vs. 1 - 10 μM) concentrations (Higashijima *et al.*, 1990; Raynor *et al.*, 1991) and within limits, the higher the concentration the greater the effect. Research done by Fischer and colleagues (1993) demonstrated that alkylamines inhibited MP-stimulated histamine release from mast cells. The mechanism causing inhibition was believed to be "nonselective perturbation of membrane lipid organization resulting in a loss of G protein activity." High concentrations of amphipathic peptides have even caused

modest stimulation of GTPase activity (Higashijima *et al.*, 1990). In contrast, elicitors are often highly specific so that elicitation may only require concentrations in the nM or μM ranges (Felix *et al.*, 1993; Granado *et al.*, 1995, Kauss and Jeblick, 1995, 1996). MP causes elicitor-like effects at elicitor-range concentrations. Specifically, MP causes the oxidative burst, phosphatidylinositol turnover and PLase A-activation in different plant species at concentrations ranging from 0.4 μM to 25 μM (Legendre *et al.*, 1992, 1993a, 1993b; Cho *et al.*, 1995; Kauss and Jeblick, 1995, 1996; Chandra *et al.*, 1996). Kauss and Jeblick (1996) have reported that maximal production of H_2O_2 occurred in response to 0.4 - 0.5 μM MP. In fact, higher MP concentrations proved to be inhibitory. Legendre and colleagues (1993b) observed that the MP concentration causing half-maximal stimulation of the oxidative burst (≈ 2.5 μM) was comparable to the concentration causing half-maximal G protein activation in animals (≈ 5 μM) (Higashijima *et al.*, 1990).

MP activity has been mimicked by GTP analogues in other plant systems, implicating G protein activation in response to MP. In two studies, GTP(γ)S, a non-hydrolyzable GTP analogue that locks G proteins into an active state, but not GDP(β)S, a similar analogue that locks G proteins into an inactive state, effected the same response as MP in tomato cells (Vera-Estrella *et al.*, 1994a, 1994b). In each case, the effects of GTP(γ)S and MP mimicked those seen in response to an incompatible interaction between *Cladosporium fulvum* and tomato cells, specifically, changes in plasma membrane redox activities and increased plasma membrane H^+-ATPase activity.

Evidence from work done by Cho and colleagues (1995) seems to rule out the direct activation of PLC by MP in cultured carrot cells. Mas7 was able to stimulate PIP-

PLC activity *in vivo*, but not *in vitro*, suggesting that a factor required to mediate the G protein activation of PLC was lost in the isolation process. It was suggested that MP may cause PLC activation by activating G proteins which directly control ion transport proteins, specifically Ca^{2+} channels [Model 5.2(A)]. This was substantiated by La^{3+} reduction of MP-induced PI turnover (Cho *et al.*, 1995). G protein involvement in regulating K^+ or Ca^{2+} channels has already been postulated (Brown and Birnbaumer, 1990; Fairley-Grenot and Assmann, 1991). In addition, a requirement for external Ca^{2+} for MP-induced cell death and the full extent of alkalinization has very recently been demonstrated (Wong, 1997). The inability of MP to effect a response in the absence of Ca^{2+} makes MP activation of PLC unlikely to be a result of direct interaction of the peptide with the enzyme. Furthermore, the requirement for external Ca^{2+} also rules out the nonspecific action of MP.

Within the recognized limitations, the data indicate that MP is eliciting the HR in isolated asparagus cells by activation of G proteins.

5.8. The relationship between GABA accumulation and the HR: causal or coincidental?

According to Model 5.2(A), MP induces Ca^{2+} influx either from the apoplast via G-protein-modulated Ca^{2+} channels in the plasma membrane and/or from the vacuole, potentiated by IP_3 or external Ca^{2+} influx (Bush, 1995). Ca^{2+} influxes lead to the activation of many target proteins, especially protein kinases and Ca^{2+}/CaM-dependent enzymes (Bush, 1993). This model explains MP-induction of GABA accumulation as well as MP induction of the oxidative burst via activation of a plasma

membrane NADPH oxidase. NAD(P)H oxidase may be activated by phosphorylation (Doke *et al.*, 1996), increased $NADP^+$ (Harding *et al.*, 1997), or by products of PLA_2 (or possibly PLD) activity (Brightman *et al.*, 1991; Qualliotine-Mann *et al.*, 1993). What is not clear is whether GABA accumulation and the HR are causally or coincidentally linked. Is it possible for the HR to occur without GABA accumulation?

To dissect the nature of the relationship, staurosporine, a general protein kinase inhibitor was employed. It was thought that if GABA synthesis was simply coincidental with the HR, inhibition of phosphorylation might block the MP-induced oxidative burst and HR [Model 5.2(A)] with GABA accumulation unhindered. Staurosporine did not decrease MP-induced GABA synthesis as was expected (see Appendix II.8.), however, it also did not prohibit O_2 uptake in response to MP (see Appendix II.9.). Thus, the data did not permit a conclusion to be made regarding the nature of the relationship between GABA accumulation and the HR. Because of the negative nature of the results, a role for phosphorylation in the HR cannot be dismissed with certainty.

While a role for G proteins in elicitor signal transduction has been implicated many times in the literature (Bolwell *et al.*, 1991; Legendre *et al.*, 1992, 1993a, 1993b; Vera-Estrella *et al.*, 1994a, 1994b; Kauss and Jeblick, 1995, 1996), only one previous report has shown G protein activation leading to GABA accumulation (Aurisano *et al.*, 1996). In this study, the G protein activator MP has been demonstrated to cause GABA accumulation in asparagus cells (Figure 4.1). This is only the second time a link between GABA accumulation and G protein signal transduction has been documented.

Just as H_2O_2 from the oxidative burst has been postulated to be involved in signaling further defense strategies in plants (Smith, 1996), hypersensitively stimulated GABA accumulation may play a role in intercellular signaling through efflux

from non-damaged cells or leakage from compromised cells (Figure 4.1). This recently generated hypothesis is based on data which demonstrate that newly synthesized GABA is subject to efflux (Chung *et al.*, 1992), that GABA appears to play a role in plant growth and development (Chen *et al.*, 1994; Baum *et al.*, 1996), and the possibility that plant cells possess plasma-membrane-located GABA receptors analogous to those found in animal nervous systems.

It is not clear whether or not GABA accumulation is causally linked to the plant HR.

Conclusions

1. MP causes GABA accumulation and efflux in asparagus cells.

2. GABA accumulation is not a marker for dead plant cells.

3. MP causes the hypersensitive death of asparagus cells.

4. MP stimulates an oxidative burst in asparagus cells.

5. The rate and extent of the MP-stimulated oxidative burst is enhanced by light.

6. H_2O_2 causes photosynthetic inhibition in asparagus cells, but does not kill them.

7. MP stimulates the degradation of H_2O_2.

8. It is not clear whether a causal relationship exists between the MP-stimulation HR and GABA accumulation.

References

Ádám A, Farkas T, Somlyai G, Hevesi M, Király Z (1989) Consequence of $O_2^{\cdot -}$ generation during a bacterially induced hypersensitive reaction in tobacco: deterioration of membrane lipids. Physiol Mol Plant Pathol **34**: 13-26

Alexandre J, Lassalles JP, Kado RT (1990) Opening of Ca^{2+} channels in isolated red beet root vacuole membrane by inositol-1,4,5-trisphosphate. Nature **343**: 567

Allen LJ (1995) The effect of mastoparan, a G protein activator, on GABA accumulation in *Asparagus sprengeri* mesophyll cells. Honours thesis. Brock University, St. Catharines, Ontario.

Apostol I, Heinstein PF, Low PS (1989) Rapid stimulation of an oxidative burst during elicitation of cultured plant cells. Plant Physiol **90**: 109-116

Arazi T, Baum G, Snedden WA, Shelp BJ, Fromm H (1995) Molecular and biochemical analysis of calmodulin interactions with the calmodulin-binding domain of plant glutamate decarboxylase. Plant Physiol **108**: 551-561

Argiolas A, Pisano JJ (1983) Facilitation of phospholipase A_2 activity by mastoparans, a new class of mast cell degranulating peptides from wasp venom. J Biol Chem **258**: 13697-13702

Asada K (1992) Ascorbate peroxidase - a hydrogen peroxide-scavenging enzyme in plants. Physiol Plant **85**: 235-241

Auh C-K, Murphy TM (1995) Plasma membrane redox enzyme is involved in the synthesis of O_2^- and H_2O_2 by *Phytophthora* elicitor-stimulated rose cells. Plant Physiol **107**: 1241-1247

Aurisano N, Bertani A, Reggiani R (1995) Involvement of calcium and calmodulin in protein and amino acid metabolism in rice roots under anoxia. Plant Cell Physiol **36**: 1525-1529

Aurisano N, Bertani A, Reggiani R (1996) Evidence for the involvement of GTP-binding proteins in the process of anaerobic γ-aminobutyrate accumulation in rice roots. J Plant Physiol **149**: 517-519

Axelrod J (1990) Receptor-mediated activation of phospholipase A_2 and arachidonic acid release in signal transduction. Biochem Soc Trans **18**: 503-507

Bach M, Schnitzler J-P, Seitz HU (1993) Elicitor-induced changes in Ca^{2+} influx, K^+ efflux, and 4-hydroxybenzoic acid synthesis in protoplasts of *Daucus carota* L. Plant Physiol **103**: 407-412

Baum G, Chen Y, Arazi T, Takatsjui H, Fromm H (1993) A plant glutamate decarboxylase containing a calmodulin binding domain: cloning, sequence, and functional analysis. J Biol Chem **268**: 19610-19617

Baum G, Lev-Yadun S, Fridmann Y, Arazi T, Katsnelson H, Zik M, Fromm H (1996) Calmodulin binding to glutamate decarboxylase is required for regulation of glutamate and GABA metabolism and normal development in plants. EMBO J **15**: 2988-2996

Benhamou N (1996) Elicitor-induced plant defence pathways. Trends Plant Sci **1**: 233-240

Berridge MJ, Irvine RF (1989) Inositol phosphates and cell signalling. Nature **341**: 197-205

Boller T (1989) Primary signals and second messengers in the reaction of plants to pathogens. In *Second Messengers in Plant Growth and Development.* (Boss WF and Morre DJ, eds) New York: Alan R. Liss Inc, pp. 227-255

Bolwell GP, Coulson V, Rodgers MW, Murphy DL, Jones D (1991) Modulation of the elicitation response in cultured French bean cells and its implication for the mechanism of signal transduction. Biochemistry **30**: 397-405

Bolwell GP, Butt VS, Davies DR, Zimmerlin A (1995) The origin of the oxidative burst in plants. Free Rad Res **23**: 517-532

Boss WF (1989) Phosphoinositide metabolism: Its relation to signal transduction in plants. In *Second Messengers in Plant Growth and Development* (Boss WF and Morre DJ, eds) New York: Alan R. Liss Inc, pp. 29-56

Bown AW (1982) An investigation into the roles of photosynthesis and respiration in H^+ efflux from aerated suspensions of *Asparagus* mesophyll cells. Plant Physiol **70**: 803-810

Bown AW, Crawford LA (1988) Evidence that H^+ efflux stimulated by redox activity is independent of plasma membrane ATPase activity. Physiol Plant **73**: 170-174

Bown A, Shelp BJ (1989) The metabolism and physiological roles of 4-aminobutyric acid. Biochem (Life Sci Adv) **8**: 21-25

Bown AW, Shelp BJ (1997) The metabolism and functions of γ-aminobutyric acid. Plant Physiol, in press

Breitkreuz KE, Shelp BJ (1995) Subcellular compartmentation of the 4-aminobutyrate shunt in protoplasts from developing soybean cotyledons. Plant Physiol **108:** 99-103

Brightman AO, Zhu XZ, Morré DJ (1991) Activation of plasma membrane NADH oxidase activity by products of phospholipase A. Plant Physiol **96**: 1314-1320

Brosnan JM, Sanders D (1990) Inositol trisphosphate-mediated Ca^{2+} release in beet microsomes is inhibited by heparin. FEBS Lett **260**: 70-72

Brown AM, Birnbaumer L (1990) Ionic channels and their regulation by G protein subunits. Annu Rev Physiol **52**: 197-213

Bush DS (1993) Regulation of cytosolic calcium in plants. Plant Physiol **103**: 7-13

Bush DS (1995) Calcium regulation in plant cells and its role in signaling. Annu Rev Plant Physiol Plant Mol Biol **46**: 95-122

Cadenas E (1989) Biochemistry of oxygen toxicity. Ann Rev Biochem **58**: 79-110

Canut H, Carrasco A, Rossignol M, Ranjeva R (1993) Is vacuole the richest store of IP_3-mobilizable calcium in plant cells? Plant Sci **90**: 135-143

Carroll AD, Fox GG, Laurie S, Phillips R, Ratcliffe RG, Stewart GR (1994) Ammonium assimilation and the role of γ-aminobutyric acid in pH homeostasis in carrot cell suspensions. Plant Physiol **106:** 513-520

Chai HB, Doke N (1987) Activation of the potential of potato leaf tissue to react hypersensitively to *Phytophthora infestans* by cytospore germination fluid and the enhancement of this potential by calcium ions. Physiol Mol Plant Pathol **30**: 27-37

Chandra S, Heinstein PF, Low PS (1996) Activation of phospholipase A by plant defense elicitors. Plant Physiol **110**: 979-986

Chasan R (1995) New openings into stomata. Plant Cell **7**: 1113-1115

Chen Y, Baum G, Fromm H (1994) The 58-kilodalton calmodulin-binding glutamate decarboxylase is a ubiquitous protein in petunia organs and its expression is developmentally regulated. Plant Physiol **106**: 1381-1387

Cho MH, Tan Z, Erneux C, Shears SB, Boss WF (1995) The effects of mastoparan on the carrot cell plasma membrane polyphosphoinositide phospholipase C. Plant Physiol **107**: 845-856

Cholewa EM (1995) Cytosolic calcium levels and stress induced γ-amino butyrate synthesis in asparagus mesophyll cells. MSc thesis. Brock University, St. Catharines, Ontario.

Cholewa E, Cholewinski AJ, Shelp BJ, Snedden WA, Bown AW (1997) Cold-shock-stimulated γ-aminobutyric acid synthesis is mediated by an increase in cytosolic Ca^{2+}, not by an increase in cytosolic H^{+}. Can J Bot **75**: 375-382

Chung I, Bown AW, Shelp BJ (1992) The production and efflux of 4-aminobutyrate in isolated mesophyll cells. Plant Physiol **99**: 659-664

Cleve RH (1995) Does the fungal elicitor arachidonic acid stimulate GABA synthesis? Honours thesis. Brock University, St. Catharines, Ontario.

Colman B, Mawson BT, Espie ES (1979) The rapid isolation of photosynthetically active mesophyll cells from *Asparagus* cladophylls. Can J Bot **57**: 1505-1510

Coté GG, Crain RC (1993) Biochemistry of phosphoinositides. Annu Rev Plant Physiol Plant Mol Biol **44**: 333-356

Dangl JL, Dietrich RA, Richberg MH (1996) Death don't have no mercy: Cell death programs in plant-microbe interactions. Plant Cell **8**: 1793-1807

Dillenschneider M, Hetherington A, Graziana A, Alibert G, Berta P, Haiech J, Ranjeva R (1986) The formation of inositol phosphate derivatives by isolated membranes from *Acer pseudoplatanus* is stimulated by guanine nucleotides. FEBS Lett **208**: 413-417

Doke N (1983) Involvement of superoxide anion generation in the hypersensitive response of potato tuber tissues to infection with an incompatible race of *Phytophthora infestans* and to the hyphal wall components. Physiol Plant Pathol **23**: 345-357

Doke N, Ohashi Y (1988) Involvement of an O_2^- generating system in the induction of necrotic lesions on tobacco leaves infected with tobacco mosaic virus. Physiol Mol Plant Pathol **32**: 163-175

Doke N, Miura Y, Sanchez LM, Park H-J, Noritake T, Yoshioka H, Kawakita K (1996) The oxidative burst protects plants against pathogen attack: mechanism and role as an emergency signal for plant bio-defence -- a review. Gene **179**: 45-51

Dong X (1995) Finding the missing pieces in the puzzle of plant disease resistance. Proc Natl Acad Sci USA **92**: 7137-7139

Drøbak BK, Watkins PAC (1994) Inositol(1,4,5)trisphosphate production in plant cells: Stimulation by the venom peptides, melittin and mastoparan. Biochem Biophys Res Commun **205**: 739-745

Ebel J, Cosio EG (1994) Elicitors of plant defense responses. Intl Rev Cytol **148**: 1-36

Einspahr KJ, Peeler TC, Thompson GA Jr (1988) Rapid changes in polyphosphoinositide metabolism associated with the response of *Dunaliella salina* to hypoosmotic shock. J Biol Chem **263**: 5775-5779

Einspahr KJ, Peeler TC, Thompson GA Jr (1989) Phosphatidylinositol 4,5-bisphosphate phospholipase C and phosphomonoesterase in *Dunaliella salina* membranes. Plant Physiol **90**: 1115-1120

Einspahr KJ, Thompson GA Jr (1990) Transmembrane signaling via phosphatidylinositol 4,5-bisphosphate hydrolysis in plants. Plant Physiol **93**: 361-366

Elliott DC, Skinner JD (1986) Calcium-dependent, phospholipid-activated protein kinase in plants. Phytochem **25**: 39-44

Fairley-Grenot K, Assmann SM (1991) Evidence for G-protein regulation of inward K^+ channel current in guard cells of fava bean. Plant Cell **3**: 1037-1044

Farmer EE, Moloshok TD, Saxton MJ, Ryan CA (1991) Oligosaccharide signaling in plants. J Biol Chem **266**: 33140-3145

Felix G, Regenass M, Boller T (1993) Specific perception of subnanomolar concentrations of chitin fragments by tomato cells: induction of extracellular alkalinization, changes in protein phosphorylation, and establishment of a refractory state. Plant J **4**: 307-316

Fischer T, Bronner C, Landry Y, Mousli M (1993) The mechanism of inhibition of alkylamines on the mast-cell peptidergic pathway. Biochim Biophys Acta **1176**: 305-312

Flor HH (1942) Inheritance of pathogenicity in *Melampsora lini*. Phytopathol **32**: 653-669

Foyer CH, Descourvières P, Kunert KJ (1994) Protection against oxygen radicals: an important defence mechanism studied in transgenic plants. Plant Cell Environ **17**: 507-523

Franklin-Tong VE, Drøbak BK, Allan AC, Watkins PAC, Trewavas AJ (1996) Growth of pollen tubes of *Papaver rhoeas* is regulated by a slow-moving calcium wave propagated by inositol 1,4,5-trisphosphate. Plant Cell **8**: 1305-1321

Gaff DF, Okong'o-ogola O (1971) The use of non-permeating pigment for testing the survival of cells. J Exp Bot **22**: 756-758

Gehring AC, Irving HR, Parish RW (1990) Effects of auxin and abscisic acid on cytosolic calcium and pH in plant cells. Proc Natl Acad Sci USA **87**: 9645-9649

Gelli A, Blumwald E (1997) Hyperpolarization-activated Ca^{2+}-permeable channels in the plasma membrane of tomato cells. J Memb Biol **155**: 35-45

Gil J, Higgins T, Rozengurt E (1991) Mastoparan, a novel mitogen for Swiss 3T3 cells, stimulates pertussis toxin-sensitive arachidonic acid release without inositol phosphate accumulation. J Cell Biol **113**: 943-950

Gilroy S, Read ND, Trewavas AJ (1990) Elevation of cytoplasmic calcium by caged calcium or caged inositol trisphosphate initiates stomatal closure. Nature **346**: 769-771

Goodwin TW, Mercer EI (1983) *Introduction to Plant Biochemistry.* Oxford: Pergamon Press, 677 pages

Granado J, Felix G, Boller T (1995) Perception of fungal sterols in plants. Plant Physiol **107**: 485-490

Hammond-Kosack KE, Jones JDG (1996) Resistance gene-dependent plant defense responses. Plant Cell **8**: 1773-1791

Harding SA, Oh S-H, Roberts DM (1997) Transgenic tobacco expressing a foreign calmodulin gene shows an enhanced production of active oxygen species. EMBO J **16**: 1137-1144

Heber U (1974) Metabolite exchange between chloroplasts and cytoplasm. Annu Rev Plant Physiol **25**: 393-421

Hedrich R, Busch H, Raschke K (1990) Ca^{2+} and nucleotide dependent regulation of voltage dependent anion channels in the plasma membrane of guard cells. EMBO J **9**: 3889-3892

Higashijima T, Wakamatsu K, Takemitsu M, Fujino M, Nakajima T, Miyazawa T (1983) Conformational change of mastoparan from wasp venom on binding with phospholipid membrane. FEBS Lett **152**: 227-230

Higashijima T, Uzu S, Nakajima T, Ross EM (1988) Mastoparan, a peptide toxin from wasp venom, mimics receptors by activating GTP-binding regulatory proteins (G-proteins). J Biol Chem **263**: 6491-6494

Higashijima T, Burnier J, Ross EM (1990) Regulation of G_i and G_o by mastoparan, related amphiphilic peptides, and hydrophobic amines. J Biol Chem **265**: 14176-14186

Higashijima T, Ross EM (1991) Mapping of the mastoparan-binding site on G proteins. J Biol Chem **266**: 12655-12661

Huang CN, Cornejo MJ, Bush DS, Jones RL (1986) Estimating viability of plant protoplasts using double and single staining. Protoplasma **135**: 80-87

Jabs T, Dietrich RA, Dangl JL (1996) Initiation of runaway cell death in an *Arabidopsis* mutant by extracellular superoxide. Science **273**: 1853-1856

Jabs T, Tschöpe M, Colling C, Hahlbrock K, Scheel D (1997) Elicitor-stimulated ion fluxes and O_2 from the oxidative burst are essential components in triggering defense gene activation and phytoalexin synthesis in parsley. Proc Natl Acad Sci USA **94**: 4800-4805

Jones DL, Kochian LV (1995) Aluminum inhibition of the inositol 1,4,5-trisphosphate signal transduction pathway in wheat roots: A role in aluminum toxicity. Plant Cell **7**: 1913-1922

Kaiser WM (1976) The effect of hydrogen peroxide on CO_2-fixation of isolated intact chloroplasts. Biochim Biophys Acta **440**: 476-482

Kaiser WM (1979) Reversible inhibition of the Calvin cycle and activation of oxidative pentose phosphate cycle in isolated intact chloroplasts by hydrogen peroxide. Planta **145**: 377-382

Kamada Y, Muto S (1994a) Stimulation by fungal elicitor of inositol phospholipid turnover in tobacco suspension culture cells. Plant Cell Physiol **35**: 397-404

Kamada Y, Muto S (1994b) Protein kinase inhibitors inhibit stimulation of inositol phospholipid turnover and induction of phenylalanine ammonia-lyase in fungal elicitor-treated tobacco suspension culture cells. Plant Cell Physiol **35**: 405-409

Kanai R, Edwards GE (1973) Purification of enzymatically isolated mesophyll protoplasts from C_3, C_4 and Crassulacean acid metabolism plants using an aqueous dextran-polyethylene glycol two-phase system. Plant Physiol **52**: 484-490

Kathiresan A, Tung P, Chinnappa CC, Reid DM (1997) γ-Aminobutyric acid stimulates ethylene biosynthesis in sunflower. Plant Physiol; in press

Kauss H, Jeblick W (1995) Pretreatment of parsley suspension cultures with salicylic acid enhances spontaneous and elicited production of H_2O_2. Plant Physiol **108**: 1171-1178

Kauss H, Jeblick W (1996) Influence of salicyclic acid on the induction of competence for H_2O_2 elicitation: comparison of ergosterol with other elicitors. Plant Physiol **111**: 755-763

Keppler LD, Novacky A (1987) The initiation of membrane lipid peroxidation during bacteria-induced hypersensitive reaction. Physiol Mol Plant Pathol **30**: 233-245

Kim HY, Coté GG, Crain RC (1996) Inositol 1,4,5-trisphosphate may mediate closure of K^+ channels by light and darkness in *Samanea saman* motor cells. Planta **198**: 279-287

Kinoshita T, Nishimura M, Shimazaki K (1995) Cytosolic concentration of Ca^{2+} regulates the plasma membrane H^+-ATPase in guard cells of fava bean. Plant Cell **7**: 1333-1342

Knight MR, Campbell AK, Smith SM, Trewavas AJ (1991) Transgenic plant aequorin reports the effects of touch and cold-shock and elicitors on cytoplasmic calcium. Nature **352**: 524-526

Knight MR, Smith SM, Trewavas AJ (1992) Wind-induced plant motion immediately increases cytosolic calcium. Proc Natl Acad Sci **89**: 4967-4971

Knight H, Trewavas AJ, Knight MR (1996) Cold calcium signaling in *Arabidopsis* involves two cellular pools and a change in calcium signature after acclimation. Plant Cell **8**: 489-503

Knogge W (1996) Fungal infection of plants. Plant Cell **8**: 1711-1722

Kurkdjian A, Guern J (1989) Intracellular pH: measurement and importance in cell activity. Annu Rev Plant Physiol **40**: 271-303

Lee Y, Assmann SM (1991) Diacylglycerols induce both ion pumping in patch-clamped guard-cell protoplasts and opening of intact stomata. Proc Natl Acad Sci USA **88**: 2127-2131

Legendre L, Heinstein PF, Low PS (1992) Evidence for participation of GTP-binding proteins in elicitation of the rapid oxidative burst in cultured soybean cells. J Biol Chem **267**: 20140-20147

Legendre L, Rueter S, Heinstein PF, Low PS (1993a) Characterization of the oligogalacturonide-induced oxidative burst in cultured soybean (*Glycine max*) cells. Plant Physiol **102**: 233-240

Legendre L, Yueh YG, Crain R, Haddock N, Heinstein PF, Low PS (1993b) Phospholipase C activation during elicitation of the oxidative burst in cultured plant cells. J Biol Chem **268**: 24559-24563

Levine A, Tenhaken R, Dixon R, Lamb C (1994) H_2O_2 from the oxidative burst orchestrates the plant hypersensitive disease resistance response. Cell **79**: 583-593

Levine A, Pennell RI, Alvarez ME, Palmer R, Lamb C (1996) Calcium-mediated apoptosis in a plant hypersensitive disease resistance response. Curr Biol **6**: 427-437

Ling V, Snedden WA, Shelp BJ, Assmann SM (1994) Analysis of a soluble calmodulin binding protein from fava bean roots: Identification of glutamate decarboxylase as a calmodulin-activated enzyme. Plant Cell **6:** 1135-1143

Low PS, Merida JR (1996) The oxidative burst in plant defense: Function and signal transduction. Physiol Plant **96**: 533-542

Ma H, Yanofsky MF, Meyerowitz EM (1990) Molecular cloning and characterization of *GPA1*, a G protein α subunit gene from *Arabidopsis thaliana*. Proc Natl Acad Sci USA **87**: 3821-3825

Ma H, Yanofsky MF, Huang H (1991) Isolation and sequence analysis of *TGA1* cDNAs encoding a tomato G protein α subunit. Gene **107**: 189-195

MacGregor KB (1997) Is superoxide generation during the oxidative burst observed when *Asparagus sprengeri* mesophyll cells are treated with mastoparan? Honours thesis. Brock University, St. Catharines, Ontario; in press

Mathieu Y, Kurkdjian A, Xia H, Guern J, Koller A, Spiro MD, O'Neill M, Albersheim P, Darvill A (1991) Membrane responses induced by oligogalacturonides in suspension-cultured tobacco cells. Plant J **1**: 333-343

McAinsh MR, Clayton H, Mansfield TA, Hetherington AM (1996) Changes in stomatal behaviour and guard cell cytosolic free calcium in response to oxidative stress. Plant Physiol **111**: 1031-1042

McCutcheon SL, Bown AW (1987) Evidence for a specific glutamate/H^+ cotransport in isolated mesophyll cells. Plant Physiol **83:** 691-697

Mehdy M (1994) Active oxygen species in plant defense against pathogens. Plant Physiol **105**: 467-472

Mehdy MC, Sharma YK, Sathasivan K, Bays NW (1996) The role of activated oxygen species in plant disease resistance. Physiol Plant **98**: 365-374

Millner PA, Causier BE (1996) G-protein coupled receptors in plant cells. J Exp Bot **47**: 983-992

Miyake C, Michihata F, Asada K (1991) Scavenging of hydrogen peroxide in prokaryotic and eukaryotic algae: acquisition of ascorbate peroxidase during the evolution of cyanobacteria. Plant Cell Physiol **32**: 33-43

Miyake C, Asada K (1992) Thylakoid-bound ascorbate peroxidase in spinach chloroplasts and photoreduction of its primary oxidation product monodehydroascorbate radicals in thylakoids. Plant Cell Physiol **33**: 541-553

Miyake C, Asada K (1994) Ferredoxin-dependent photoreduction of the monodehydroascorbate radical in spinach thylakoids. Plant Cell Physiol **35**: 539-549

Morré DJ, Brightman AO, Wu L-Y, Barr R, Leak B, Crane FL (1988) Role of plasma membrane redox activities in elongation growth in plants. Physiol Plant **73**: 187-193

Morré DJ, Brightman AO, Barr R, Davidson M, Crane FL (1993) NADH oxidase activity of plasma membranes of soybean hypocotyls is activated by guanine nucleotides. Plant Physiol **102**: 595-602

Munnik T, Musgrave A, de Vrije T (1994) Rapid turnover of polyphosphoinositides in carnation flower petals. Planta **193**: 89-98

Munnik T, Arisz SA, de Vrije T, Musgrave A (1995) G protein activation stimulates phospholipase D signaling in plants. Plant Cell **7**: 2197-2210

Munnik T, de Vrije T, Irvine RF, Musgrave A (1996) Identification of diacylglycerol pyrophosphate as a novel metabolic product of phosphatidic acid during G-protein activation in plants. J Biol Chem **271**: 15708-15715

Neubauer C, Schreiber U (1988) Photochemical and non-photochemical quenching of chlorophyll fluorescence induced by hydrogen peroxide. Z Naturforsch **44c**: 262-270

Neufeld E, Bown AW (1987) A plasmamembrane redox system and proton transport in isolated mesophyll cells. Plant Physiol **83**: 895-899

Nürnberger T, Wirtz W, Nennstiel D, Hahlbrock K, Jabs T, Zimmerman S, Scheel D (1997) Signal perception and intracellular signal transduction in plant pathogen defense. J Receptor Signal Trans Res **17**: 127-136

Okano Y, Takagi H, Tohmatsu T, Nakashima S, Kuroda Y, Saito K, Nozawa Y (1985) A wasp venom mastoparan-induced polyphosphoinositide breakdown in rat peritoneal mast cells. FEBS Lett **188**: 363-366

Oláh Z, Kiss Z (1986) Occurrence of lipid and phorbol ester activated protein kinase in wheat cells. FEBS Lett **195**: 33-37

Parsons R, Baker A (1996) Cycling of amino compounds in symbiotic lupin. J Exp Bot **47**: 421-429

Pavlovkin J, Novacky A, Ullrich-Eberius CI (1986) Membrane potential changes during bacteria-induced hypersensitive reaction. Physiol Mol Plant Pathol **28**: 125-135

Peever TL, Higgins VJ (1989) Electrolyte leakage, lipoxygenase, and lipid peroxidation induced in tomato leaf tissue by specific and nonspecific elicitors from *Cladosporium fulvum*. Plant Physiol **90**: 867-875

Peterson RB, Aylor DE (1995) Chlorophyll fluorescence induction in leaves of *Phaseolus vulgaris* infected with bean rust (*Uromyces appendiculatus*). Plant Physiol **108**: 163-171

Price AH, Taylor A, Ripley SJ, Griffiths A, Trewavas AJ, Knight MR (1994) Oxidative signals in tobacco increase cytosolic calcium. Plant Cell **6**: 1301-1310

Price A, Knight M, Knight H, Cuin T, Tomos D, Ashendon T (1996) Cytosolic calcium and oxidative plant stress. Biochem Soc Trans **24**: 479-483

Qualliotine-Mann D, Agwu DE, Ellenburg MD, McCall CE, McPhail LC (1993) Phosphatidic acid and diacylglycerol synergize in a cell-free system for activation of NADPH oxidase from human neutrophils. J Biol Chem **268**: 23843-23849

Ramputh A-I, Bown AW (1996) Rapid γ-aminobutyric acid synthesis and the inhibition of the growth and development of oblique-banded leaf-roller larvae. Plant Physiol **111**: 1349-1352

Raynor RL, Zheng B, Kuo JF (1991) Membrane interactions of amphiphilic polypeptides mastoparan, melittin, polymyxin B, and cardiotoxin: differential inhibition of protein kinase C, Ca^{2+}/calmodulin-dependent protein kinase II and synaptosomal membrane Na,K-ATPase, and Na^{+} pump and differentiation of HL60 cells. J Biol Chem **266**: 2753-2758

Roberts JKM, Hooks MA, Miaullis AP, Edwards S, Webster C (1992) Contribution of malate and amino acid metabolism to cytoplasmic pH regulation in hypoxic maize root tips studied using nuclear magnetic resonance spectroscopy. Plant Physiol **98**: 480-487

Robertson D, Davies DR, Gerrish C, Jupe SC, Bolwell GP (1995) Rapid changes in oxidative metabolism as a consequence of elicitor treatment of suspension-cultured cells of French bean (*Phaseolus vulgaris* L.). Plant Mol Biol **27**: 59-67

Rogers KR, Albert R, Anderson AJ (1988) Lipid peroxidation is a consequence of elicitor activity. Plant Physiol **86**: 547-553

Ross EM, Higashijima T (1994) Regulation of G-protein activation by mastoparans and other cationic peptides. Meth Enzymol **237**: 26-37

Rotman, Papermaster (1966) Membrane properties of living mammalian cells as studied by enzymatic hydrolysis of fluorogenic esters. Proc Natl Acad Sci USA **55**: 134-141

Rubinstein B, Stern AI, Stout RG (1984) Redox activity at the surface of oat root cells. Plant Physiol **76**: 386-391

Salzer P, Hebe G, Reith A, Zitterell-Haid B, Stransky H, Gaschler K, Hager A (1996) Rapid reactions of spruce cells to elicitors released from the ectomycorrhizal fungus *Hebeloma crustuliniforme*, and inactivation of these elicitors by extracellular spruce cell enzymes. Planta **198**: 118-126

Satya Narayan V, Nair PM (1990) Metabolism, enzymology and possible roles of 4-aminobutyrate in higher plants. Phytochem **29**: 367-375

Schafer A, Bygrave F, Matzenauer S, Marmé D (1985) Identification of a calcium- and phospholipid-dependent protein kinase in plant tissue. FEBS Lett **187**: 25-28

Scanlon CH, Martinec J, Macháčková I, Rolph CE, Lumsden PJ (1996) Identification and preliminary characterization of a Ca^{2+}-dependent high-affinity binding site for inositol-1,4,5-trisphosphate from *Chenopodium rubrum*. Plant Physiol **110**: 867-874

Scheel D, Parker JE (1990) Elicitor recognition and signal transduction in plant defense gene activation. Z. Naturforsch. **45**: 569-575

Scherer GFE (1992) Stimulation of growth and phospholipase A_2 by the peptides mastoparan and melittin and by the auxin 2,4-dichlorophenoxyacetic acid. Plant Growth Regul **11**: 153-157

Scherer GFE, André B (1989) A rapid response to a plant hormone: auxin stimulates phospholipase A_2 *in vivo* and *in vitro*. Biochem Biophys Res Commun **163**: 111-117

Schreiber U, Schliwa U, Bilger W (1986) Continuous recording of photochemical and non-photochemical chlorophyll fluorescence quenching with a new type of modulation fluorometer. Photosyn Res **10**: 51-62

Schreiber U, Reising H, Neubauer C (1991) Contrasting pH-optima of light-driven O_2- and H_2O_2-reduction in spinach chloroplasts as measured *via* chlorophyll fluorescence quenching. Z Naturforsch **46c**: 635-643

Schroeder JI, Hagiwara S (1989) Cytosolic calcium regulates ion channels in the plasma membrane of *Vicia faba* guard cells. Nature **338**: 427-430

Schumaker K (1996) Spikes and waves: Calcium-mediated signaling in tip-growing cells. Plant Cell **8**: 1915-1916

Schwacke R, Hager A (1992) Fungal elicitors induce a transient release of active oxygen species from cultured spruce cells that is dependent on Ca^{2+} and protein-kinase activity. Planta **187**: 136-141

Smith CJ (1996) Accumulation of phytoalexins: defence mechanism and stimulus response system. New Phytologist **132**: 1-45

Smoleńska-Sym G, Kacperska A (1996) Inositol 1,4,5-trisphosphate formation in leaves of winter oilseed rape plants in response to freezing, tissue water potential and abscisic acid. Physiol Plant **96**: 692-698

Snedden WA, Chung I, Pauls RH, Bown AW (1992) Proton/L-glutamate symport and the regulation of intracellular pH in isolated mesophyll cells. Plant Physiol **99**: 665-671

Snedden WA, Arazi T, Fromm H, Shelp BJ (1995) Calcium/calmodulin activation of soybean glutamate decarboxylase. Plant Physiol **108**: 543-549

Speksnijder JE, Miller AL, Weisenseel MH, Chen T-H, Jaffe LF (1989) Calcium buffer injections block fucoid egg development by facilitating calcium diffusion. Proc Natl Acad Sci USA **86**: 6607-6611

Sutherland MW (1991) The generation of oxygen radicals during host plant responses to infection. Physiol Mol Plant Pathol **39**: 79-93

Takeda T, Yokota A, Shigeoka S (1995) Resistance of photosynthesis to hydrogen peroxide in algae. Plant Cell Physiol **36**: 1089-1095

Terryn N, Van Montagu M, Inzé D (1993) GTP-binding proteins in plants. Plant Mol Biol **22**: 143-152

Toyoda K, Shiraishi T, Yoshioka H, Yamada T, Ichinose Y, Oku H (1992) Regulation of polyphosphoinositide metabolism in pea plasma membranes by elicitor and suppressor from a pea pathogen, *Mycosphaerella pinodes*. Plant Cell Physiol **33**: 445-452

Trewavas A, Read N, Campbell AK, Knight M (1996) Transduction of Ca^{2+} signals in plant cells and compartmentalization of the Ca^{2+} signal. Biochem Soc Trans **24**: 971-974

Tucker EB, Boss WF (1996) Mastoparan-induced intracellular Ca^{2+} fluxes may regulate cell-to-cell communication in plants. Plant Physiol **111**: 459-467

Vera-Estrella R, Blumwald E, Higgins VJ (1992) Effect of specific elicitors of *Cladosporium fulvum* on tomato suspension cells: evidence for the involvement of active oxygen species. Plant Physiol **99**: 1208-1215

Vera-Estrella R, Barkla BJ, Higgins VJ, Blumwald E (1994a) Plant defense response to fungal pathogens: activation of host-plasma membrane H^{+}-ATPase by elicitor-induced enzyme dephosphorylation. Plant Physiol **104**: 209-215

Vera-Estrella R, Higgins VJ, Blumwald E (1994b) Plant defense response to fungal pathogens: II. G-protein-mediated changes in host plasma membrane redox reactions. Plant Physiol **106**: 97-102

Vianello A, Macrì F (1989) NAD(P)H oxidation elicits anion superoxide formation in radish plasmalemma vesicles. Biochim Biophys Acta **980**: 202-208

Wallace W, Secor J, Schrader LE (1984) Rapid accumulation of γ-aminobutyric acid and alanine in soybean leaves in response to an abrupt transfer to lower temperature, darkness, or mechanical manipulation. Plant Physiol **75**: 170-175

Ward JM, Schroeder JI (1994) Calcium-activated K^+ channels and calcium-induced calcium release by slow vacuolar ion channels in guard cell vacuoles implicated in the control of stomatal closure. Plant Cell **6**: 669-683

Warm E, Laties GG (1982) Quantification of hydrogen peroxide in plant extracts by the chemiluminescence reaction with luminol. Phytochem **21**: 827-831

Warpeha KMF, Hamm HE, Rasenick MM, Kaufman LS (1991) A blue-light-activated GTP-binding protein in the plasma membranes of etiolated peas. Proc Natl Acad Sci USA **88**: 8925-8929

Wevelsiep L, Kogel K-H, Knogge W (1991) Purification and characterization of peptides from *Rhynchosporium secalis* inducing necrosis in barley. Physiol Mol Plant Pathol **39**: 471-482

White IR, Wise A, Millner PA (1993) Evidence for G-protein-linked receptors in higher plants: stimulation of GTP-gamma-S binding to membrane fractions by the mastoparan analogue mas 7. Planta **191**: 285-288

Widholm JM (1972) The use of fluorescein diacetate and phenosafranine for determining viability of cultured plant cells. Stain Technol **47**: 189-194

Wiess CA, Garnaat CW, Mukai K, Hu Y, Ma H (1994) Isolation of cDNAs encoding guanine nucleotide-binding protein β-subunit homologues from maize (ZGB1) and *Arabidopsis* (AGB1). Proc Natl Acad Sci USA **91**: 9554-9558

Withers LA (1985) Cryopreservation and storage of germplasm. In *Plant Cell Culture, A Practical Approach* (Dixon RA, ed.) Washington DC: IRL Press, pp. 184,185

Wong R (1997) The role of calcium in plant cell death, the hypersensitive response and GABA accumulation in *Asparagus sprengeri* mesophyll cells. Honours thesis. Brock University, St. Catharines, Ontario.

Xing T, Higgins VJ, Blumwald E (1996) Regulation of plant defense response to fungal pathogens: two types of protein kinases in the reversible phosphorylation of the host plasma membrane H^+-ATPase. Plant Cell **8**: 555-564

Zhang Z, Collinge DB, Thordal-Christensen H (1995) Germin-like oxalate oxidase, a H_2O_2-producing enzyme accumulates in barley attacked by the powdery mildew fungus. Plant J **8**: 139-145

Appendix I

GABA Calibration Graph:
Absorbance Change as a Function of GABA Concentration

One hundred ml of 0.001 M GABA was prepared. Ten ml of this was diluted to 100 ml to give a 0.001 M standard GABA solution. Dilutions of this solution with 4 ml of 5 mM MES buffer, pH 6.0 were performed to give GABA solutions containing from 0 to 20 nmols of GABA. These solutions were dried down and GABA was redissolved in 500 μl of 0.1 M potassium pyrophosphate buffer, pH 8.6. GABA determination was performed in duplicate with the gabase assay. The change in absorbance at 340 nm was plotted against nmols of standard GABA. Each point represents the mean of three experiments.

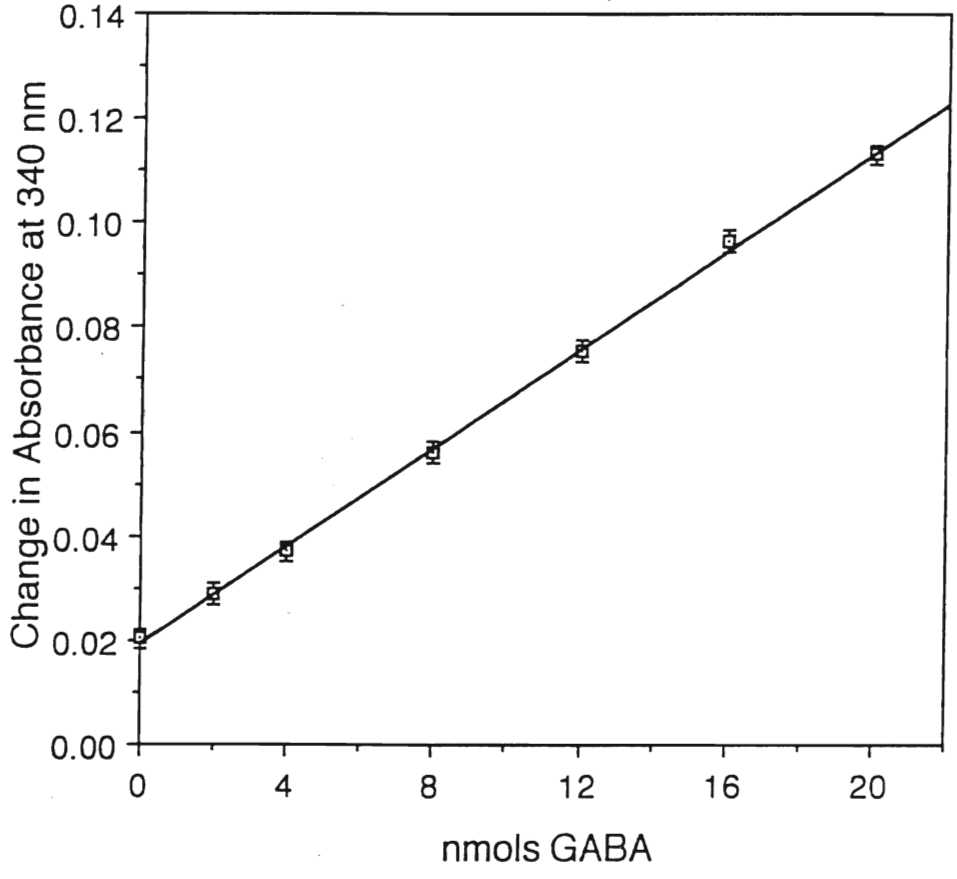

Appendix II

The following questions were asked but experiments to test them gave negative results in which the chemical of interest had no effect or control and experimental values were not significantly different:

1. Does the addition of catalase (0.18 μM) 10 s before and 10 s after MP addition diminish the rate of O_2 consumption? (n = 2)
2. Does the addition of sodium dithionite crystals following MP-stimulated O_2 uptake cause a further decrease in O_2? (n = 4)
3. Does the protonophore nigericin (6.7 μM) 1 min before or 15 s after MP (6.6 μM) eliminate nonphotochemical quenching due to MP? (n = 3)
4. Do H_2O_2 concentrations ranging from 0.5 mM to 50 mM cause significant loss of cell viability within 36 min? (n = 3)
5. Does 2 mM H_2O_2 induce GABA accumulation within 16 min? (n = 3)
6. Does the addition of superoxide dismutase (SOD) (50 units) plus MP (25 μM) decrease the % of nonviable cells as compared to MP alone? (n = 3)
7. Does the addition of SOD (112.4 units) plus MP (66 μM) result in the accumulation of H_2O_2 as detected with the luminol assay? (n = 2)
8. Does the protein kinase inhibitor staurosporine (1 μM) inhibit MP-stimulated GABA accumulation within 16 min? (n = 3)
9. Does staurosporine (5.4 μM or 25 μM) preincubated with asparagus cells for 15 min inhibit O_2 uptake in response to 6.6 μM MP? (n = 3)

"There is no such thing as a failed experiment. It is nature trying to tell you something."

A.W. Bown, 1997